Università degli Studi di Torino

Scuola di Dottorato in
Scienze della Natura e Tecnologie Innovative

Dottorato in Scienze Farmaceutiche e Biomolecolari (XXIX ciclo)

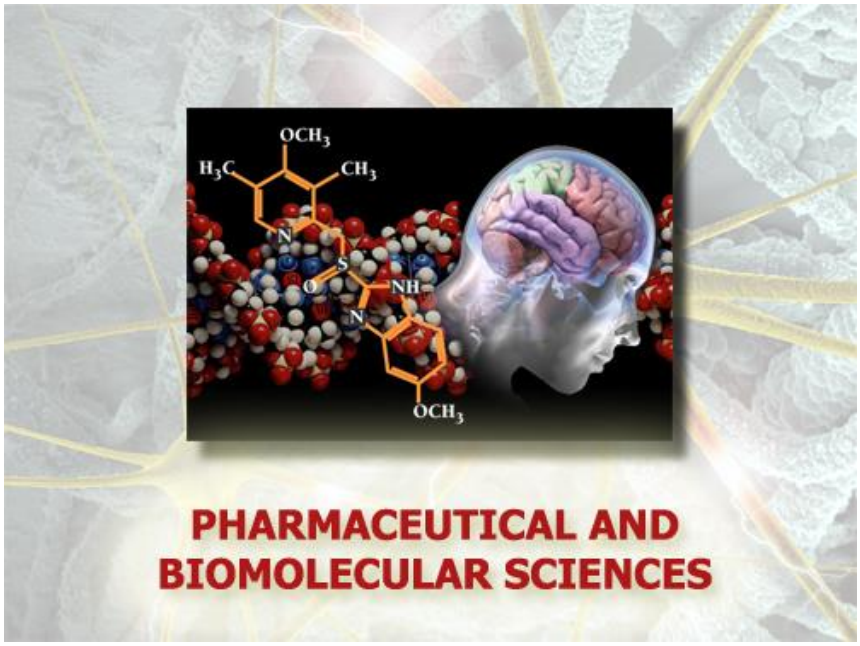

Effects of the Earth's magnetic field on plant growth, development and evolution

Candidato/a: Chiara Agliassa **Tutor(s): Prof. Massimo Emilio Maffei**

Università degli Studi di Torino

Dottorato in
Scienze Farmaceutiche e Biomolecolari

Tesi svolta presso il
Dipartimento di Scienze della Vita e Biologia dei Sistemi

CICLO: XXX

TITOLO DELLA TESI: Effects of Earth's magnetic field on plant growth, development and evolution

TESI PRESENTATA DA: Chiara Agliassa

TUTOR(S): Prof. Massimo Emilio Maffei

COORDINATORE DEL DOTTORATO: Prof. Gianmario Martra

ANNI ACCADEMICI: 2014-2015-2016-2017

SETTORE SCIENTIFICO-DISCIPLINARE DI AFFERENZA*: BIO/04
(*N.B. Nel caso di più settori disciplinari interessati, deve essere indicato quello più presente nella trattazione della tesi).

“***Be happy while you’re living, for you’re a long time dead”***
Scottish Proverb

TABLE OF CONTENTS

INTRODUCTION

The geomagnetic field (GMF) origin, intensity and direction

The Earth's magnetic field or geomagnetic field (GMF) is a natural physical phenomenon observable on the Earth. Adopting the definition by Glatzmaiers and Roberts (1995), the GMF can be described as a dominant dipolar field at the surface of the Earth with an axis which on the average lies closed to the Earth's rotation geographical axis.

A magnetic field (MF) is known to be the combination of magnetic materials and electric currents. The GMF originates in the Earth's outer fluid metallic core which is well above the Curie point (at which metals lose their ferromagnetic properties) and is sustained by the electrical currents which circulate in this ocean of liquid iron. The convection of molten iron together with the Coriolis effect caused by the overall planetary rotation tends to produce these "electric currents" in rolls aligned along the north-south polar axis. When a conducting fluid flows across an existing MF, electric currents are induced, thus creating another magnetic field. The new induced MF reinforces the original MF, creating a dynamo which sustains itself. Nowadays, the GMF origin theory is correlated to the above illustrated *dynamo hypothesis,* which was firstly introduced by Sir Joseph Larmor in 1919 to account for the magnetic field of sunspots (Figure 1).

The Earth's magnetic field is a solenoidal vector field with 3 components: inclination, declination and intensity (Merrill and McFadden, 1995). Magnetic field lines emerge from the planet forming an angle in relation to the Earth's surface that varies with the latitude. This is referred to as the inclination of the field. In contrast, the declination refers to the angle of the magnetic field lines with respect to true geographic North, reflecting the direction a compass needle points. The intensity of the field is measured in terms of its flux density (B). B is the vector that describes electrodynamic phenomena deriving from the field and it is measured in Tesla (symbol: T), defined as:

$$\mathrm{T} = \mathrm{N}\frac{\mathrm{s}}{\mathrm{C\,m}} = \mathrm{V}\frac{\mathrm{s}}{\mathrm{m}^2} = \frac{\mathrm{Wb}}{\mathrm{m}^2}$$

In SI unit, the magnetic flux (ϕ) is measured in Weber (Wb) and represents the product of B and the area that is filled by the magnetic field ($\mathrm{Wb} = \mathrm{T\,m}^2$). The GMF intensity as well as its direction are subjected to local differences at the Earth's surface. Its strength values range from less than 30 μT at the south Atlantic anomaly level (including most of South America and South Africa) to almost 70 μT around the magnetic poles in northern Canada and south of Africa. As for the direction, its parallel component is maximal at the equator (about 33 μT), while its perpendicular component shows its maximal at the magnetic poles (about 67 μT).

The GMF is not stable, it is subjected to variations on time scales from milliseconds to millions of years (Jacobs and Sinno, 1960). The average value of its flux density at the surface of the Earth is influenced by changes in the Earth's interior magnetism together with fluctuations of external variables such as the solar activity and other atmospheric events (Valet, 2003). The geomagnetic field has a regular small variation with a fundamental period of 24 hours. This variation is easiest to observe during periods of low solar activity when large irregular disturbances are less frequent. Geomagnetic storms, sub-storms, and pulsations are the most noteworthy manifestations of the geomagnetic activity, which induces daily to weekly changes in GMF circadian rhythmicity. In particular, they affect the electric currents of the magnetosphere and ionosphere , which are both external sources of the GMF, but lower than the interior Earth's MF by several orders of magnitude (Valet, 2003).

Together with changes in its intensity, the GMF is subjected to reversion in its polarity, on timescales of millennia. During the so called GMF reversals or excursions usually a few

thousand years long, the GMF strength is strongly reduced and can even exhibit low-frequency perturbations (Crain, 1971). Considering the key role of GMF in protecting the Earth by the solar wind charge particles, these events abolish the shielding of our planet from the cosmic rays (Leske *et al.*, 1995).

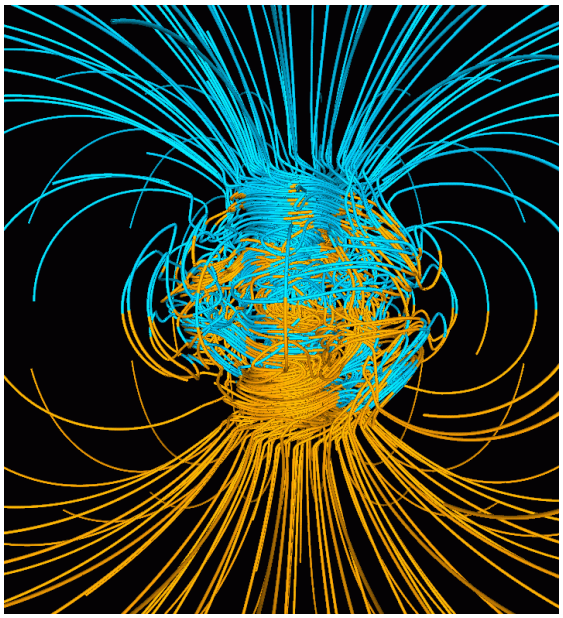

Figure 1: A snapshot of the 3D magnetic field structure simulated with the geo-dynamo model. Magnetic field lines are blue where the field is directed inward and yellow where directed outward. The rotation axis of the model Earth is vertical and through the center. A transition occurs at the core-mantle boundary from the intense, complicated field structure in the fluid core, where the field is generated, to the smooth, potential field structure outside the core. The field lines are drawn out to two Earth radii. Magnetic field is wrapped around the "tangent cylinder" due to the shear of the zonal fluid flow (Glatzmaiers and Roberts, 1995).

The GMF as a possible evolution driving force

Along the evolutionary and geological timeline of the Earth, the GMF has always been a natural environmental element. Considering the changes that affected its intensity and polarization in time and space, it is legitimate to assume that the GMF could act as an abiotic stress factor on living organisms. For a long time, most scientists have casted doubt on the possibility of biological responses to geomagnetic activity. The main reason for these doubts is that the energy of geomagnetic fluctuations that comprise geomagnetic activity is much lower than the thermal noise of biological systems (Krylov, 2017), thus marking the GMF as a weak magnetic field. Despite all doubts, the number of empirical findings describing significant correlations between geomagnetic activity and biological parameters has steadily increased over time (Krylov, 2017). Moreover, joint analysis of the fossil record and paleomagnetic data point out a correlation between fossil pattern of extinction, speciation and geomagnetic polarity reversals. This trend is demonstrated for both marine and terrestrial faunal organisms (Buchachenko, 2016). The greatest incidence of high-energy particles and UV radiations able to reach the Earth surface during GMF reversals could be one of the reason of the massive extinction and speciation related to this event. In fact, mass extinctions have involved also marine life that is effectively shielded from cosmic radiation and UV (Crain, 1971). Moreover, considering that cosmic rays produce only a small percentage of all observed genome mutations (0,6%), they cannot be responsible of an evolutionary discontinuity (Crain, 1971). Thereby, a simpler and straight explanation of this issue is that GMF has direct bioeffects on living organisms. The GMF is not shielded by seawater and it can freely penetrate biological tissues and operate on both marine and terrestrial organisms with equal effectiveness.

Periods of GMF polarity reversal last from a minimum of 1000 yrs to a maximum of 13000 yrs (Crain, 1971; Glatzmaiers and Roberts, 1995). Thereby, many consecutive generations of all kingdoms of organisms would have been exposed to an environment with a greatly reduced magnetic field, thus possibly affecting their evolution. Recently, it has been proved that periods of normal polarity transitions overlapped with the diversification of most of the familial Angiosperm lineages (Occhipinti, De Santis and Maffei, 2014)(Figure 2). Therefore, together with its intensity reduction during polarity reversals, GMF could have even affected plant evolution by its polarity.

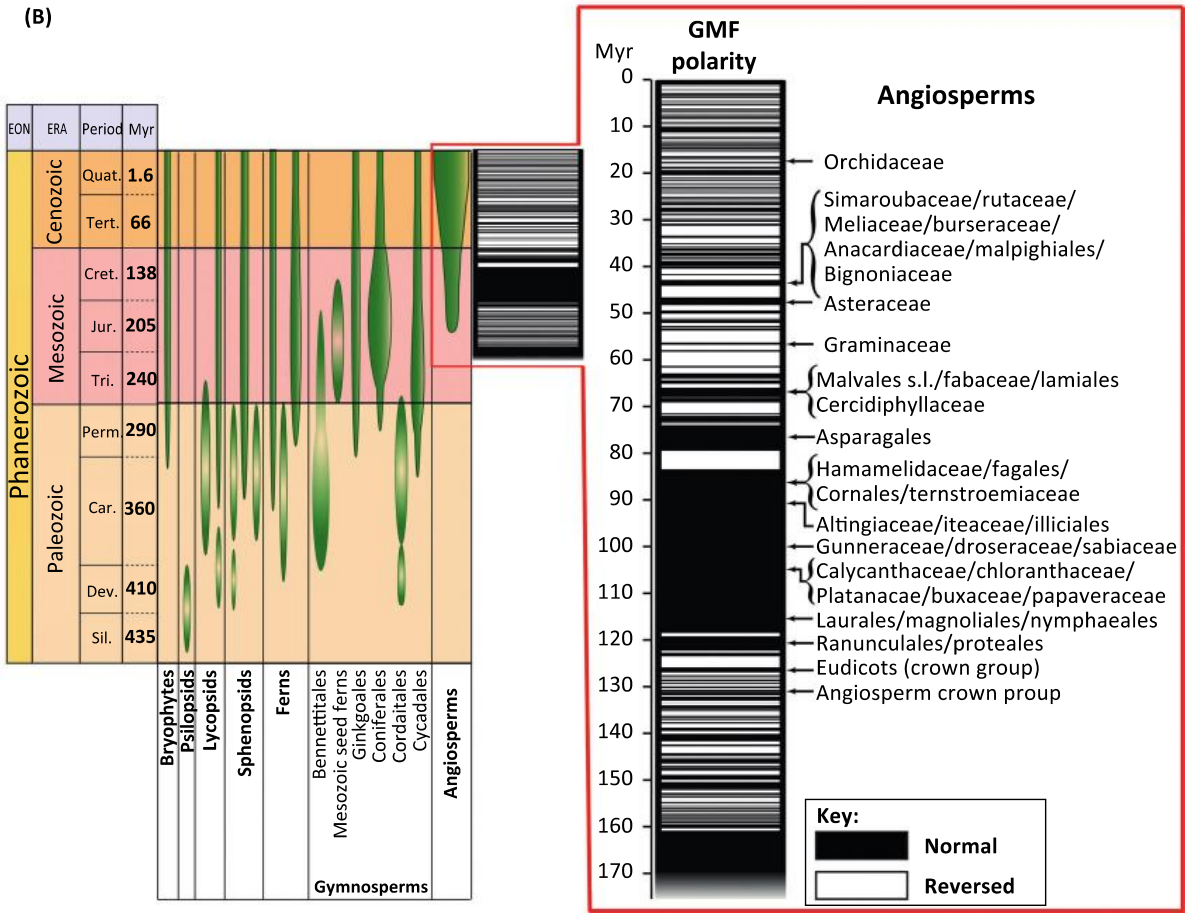

Figure 2: Influence of GMF polarity on plant evolution: the evolutionary history of plants (on the left); a direct comparison between GMF polarity and the diversification of Angiosperms (on the right) (Occhipinti, De Santis and Maffei, 2014).

The weak magnetic field (WMF) affects biological processes

Magneto-biological experiments have been conducted to highlight the sensitivity of biological systems to permanent and alternating MFs. It has been demonstrated that the ability to respond to magnetic fields is ubiquitous and universal among all kingdoms of organisms (Buchachenko, 2016). Interestingly, the GMF appears to influence the circadian biological processes in animals, thus having been proposed as an endogenous clock entertainer in animals (Bliss and Heppner, 1976; Brown, 1976; Yoshii, Ahmad and Helfrich-Förster, 2009). In all living organisms, MF-induced bioeffects are present at a biochemical, molecular, cellular and whole organism level and they depend upon the intensity, amplitude, time and frequency of applied fields (Ghodbane *et al.*, 2013). In general, four different types of magnetic fields have mainly been employed in experimental conditions:

a) Weak static homogeneous magnetic field from 0 to about 100 μT (including the GMF values). It can be divided into:

- weak or low magnetic field (WMF) referred to intensities from 100 nT to 0.5 mT;
- super weak or conditionally zero field (also called Near Null Magnetic Field, NNMF) related to intensities below 100 nT.

b) Strong homogenous magnetic field (mT to T);
c) Strong inhomogeneous magnetic field;
d) Extremely low frequency (ELF) magnetic field of low to moderate (several hundred micro Teslas) magnetic flux densities.

Amongst these four types of experimental conditions, only the weak static fields contribute directly to the question whether organisms can detect the GMF or not, even though much useful information can also be extracted from other treatments (Galland and Pazur, 2005).
Magnetic fields lower than the GMF have been created in laboratory using different techniques; one method consists in surrounding the experimental zone by ferromagnetic metal plates with a high-magnetic-permeability (such as "mu-metal"). This solution allows to deviate the flux lines of the external magnetic field and to concentrate them within the metal plates, this way screening the experimental zone from the external magnetic field. However, this screening approach is prohibitively expensive, and it is technically infeasible to build large exposure chambers (> 3 m^3). Moreover, this method forces plants to grow in unrealistic environmental conditions (air circulation, temperature, lighting), which affects many natural plant responses (e.g., light, temperature, etc.) (Maffei, 2014).
Alternatively, it is possible to obtain a reduced MF in a more natural environment by using Helmholtz coils. A Helmholtz coil is a device that can be used for producing a region of nearly-uniform magnetic field and it consists of a pair of two identical (usually circular) magnetic solenoids. Solenoids are placed symmetrically along a common axis and separated by a distance *h* equal to the radius *R* of the coil. Each coil carries an equal electric current in the same direction, so that a stable and constant $\mathbf{B_{axis}}$ component (parallel to the coil pair axis) is produced in the middle of the coil pair in order to compensate the GMF (Maffei, 2014).

Plants respond to WMF

Under MF values higher than GMF, many plants processes, such as germination, leaf movement, stomata conductance, root and shoot growth, gravitropic-related response, photosynthesis and redox status-related responses are affected (Maffei, 2014). Despite the lack of experiments performed under WMF conditions with respect to those testing the effects of high magnetic field on plants, a large body of data demonstrates plant susceptibility even to WMF (Maffei, 2014). Some of the experiments carried out from 1977 up to now are reported below, showing the complexity and contradiction of plant responses:

- From a morphological point of view, WMF seems to affect the growth and development of different plant organs, usually in a contradictory way. For example, the development of primary roots was influenced by WMF during early germination stages. While a growth inhibition was observed in sugar beet, wheat and pea primary roots after the first 4 days of WMF exposure, a later root elongation partially compensated the reduction compared to GMF-exposed controls (Belyavskaya, 2004). In another set of experiments, 3-5-day old wheat seedlings grew slower in a wide range of WMF (from 0.20 nT to 0.1 mT) than in GMF conditions, while a small increase in the pea seedlings length was observed at 40 μT and 0.5 μT (Bogatina *et al.*, 1978, 1979). Differently, 3-day old pea epicotyls exposed to WMF for 24h in the darkness were longer than in GMF conditions (Negishi *et al.*, 1999).
- Considering plant biomass, *in vitro* experiments showed that its production from plant tissue cultures is either stimulated or inhibited under WMF conditions. It depended upon the species, genotype, type of initial explant, treatment duration and even

culture medium (Rakosy-Tican, Aorori and Morariu, 2005). Similarly, even the fresh weight of pot-grown seedlings was differently affected by WMF depending on the plant species (Lebedev *et al.*, 1977). Considering plant later developmental stages, *Arabidopsis thaliana* biomass accumulation was significantly suppressed at the time of switching from vegetative to reproductive growth under WMF (Xu *et al.*, 2013).

- Flowering time is also affected by WMF: *Arabidopsis thaliana* growth in NNMF conditions reached flowering ca. 5 day later than in normal GMF (Xu *et al.*, 2012, 2013);
- WMF has also demonstrated effects at the cellular cycle level. For example, pea, flax and lentil root meristems showed a delay of the pre-synthetic G_1 phase and post synthetic G_2 phase under WMF. Moreover, a decrease in the functional genome activities occurred in the early G_1 phase under WMF conditions compared to GMF control (Fomicheva *et al.*, 1992; Fomicheva, Govoroon and Danilov, 1992)
- WMF also causes alterations in cellular structures. As an example, it induced a noticeable accumulation of lipid bodies, together with a development of lytic compartments (vacuoles, cytosegresomes, and paramural bodies) and a reduction of phytoferritin in plastids of meristem root cells. Moreover, mitochondria seemed to be the WMF most sensitive organelles due to their cellular size and relative volume increment and cristae reduction under this condition (Belyavskaya, 2001).
- Furthermore, MF intensity seems to interfere with the chemiosmotic equilibrium in plant cells. WMF increased the rate of water absorption and osmotic pressure of cell sap at the middle part of pea epicotyl (Negishi *et al.*, 1999). Experimental data provided evidence that WMF alters water relations also in seeds, and this effect might explain the reported alterations in their germination rate (Reina, Pascual and Fundora, 2001). Moreover, several experiments showed that WMF causes alterations in the mobilization of ions and that Ca^{2+} entry into the cytosol might constitute an early MF sensing mechanism (Belyavskaya, 2001).

Physical models for explaining WMF perception in plants

Despite the evidence that a WMF has effects on living organisms, the molecules and mechanisms that mediate the sensory transduction are far from being elucidated. So far, amongst the physical processes and models that have been theorized to explain the fundamental nature of bioeffects of weak MF on living organisms (Belyavskaya, 2004), the ferrimagnetism and the ion cyclotron resonance (ICR), together with the radical pair mechanism (RPM) appear to be the most suitable for trying to identify the WMF mode of action on plants.

On the one hand, the magnetite-based hypothesis predicts the existence of a mechanosensitive channel attached to a ferrimagnetic structure made of an iron oxide such as magnetite (Fe_3O_4) which is able to perceive MF (Winklhofer and Kirschvink, 2010). This conceptually simple idea is tenable since it is known that numerous species are able to form biogenic magnetite. The best examples are magneto-tactic bacteria, which generate a chain of intracellular magnetite crystals (Uebe and Schüler, 2016). They employ this internal compass needle to guide their swimming along the incline of the magnetic field vector to deeper waters with favorable redox conditions. Magnetite particles, which are ubiquitous in the animal kingdom, were reported to be absent in higher plants (Frankel, 1990). More recently, however, “botanical magnetite” has been detected in disrupted grass cell (Gajdardziska-Josifovska *et al.*, 2001). Investigations have even shown that phytoferritin occurs in plant cells as crystalline magnetite and hematite (McClean *et al.*, 2001).

On the other hand, the ion-cyclotron resonance (ICR) model assumes that Ca^{2+} ions moving helically along geomagnetic field flux lines are accelerated by cyclotron resonance generated

by an extremely low frequency (ELF) MF superposed on the GMF. This results in increased Ca^{2+} influx via calcium channels aligned with the GMF, thus altering equilibria of biochemical reactions(Sandweiss, 1990). However, the ICR model explains only the perception of ELF MF (around 50-60 Hz) that occurs during geomagnetic activity or that is induced by humans.
Alternatively, the radical pair mechanism (RPM) is one of the most reliable theories of biochemical responses to MF. RPM is indeed the only physically plausible mechanism by which the magnetic interactions that are ten orders weaker than the average thermal energy, k_BT, can affect the total chemical energy balance (Occhipinti, De Santis and Maffei, 2014). The basis of this theory lays in the fact that magnetic interactions with reactants are the only ones able to change the spin of electrons, whereas a chemical reaction is normally allowed only if the total spin of products is the same as that of reagents, following the law of the angular momentum conservation (Hore and Mouritsen, 2016). MF controls the singlet-triplet states (antiparallel and parallel electron spin respectively) of a radical pair population and, consequently, the reaction pathways and chemical reactivity (Messiha *et al.*, 2014; Buchachenko, 2016). The radical pair mechanism is known to be at the base of many phosphorylation dependent enzymatic processes, when mediated by magnetic nuclei (Buchachenko, 2016; Jones, 2016). Recently, because of its radical pair mechanism, cryptochrome has been identified as a probable magnetic compass in birds, which use the GMF as a direction for their migration (Wiltschko and Wiltschko, 2005). Cryptochromes are blue light photoreceptors that are present not only in animals, but also in plants. Thereby, the hypothesis of a cryptochrome-mediated MF perception in plants is more than plausible.

Arabidopsis thaliana cryptochromes as possible magneto-sensors

Cryptochromes are receptors for blue and UV-A light, that share sequence similarity to DNA photolyases. They are present in all eukaryotes and bacteria (not in Archaea) organs and tissues. There are three major subfamilies of cryptochromes: animal cryptochromes, plant cryptochromes and CRY-DASHes. CRY-DASH proteins may play a role in the repair of cyclobutene pyrimidine dimers, thus representing the only CRY family which has not lost DNA photolyase activity during evolution (Liu *et al.*, 2016). Differently, animal cryptochromes are a component of the circadian system that controls daily physiological and behavioral rhythms. Therefore, the observed influence of the GMF on animals' circadian clocks seems to be mediated by cryptochromes (Yoshii, Ahmad and Helfrich-Förster, 2009). Whereas, plant cryptochromes have a key role in photomorphogenic responses and photoperiodic flowering. *Arabidopsis thaliana* encodes three different CRYs: CRY1, CRY2, CRY3 (the last one is a CRY-DASH protein). CRY1 and CRY2 are blue-light photoreceptors that can exist as dimers. CRY1 is present both in the cytoplasm and in the nucleus, while CRY2 is localized predominantly in the nucleus. Arabidopsis cryptochromes possess two domains: a N-terminal photolyase-related (PHR) region and a C-terminal extension (CCE) domain. The CEE region is variable both in length and sequence: CRY1 and CRY2 are 180 and 110 amino-acid residues in length, respectively. This domain plays an important role in the rely of CRY signaling to downstream components. On the other hand, the PHR region has a highly conserved sequence composed by 500 amino acids folded in an α/β domain and a helical domain, which are connected by a variable loop that wraps around the α/β domain. PHR region is responsible of dimer formation and can bind two chromophores, flavin adenine dinucleotide (FAD) and pterin which acts as a secondary chromophore (Yang *et al.*, 2017). FAD is incorporated in the FAD-access cavity, it is not covalently bound, and it is free to interact with solvent. FAD cavities of CRY1 can also interact with an ATP analog. FAD can acquire interconvertible redox forms: FAD, FADH•, $FADH^-$ and FADH+. FAD is the resting state and is accumulated under long dark period. Only upon blue light FAD is converted in FADH•, leading cryptochrome to acquire its active signaling

form. Recently, a combination of quantum biology and molecular dynamics simulations on Arabidopsis cryptochrome isoform 1 has demonstrated that after photoexcitation an electron transfer from three tryptophan amino acids to FAD leads to the formation of a FADH• and Trp• radical pair in singlet state that can have a magnetic response even induced by a weak external magnetic field (Solov'yov, Chandler and Schulten, 2007; Kattnig, Solov'yov and Hore, 2016)

WMF influences the radical pair originated after Arabidopsis cryptochrome excitation

FADH• + Trp• lifetime is about 6 μs, a time frame long enough for possible interconversion and control of the overall spin state by an external magnetic field. Depending on its intensity, the external MF can differently interfere with the so-called hyperfine interaction of magnetic nuclei with the unpaired electron spins.

FADH• signal is quenched in two ways: (1) FADH• can absorb a second, blue-green, light photon and be converted to the fully reduced inactive form $FADH^-$ that under dark and aerobic condition is reverted back to the initial FAD state. (2) An electron back-transfer from FADH• to Trp•, leads to the formation of FADH+ that decays quickly to the fully oxidized FAD via deprotonation.

The MF control of the radical pair spin state leads to a cryptochrome magnetic response changing the kinetic of the first way and inhibiting the second way (which cannot occur in triplet state) (Solov'yov, Chandler and Schulten, 2007)(Figure 3). Despite the observed influence of WMF on the cryptochrome flavin-tryptophan radical pair, the occurrence of magnetic effects on plants could also be not exhibited dependently from this factor (Buchachenko, 2016). Actually, evaluating WMF influence on the processes downstream cryptochrome activation is the only way to assess whether cryptochromes are able to perceive WMF inducing a signal cascade in plants.

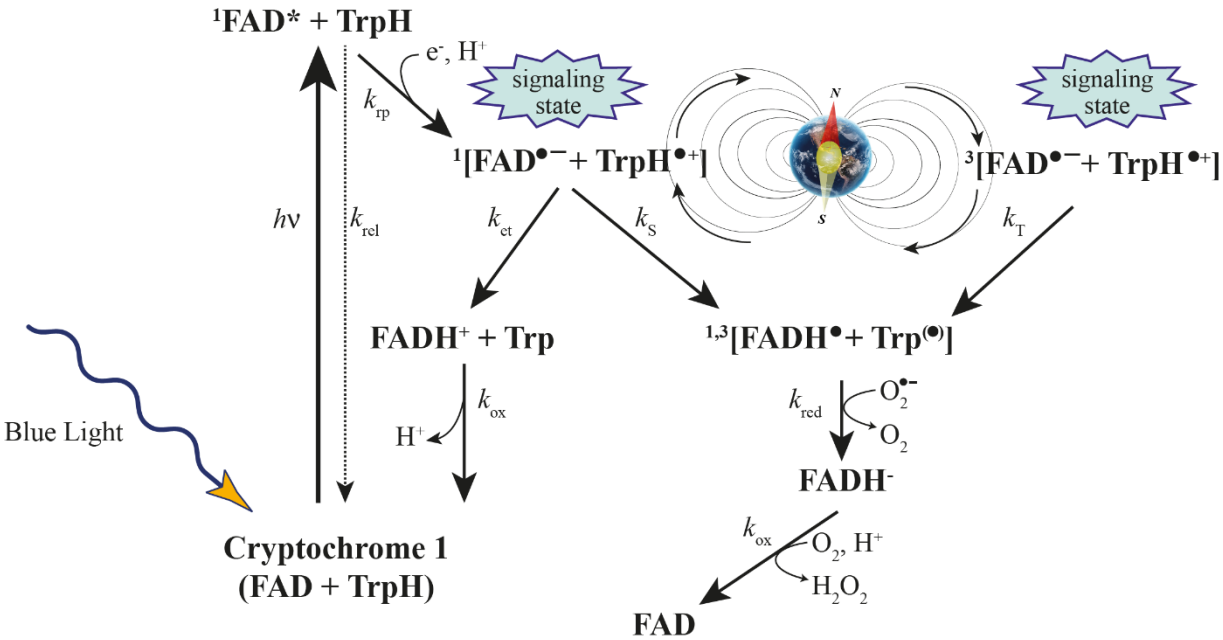

Figure 3: Blue light activates cryptochrome through absorbing a photon by the flavin cofactor. FAD becomes promoted to an excited FAD^* state and receives an electron from a nearby tryptophan, leading to the formation of the [FADH• + Trp•] radical pair, which exists in singlet $^{(1)}$ and triplet $^{(3)}$ overall electron spin states by coherent geomagnetic field-dependent interconversions. Under aerobic conditions, $FADH^•$ slowly reverts back to the initial inactive FAD state through the also inactive $FADH^-$ state of the flavin cofactor (Maffei, 2014).

Cryptochrome-related physiological responses in Arabidopsis and magnetic field (MF) influence

After CRY1 and CRY2 photoactivation by phosphorylation, their CCE domain acquires a negative charge thus allowing a conformational change of the closed dark-promoted CRY structure. The light- induced change in cryptochrome conformation is directly related to the signal transduction pathway downstream its activation. Cryptochromes regulate many biological processes such as the suppression of seedling stem growth, the de-etiolation of seedlings, chlorophyll and anthocyanin synthesis and the promotion of leaf and cotyledon expansion (known as photomorphogenic responses), the control of flowering time, the regulation of stomatal opening, the resetting of the circadian oscillator and the programmed cell death (Yang *et al.*, 2017). Along with cryptochromes, the red-light photoreceptors phytochromes (PHYs), the blue light LOV domain containing F box photoreceptors (ZEITLUPE (ZTL), FLAVIN-BINDING KELCH REPEAT F-BOX 1 (FKF1) and LOV-KELCH PROTEIN 2(LKP2)) and the blue light photoreceptors phototropins (PHOTs) mediate these processes dependently from light quality, quantity and intensity. To this aim, photoreceptors activate a complex signal network that approximately involves 30% of Arabidopsis genome (Ma *et al.*, 2001).
Amongst the photoreceptors- promoted processes, the resetting of the circadian time is directly linked to plant growth-promoting processes and flowering time (Shim, Kubota and Imaizumi, 2017). Indeed, the circadian clock controls the diurnal amplitude and phasing of a wide variety of rhythmic phenomena in plants (e.g., flowering time, hypocotyl expansion and gene expression).

Circadian clocks are endogenous and self-sustaining timekeeping networks, thus able to persist as free rhythms under constant environmental conditions (such as constant light or dark, and constant temperature) (Nohales and Kay, 2016). The circadian clock is composed by three interlocked loops differently expressed during the day. The morning loop is composed by CIRCADIAN CLOCK ASSOCIATED 1 (CCA1) and LATE ELONGATED HYPOCOTYL 1 (LHY) that activate PSEUDO-RESPONSE REGULATOR 7 (PRR7) and PSEUDO RESPONSE REGULATOR 9 (PRR9) which in turn repress the MYB transcription factors. The central loop is composed by CCA1 and LHY that repress transcription of the evening expressed genes *TIMING OF CAB EXPRESSION 1* (*TOC1*) and *GIGANTEA* (*GI*) instead. On the opposite, TOC1 and GI activates transcription of *LHY* and *CCA1* (Fornara, de Montaigu and Coupland, 2010; Nohales and Kay, 2016). Three additional evening clock proteins (EC) associate into a hub and maintain the repression of morning and evening oscillator components. This complex comprises LUX ARRYTHMO (LUX), a MYB like GARP transcription factor, and EARLY FLOWERING 3 (ELF3) and EARLY FLOWERING 4 (ELF4), two unrelated plant specific proteins. The EC components are repressed by CCA1 and LHY in the morning and by TOC1 in the evening, and mutation of any of the components results in arrhythmia (Nohales and Kay, 2016). Circadian rhythms are characterized by an amplitude which is the extent of an oscillatory movement, a phase which is the instantaneous state of an oscillation within a period, and a period which is the time taken for a complete oscillation to take place. Light and temperature can be called zeitgebers (ZT, “time giver”) because of their capability to reset circadian rhythms, modifying the period length from the free run period to the 24 h under normal Light/Dark (LD) or temperature cycles (Más, 2005). In particular, light can modulate the expression of several clock genes at many levels and at different time of the day (Harmer, 2009) (Figure 4). The response to light can be gated by the clock itself, since *PHY*s and *CRY*s transcription as well as *FKF1* expression are clock regulated (Hall *et al.*, 2001; Shim, Kubota and Imaizumi, 2017). Some photoreceptors can directly interact with clock components (Song *et al.*, 2014) or with light-signaling intermediates such as the PHYTOCHROME INTERACTING FACTORS (PIFs), which are bound to

the promoters of light responsive genes including *CCA1* and *LHY* and mediate the photomorphogenesis process (Martinez-Garcia, Huq and Quail, 2000). CONSTITUTIVELY PHOTOMORPHOGENIC 1 (COP1) interaction with the CRYs has been linked with the protein regulation of GI (Xu, Zhu and Deng, 2016) and is essential for both the flowering and the photomorphogenesis process. The main function of COP1/SPA complexes is to target CONSTANS (CO) and HYPOCOTYL ELONGATION 5 (HY5) for ubiquitination, and their eventual degradation (Osterlund *et al.*, 2000; L. J. Liu *et al.*, 2008). CRY1 and CRY2 photoactivation allows the binding with COP1/SPA complexes, inactivating them (Sarid-Krebs *et al.*, 2015).

Regarding flowering time, CRY1 and CRY2 gene expression regulating mechanism is mostly linked to CONSTANS (CO), a key transcription factor known for promoting the expression of the florigen (*FLOWERING LOCUS T (FT*)) under LD conditions (Fornara, de Montaigu and Coupland, 2010). CRY2 can also bind CRYPTOCHROME-INTERACTING BASIC HELIX- LOOP-HELIXs (CIBs), a group of proteins that directly promote flowering, by inducing *FT* expression (Yang *et al.*, 2017). Blue light LOV domain containing F box photoreceptors also promote flowering by enhancing CO protein and *CO* and *FT* transcript level. In particular, FKF1 and GI together promotes the degradation of CYCLING DOF FACTOR (CDF), which are *CO* repressors. Moreover, it is the coincidence between the circadian rhythms of *CO*, *GI* and *FKF1* and exposure to light under long days that determines whether CO is stabilized to promote flowering (Song *et al.*, 2014). Differently, PHYB is known to reduce CO level under red light, while PHYA promotes flowering by stabilizing CO level under far red light such as the complex composed by PHYA, CRY1 and CRY2 under blue light conditions (Sánchez-Lamas, Lorenzo and Cerdán, 2016) (Figure 4). Along with the photoperiod pathway, which is located in the vasculature, photoreceptors, in particular phytochromes, are also able to interact with other flowering pathways, such as the vernalization and the gibberellin ones (Endo, Araki and Nagatani, 2016). Therefore, the flowering control time is a complex process that is not only influenced by light perception and wavelength, but also other environmental variables, such as temperature changes, are able to interfere (Fornara, de Montaigu and Coupland, 2010).

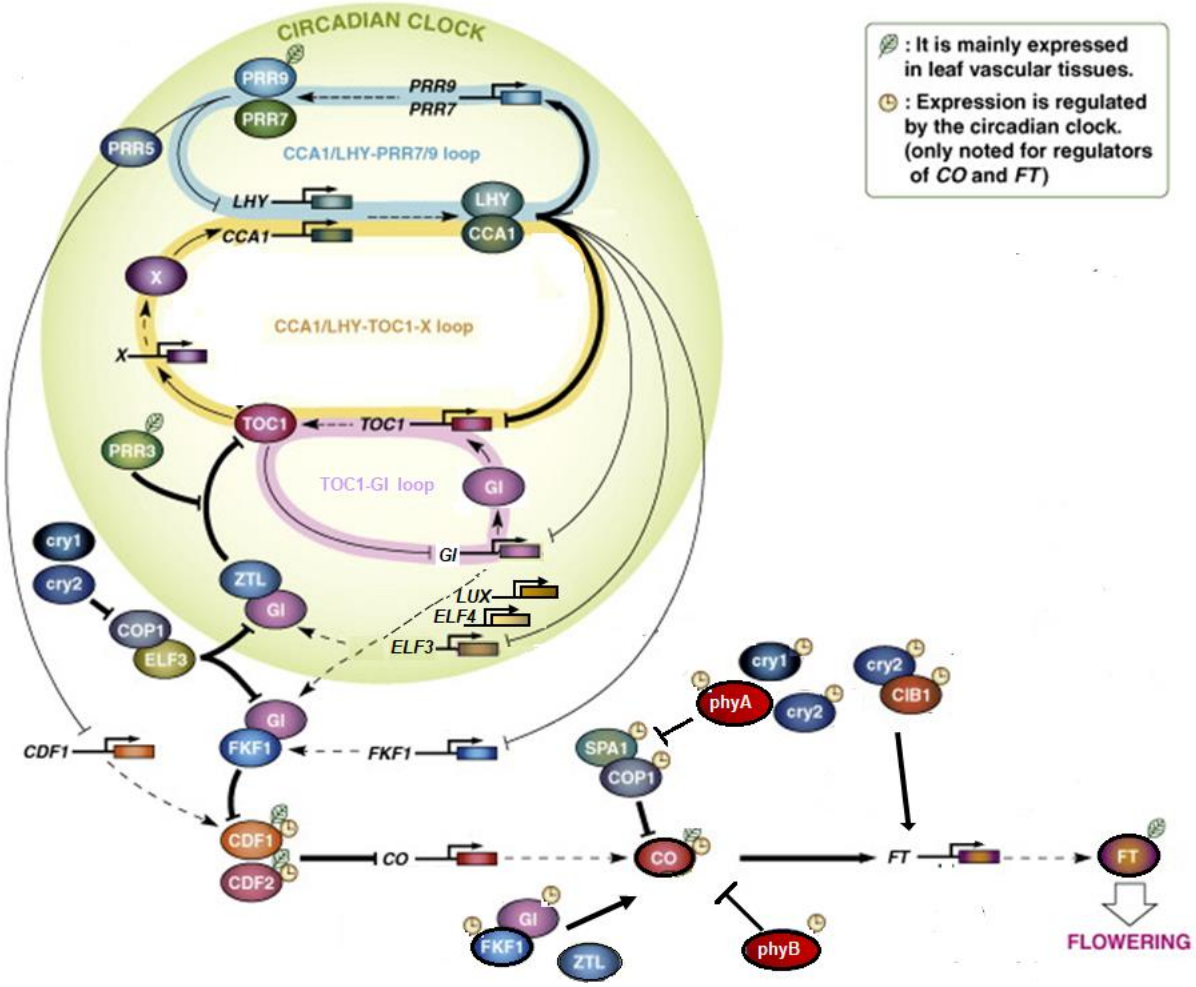

Figure 4: Clock and photoperiod dependence of flowering time induction mechanism. The diagram that is outside the pale green circle area denotes the clock-regulated photoperiodic pathway. Oval symbols depict proteins and overlapping ovals indicate protein complexes. Thick solid lines denote direct physical interactions, while thin solid lines denote genetic interactions. The dotted lines depict transcription and translation. Adapted from Imaizumi, 2010.

Like flowering induction, the photomorphogenic response is known to be based on convergence mechanisms, including photoreceptor interactions, direct signal convergence on common intermediates and indirect signal convergence on transcription factors known to promote photomorphogenesis when the COP1/SPA ubiquitination activity is silenced under light (Usami *et al.*, 2004). The photoactivated CRY2 and in particular CRY1 are known to reduce the COP1/SPA promoted degradation of the key transcription factor HY5, which directly promotes the transcription of genes connected to the photomorphogenic response, such as genes connected to anthocyanin synthesis (i.e. *CALCONE SHYNTASE, CHS*) and directly related to auxin signaling (Lee *et al.*, 2007). CRY1 and CRY2 are also known to interact with PIFs, a class of transcription factors involved in many plant light-mediated responses, including the repression of the de-etiolation response (Yang *et al.*, 2017). Phytochromes (PHYA and PHYB) are able to directly interfere with the COP1/SPA complex and PIF degradation both under blue and red light (Tsuchida-Mayama *et al.*, 2010). Last but not least, PHOT1 can contribute to de-etiolation processes, by affecting hypocotyl growth in the absence of a functional cryptochrome (Lin, 2002) and by promoting a very early hypocotyl initial growth inhibition 30 s after blue light exposure (Kang *et al.*, 2008).

MF intensities affect cryptochrome dependent responses in a controversial manner

Experiments on Arabidopsis have suggested that magnetic intensity affects light and cryptochrome-dependent growth responses, i.e. by influencing flowering time, hypocotyl growth and anthocyanin accumulation (Ahmad *et al.*, 2007; Xu *et al.*, 2012). In particular, near null MF delays Arabidopsis flowering time with respect to GMF conditions under a LD photocycle, affecting *CO*, *FT* and *PHYB* expression (Xu *et al.*, 2012). On the one hand, the NNMF-induced flowering delay appears to be mediated by cryptochrome (Xu *et al.*, 2015) and its associated changes in the auxin (Xu *et al.*, 2018) and gibberellin (Xu *et al.*, 2017) signaling pathways under 6 h 10 µmol/$m^{-2}sec^{-1}$ blue light/ 6h dark photocycle. On the other hand, cryptochrome-mediated MF effects on plant early growth stages are often contradictory and seldom reproducible (Maffei, 2014). Under LD conditions, hypocotyl growth appears to be reduced under a near-null magnetic field with respect to GMF condition (Xu *et al.*, 2012). Ahmad *et al*. (2007) showed that a 500 µT MF enhances hypocotyl growth inhibition as well as anthocyanin accumulation under continuous blue light in a cryptochrome dependent manner. However, under the same experimental conditions, Harris *et al.* (2009) did not observed any MF-mediated influence on hypocotyl lengths, anthocyanin accumulation and the expression of cryptochrome-cascade related genes (*CHS* and *HY5*). Therefore, although a modification of the activated state of cryptochromes has been demonstrated under MF higher or weaker than the local GMF in terms of changes in both their phosphorylation and degradation status (Ahmad *et al.*, 2007; Xu *et al.*, 2014), the involvement of cryptochrome in Arabidopsis magneto-reception mechanism and its actual role in mediating the signal cascade connected to GMF perception is still unclear.

AIMS AND STRUCTURE OF THE THESIS

As mentioned above, the GMF is known to affect plant growth usually in a specie-specific manner and its variation in intensity and polarity could be eventually related to Angiosperm evolution. Despite the plethora of studies on MF higher than the Earth's MF, a lower number of research works focus on Near Null MF effects on plants, whereas the influence of GMF polarity on plant growth has never been investigated so far. NNMF-induced delay in Arabidopsis flowering appears to be a key point to correlate the occurrence of Angiosperm speciation to the GMF polarity, since the reduction of GMF during its reversals could have affected the rate of plant reproduction. Despite the observed cryptochrome-mediated flowering delay under blue light in the absence of MF, the effect of NNMF on Arabidopsis flowering time under LD white light conditions has not been exhaustively investigated so far. Therefore, this observation, together with the contradictory results related to MF-influence on plant processes mediated by cryptochrome reported in literature, suggests that the exclusive role of cryptochrome as magnetoreceptor has to be further investigated. Last but not least, although the GMF can influence animals' circadian clock since cryptochrome is a component of the endogenous clock in animals, the effect of the GMF on plants' circadian clock has not been investigated so far.

Considering this background, the main aims of this work are:

- to corroborate the hypothesis of GMF involvement in plant evolution, considering its effect on plant growth under different GMF polarity and in NNMF conditions;
- to further investigate the mechanism of GMF sensing in plants by:
    - discriminating the gene pathways that seem to be mostly affected by the absence of the GMF in the flowering process, in order to deepen in the molecular bases of NNMF-induced flowering delay and thus better knowing the response downstream the GMF sensing.
    - ascertaining the light-dependence of the response to the GMF and the level of cryptochrome involvement in this process, using photomorphogenesis as the analysed process.
    - evaluating the possible GMF influence on the internal clock rhythm.

The breakdown structure of this thesis is organized in four main actions.
In the first, the different Arabidopsis response to normal and reverse magnetic field has been assessed in roots and leaves separately, both from a morphological and gene expression point of view.
The second is focused on the molecular basis of NNMF-induced delay in Arabidopsis flowering under LD conditions analysed by evaluating NNMF-induced changes on the expression of all the key rosette and flowering meristem gene pathways in a time course experiment. Considering the complexity of the flowering induction process and the different pathways involved in its promotion, focusing on the NNMF-dependent regulation of the flowering gene expression could be a key point for assessing the events downstream GMF perception.
In the third, the light-dependent response to the GMF has been explicated analyzing Arabidopsis photomorphogenic response at the shoot and root level. Photoreceptor contribution to Arabidopsis response to the GMF has been discriminated using both biomolecular and immunoblotting approaches on wild type and photoceptor mutant lines.
In the fourth, attention has been particularly given to Arabidopsis clock genes, whose expression has been further investigated in a time course experiment in presence and in absence of GMF to verify whether the GMF affects the endogenous clock period and amplitude.

MATERIAL AND METHODS

Plant material and growth conditions

In vitro *studies*

For the reversal GMF experiment*, Arabidopsis thaliana* ecotype Columbia 0 (Col 0) wild type (WT) seeds were surface sterilized with 70 % v/v ethanol for 2 min and then with 5% w/v calcium hypochlorite for 5 min. After 3 to 4 washes with sterile water, seeds were sown on the surface of sterile agar plates (12x12 cm) containing half-strength Murashige and Skoog (MS) medium (Murashige and Skoog, 1962). Plates were vernalized for 48 h and then exposed vertically under a homogenous and continuous white light source at 120 µmol m^{-2} s^{-1} and 21°C (±1.5) for 24 h to induce germination. WT seedlings were transferred in the same laboratory and at the same time, either under a reversed GMF produced by the triaxial Helmholtz coils or at natural GMF conditions and exposed to long-day (16 h/8 h) 150 µmol m^{-2} s^{-1} white light for 10 days.

For photomorphogenic studies, *Arabidopsis thaliana* ecotype Col 0 WT, *cry1cry2*, *phyA*, *phyAphyB* and *phot1* mutant seeds were surface sterilized and vernalized as mentioned earlier. After the germination induction, seedlings were kept in the darkness at room temperature for 72 h. Plates were then transferred, in the same laboratory and at the same time, either under the NNMF produced by the triaxial Helmholtz coils or at natural GMF conditions and exposed to different light regimes for a variable time, depending on the set of the experiment.
For gene expression experiments, WT seedlings were exposed for 72 h to different light regimes, depending on the set up of the experiment: (i) 16-8 h light/darkness photoperiod (white light 150 µmol m^{-2} s^{-1}), (ii) continuous darkness, (iii) 150 µmol m^{-2} s^{-1}continuous white light; differently, WT seedlings along with *cry1cry2, phyAphyB* and *phot1* were exposed for 72 h to (iv) 20 µmol m^{-2} s^{-1} continuous blue light, and (v) 60 µmol m^{-2} s^{-1} continuous red light.
For immunoblotting analysis, different exposure times and light fluences were adopted to selectively verify photoreceptor activation. To monitor differences in CRY2 degradation, WT, *phyA* and *phyAphyB* plants were exposed to 0.5 µmol m^{-2} sec^{-1} blue light for 8 h. A blue light fluence different from the one used in gene expression experiments was applied, since PHYA appears to mediate CRY2 degradation under low blue light fluences according to Weidler *et al.* (2012). To evaluate the phosphorylation level of CRY1 and PHOT1, 20 µmol m^{-2} sec^{-1} blue light was used to irradiate WT, *phot1, cry1cry2* and *phyAphyB* seedlings for 15 minutes. To check the possible influence of the GMF on PHYA and PHYB degradation, WT, *cry1cry2* and *phot1* plants were exposed under 60 µmol m^{-2} sec^{-1} red light for 3 h and 9 h, respectively.

For the clock experiment, *Arabidopsis thaliana* ecotype Col 0 WT seeds were sterilized and vernalized as mentioned before. After the germination induction, seeds were exposed to 150 µmol m^{-2} s^{-1} white light (16 h light/ 8 h dark) for 7 days. Treated plates were then transferred at ZT (dawn) under the triaxial Helmoltz coils system, whereas control plates were kept under GMF conditions. Half of the plates were maintained under LD white light conditions, while the others were kept in the darkness. All the treatments lasted 4 days. To guarantee the material collection every 4 hours after the treatment, every replicate was divided in two experimental settings.

In vivo *studies*

For the flowering experiment*, Arabidopsis thaliana* ecotype Col 0 WT and *cry1cry2* seeds were sown in 8 cm diameter polyethylene pots filled with soil prepared with a mixture of peat and vermiculite (2:1) and exposed to homogenous irradiation for 16 h at 200 µmol m^{-2} s^{-1}, at 21°C

(±1.5°C) under GMF control and NNMF treatment conditions (triaxial Helmoltz coils system). All plants were grown until full bloom and WT plants were used for gene expression analyses.

WT plants were also kept in the triaxial coils for seed collection and seeds were re-sown in the triaxial coils for three generations. WT seeds from plants growing inside the GMF control system were collected and kept in small Petri dishes under NNMF conditions. These seeds (F1 WT NNMF) were sown in pots as described above and plants were allowed to grow until full bloom. Seeds of F1 WT NNMF (called F2 WT NNMF) were then kept in Petri dishes under NNMF conditions and sown in pots in order to obtain a third generation of plants experiencing NNMF conditions. These plants were then exposed to GMF conditions.

GMF control system

In order to reverse the GMF polarity or to reduce the GMF, an octagonal triaxial Helmholtz coils (THC) system was used (Figure 5). This system is able to compensate the GMF in all three space dimensions with an exceptional time-stability and homogeneity and its coils shape and dimension allow to obtain a spherical volume (25 x 25 x 25 cm^3) of GMF compensation sufficient for plant growth experiments, hosting several Petri plates or small pots. The coil diameter (CD) and the separations between the Helmholtz coils (SH) are the following: X, CD = 128 cm, SH = 55 cm; Y, CD = 150, SH = 67; Z, CD = 135, SH = 59.
Each coils pair was connected to a DC power supply (dual range: 0-8V/5A and 0-20V/2.5A, 50W), which is controlled from a computer via a GPIB connection. A Bartington Mag-03 three-axis magnetometer probe, which was connected to the same computer, was inserted in the middle of the THC. The real-time measure of $\mathbf{B_{x,y,z}}$, at the probe position was done, collecting 10 s interval data which were transformed in total B by a software (VEE, Agilent Technologies) using the following equation:

$$B = \sqrt{B_x^2 + B_y^2 + B_z^2}$$

After using the values reported by the software to know the actual value of the GMF, the voltage of the power supplies was manually set in order to obtain a vector able to reverse or reduce the GMF. A constant compensation of the GMF was achieved by a continuous control of magnetic field values through reading of magnetometer values and voltage compensation. To obtain a reversed phase GMF, after calculating the orientation of a field with the same strength and same vertical component of the GMF, the voltages of the power supplies were set to generate a new field with the same magnitude as the GMF but with an inverse polarity. To reduce the GMF values to NNMF, the DC power supplies voltages were set in order to obtain a current able to compensate the GMF values, thus producing a field strength of 40 nT (1000 times less than the GMF intensity).

To rule out potential subtle heating or vibrational effects either from the coils themselves or from the electronics used to control the coils, Sham exposure experiments were performed. The field was kept equal to that of the GMF but the direction (i.e. “North, East or West”) of the horizontal component of the field was altered with equal currents in the triaxial coils compared to the field reversal or NNMF condition by altering the voltage of the coils.

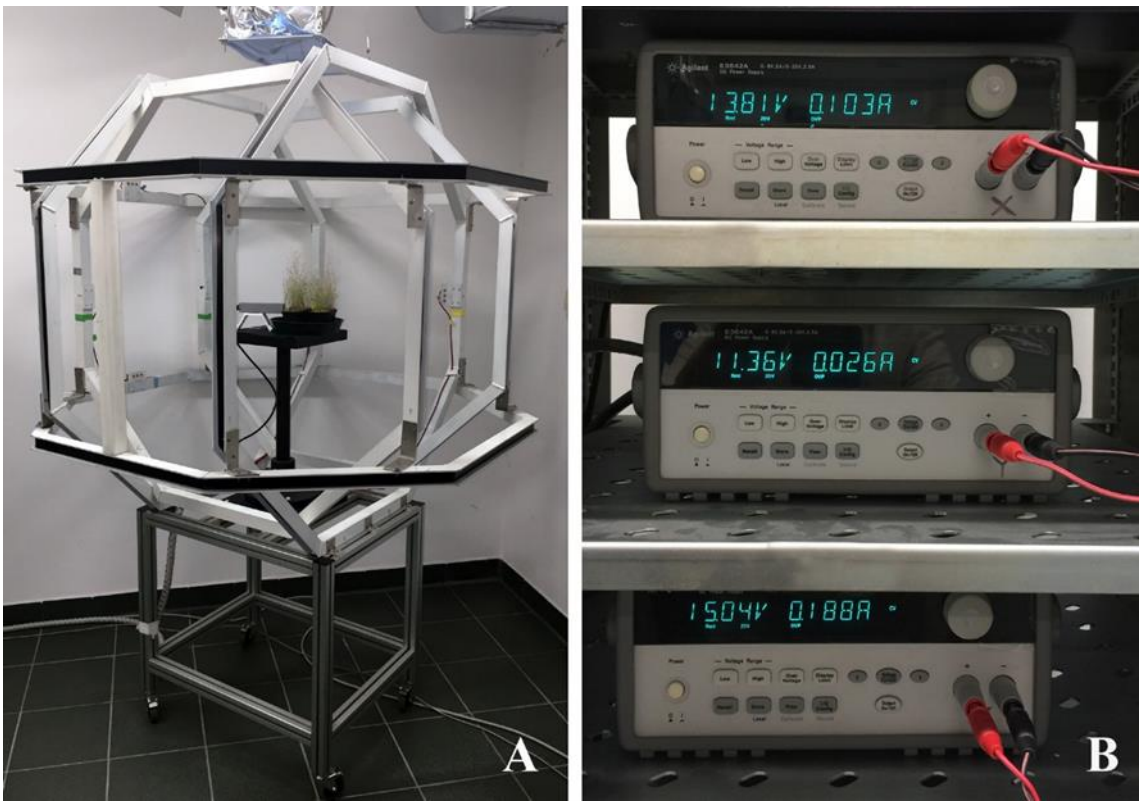

Figure 5: A) Triaxial Helmholtz coil system used in this work. B) Computer controlled power supply system.

Light sources

Under both GMF and NNMF conditions, white light was provided by a high-pressure sodium lamp source (SILVANIA, Grolux 600W, Belgium) using a gelatin film for spotlight to reduce the red component of lamps, whereas red light by an array of LEDs (SUPERLIGHT, Ultra bright LED, λ 645-665 nm, peak emission at 655 nm) and blue light by an array of LEDs (SUPERLIGHT, Ultra bright LED, λ 465-475 nm, peak emission at 470 nm).

Continuous darkness exposed plates were kept in paper boxes internally covered by a black cardboard.

Morphological analysis

For the reversal GMF experiment, pictures of Petri dishes were taken after 10 days exposure to the treatment. The ImageJ software was used to calculate root length and leaf area.

For the photomorphogenic studies, plates were photographed just before being sampled. All plate images were used to measure hypocotyl and root lengths. Image analysis was performed using ImageJ software.

For the flowering experiment, pictures were taken for the first generation of plants and the phenotypic parameters (leaf area index and stem length) were analysed by ImageJ and then plotted as a function of time. The days to flowering for all the plant generations as well as the rosette leaf number at flowering time were also calculated. The occurrence of all the reproductive phenological phases of plants, even along the generation experiment, was expressed in terms of days after sowing (DAS).

Gene expression analysis

Plant material collection

For the reversal GMF experiment, Arabidopsis roots and leaves were separately collected exactly 10 days after each treatment, immediately frozen in liquid N_2 and kept at -80°C for

further analysis. Thirty mg of frozen leaves and 10 mg of frozen roots were used for RNA extraction.
For the photomorphogenic studies, Arabidopsis shoots and roots were separately harvested in liquid nitrogen after 72 h treatment. Thirty mg of frozen shoots and 10 mg of frozen roots were used for RNA extraction.
For the flowering experiment, rosette leaves and floral meristems from WT plants growing in GMF and NNMF conditions were collected at noon (6 hours after ZT, dawn) and immediately frozen in liquid nitrogen. The plant material collection lasted from 17 DAS to 28 DAS for the rosette, whereas from 21 to 30 DAS for the meristem. Fifty mg of frozen leaf material and 10 mg of frozen meristems were used for RNA extraction.
For the clock experiment, 20 Arabidopsis seedlings were harvested in liquid nitrogen every 4 hours since the treatment beginning and then used for RNA extraction.

RNA isolation and cDNA synthesis

Total shoot, leaf rosette and seedling RNA was isolated using the Agilent Plant RNA Isolation Mini Kit (Agilent Technologies, Santa Clara, CA, US), whereas total root and meristem RNA was isolated using the RNAeasy Micro Kit (Qiagen, Hilden, Germany), following manufacturer's protocols. RNA quality was checked by using the RNA 6000 Nano kit and the Agilent 2100 Bioanalyzer (Agilent Technologies) in accordance with manufacturer's instructions. Whereas, RNA quantity was verified spectrophotometrically by using a NanoDrop ND-1000 (Thermo Fisher Scientific, Waltham, MA, US).
cDNA was synthesized starting from 1 µg of RNA using the High Capacity cDNA Reverse Transcription kit (Applied Biosystem, Foster City, CA, US), following manufacturer's recommendations.

Quantitative real time-PCR (qPCR)

The qPCR experiments were run on a Stratagene Mx3000P Real-Time System (La Jolla, CA, USA) using SYBR green I with ROX as an internal loading standard. The reaction mixture was 10 µL, containing 5 µL of 2X Maxima^{TM} SYBR Green qPCR Master Mix (Fermentas International, Inc, Burlington, ON, Canada), 0.6 µL of 1:5 diluted cDNA (for roots and meristems) and 0.6 µL of 1:10 diluted cDNA (for shoot, rosette leaves and seedlings) and 300 nM primers (Integrated DNA Technologies, Coralville, IA, US). Non-template controls (water template) were included. Primers were designed using Primer 3.0 software (Rozen and Skaletsky, 2000) (Table 1).
Four different reference genes *ACTIN1* (*ACT1*, At2g37620); *CYTOPLASMIC GLYCERALDEHYDE-3-PHOSPHATE DEHYDROGENASE* (*GAPC2, At1g13440*); *ELONGATION FACTOR 1B ALPHA-SUBUNIT 2* (*eEF1Balpha2*, At5g19510); *UBIQUITIN SPECIFIC PROTEASE 6* (*UBP6*, At1g51710) were selected for all the experiments. The following qPCR conditions were used: *ACT1*, *GAPC2, UBP6*: 10 min at 95°C, 45 cycles of 15 s at 95°C, 20 s at 57°C, and 30 s at 72°C, 1 min at 95°C, 30 s at 55°C, 30 s at 95°C; *eEF1Balpha2*: 10 min at 95°C; 45 cycles of 15 s at 95°C, 30 s at 57°C, and 30 s at 72°C; 1 min at 95°C, 30 s at 55°C, 30 s at 95°C. The best of the four genes was selected using the Normfinder software; the most stable gene was always *eEF1Balpha2.*
In the reversal experiment, the following genes were analysed: *ASCORBATE PEROXIDASE1* (*APX1*, At1g07890), *CRUCIFERIN 3* (*CRU3*, At4g28520), *CATALASE3* (*CAT3*, At1g20620), *COPPER TRANSPORT PROTEIN1* (*COPT1,* At5g52760), *FE SUPEROXIDE DISMUTASE 1 (FeSOD1*, At4g25100), *NADPH/RESPIRATORY BURST OXIDASE PROTEIN D (RbohD*, At5g47910), *REDOX RESPONSIVE TRANSCRIPTION FACTOR1* (*RRTF1,* At4g34410), and *THYLAKOIDAL ASCORBATE PEROXIDASE* (*TAPX,* At1g77490). Specifically, qPCR conditions were the following: *CRU3*, *COPT1*, *RRTF1*: 10 min at 95°C, 40 cycles of 15 s at 95°C, 30 sec at 58°C, and 30 sec at 72°C; 1 min at 95°C, 30 s at 55°C, 30 s at 95°C; *APX1*, *CAT3*, *FeSOD1, RbohD*, *TAPX*: 10 min at 95°C, 40

cycles of 15 s at 95°C, 20 sec at 57°C, and 30 sec at 72°C; 1 min at 95°C, 30 s at 55°C, 30 s at 95°C.

In the photomorphogenic studies, the following genes were analysed: *ANTHOCYANIDIN SYNTHASE* (*ANS*, At4g22880), *CHALCONE SYNTHASE* (*CHS*, At5g13930); *CONSTANS* (*CO*, At5g15840); *GLUTATHIONE S-TRANSFERASE (GST*, At1g1037); *ELONGATED HYPOCOTYL 5 (HY5*, At5g11260); *HY5-HOMOLOG (HYH*, At3g17609); *LONG AFTER FAR-RED LIGHT 1* (*LAF1;* At4g25560); *NUCLEOSIDE DIPHOSPHATE KINASE 2 (NDPK2*, At5g63310); *PHYTOCHROME INTERACTING FACTOR 3* (*PIF3,* At1g09530); *PIN-FORMED 1 (PIN1*, At1g73590); *PIN-FORMED 3 (PIN3*, At1g70940); *PHYTOCHROME KINASE SUBSTRATE 1 (PKS1*, At2g02950). Specifically, qPCR conditions were the following: *ANS, CHS, CO, LAF1, NDPK2, PIF3, PIN1, PIN3, PKS1*: 10 min at 95°C, 45 cycles of 15 s at 95°C, 20 s at 57°C, and 30 s at 72°C, 1 min at 95°C, 30 s at 55°C, 30 s at 95°C; *GST*:10 min at 95°C; 45 cycles of 15 s at 95°C, 20 s at 59°C, and 30 s at 72°C; 1 min at 95°C, 30 s at 55°C, 30 s at 95°C; *HYH*:10 min at 95°C; 45 cycles of 15 s at 95°C, 20 s at 58°C, and 30 s at 72°C; 1 min at 95°C, 30 s at 55°C, 30 s at 95°C; *HY5*:10 min at 95°C; 45 cycles of 15 s at 95°C, 20 s at 56°C, and 30 s at 72°C; 1 min at 95°C, 30 s at 55°C, 30 s at 95°C.

In the flowering experiment, the following genes were analysed: *AGAMOUS-LIKE 24* (*AGL24*, At4g24540); *APETALA1* (*AP1*, At1g69120); *CIRCADIAN CLOCK ASSOCIATED 1* (*CCA1,* At2g46830); *CONSTANS* (*CO*, At5g15840); *ATBZIP14* (*FD*, At4g35900*); FLAVIN-BINDING KELCH REPEAT F-BOX 1* (*FK*F1. At1g68050); *FLOWERING LOCUS C* (*FLC*, At5g10140); *FRIGIDA* (*FRI*, At4g00650); *FLOWERING LOCUS T* (*FT*, At1g65480); *GIBBERELLIN 2-OXIDASE 1* (*GA2ox1*, At1g78440); *GIBBERELLIN 20-OXIDASE1* (*GA20ox1*, At4g25420); *GIBBERELLIN 20 OXIDASE2* (*GA20ox2*, At5g51810); *GIGANTEA* (*GI*, At1g22770); *JMJC DOMAIN-CONTAINING HISTONE DEMETHYLASES 14* (*JMJ14*, At4g20400); *LEAFY* (*LFY*, At5g61850,); *LATE ELONGATED HYPOCOTYL* (*LHY*, At1g01060); *NAC TRANSCRIPTION FACTOR 50* (*NAC050*, At3g10480); *NAC TRANSCRIPTION FACTOR 52* (*NAC052*, At3g10490); *SET DOMAIN GROUP 26* (*SDG26*, At1g76710); *SUPPRESSOR OF OVEREXPRESSION OF CONSTANS 1* (*SOC1*, At2g45660); *SHOOTMERISTEMLESS* (*STM*, At1g62360,); *SHORT VEGETATIVE PHASE* (*SVP*, At2g22540); *TERMINAL FLOWER1* (*TFL1*, At5g03840); *TIMING OF CAB 1* (*TOC1*, At5g61380); *TWIN SISTER OF FT* (*TSF*, At4g20370); *WUSCHEL* (*WUS*, At2g17950). For all the genes the qPCR conditions were the following: 10 min at 95°C, 45 cycles of 15 s at 95°C, 20 s at 57°C, and 30 s at 72°C, 1 min at 95°C, 30 s at 55°C, 30 s at 95°C.

In the clock experiment, the following gene were analysed: *LATE ELONGATED HYPOCOTYL* (*LHY*) and *PSEUDO-RESPONSIVE REGULATOR 7* (*PRR7*). The qPCR conditions were the following: 10 min at 95°C, 45 cycles of 15 s at 95°C, 20 s at 57°C, and 30 s at 72°C, 1 min at 95°C, 30 s at 55°C, 30 s at 95°C.

Fluorescence was read following each annealing and extension phase. All runs were followed by a melting curve analysis from 55°C to 95°C. The linear range of template concentration to threshold cycle value (Ct value) was determined by preparing a dilution series, using cDNA from three independent RNA extractions analysed in three technical replicates. Primer efficiencies for all primer pairs were calculated using the standard curve method. All amplification plots were analysed with the Mx3000P^{TM} software to obtain Ct values. Relative RNA levels were calibrated and normalized with the level of *eEF1Balpha2* mRNA (Pfaffl, 2001).

Table 1: Primers used in this work

Gene Code	Gene	Forward primer (5'-3')	Reverse primer (5'-3')
REFERENCE GENES			
At2g37620	*ACT1*	TGCACTTCCACATGCTATCC	GAGCTGGTTTTGGCTGTCTC
At5g19510	*eEF1Balpha2*	ACTTGTACCAGTTGGTTATGGG	CTGGATGTACTCGTTGTTAGGC
At1g13440	*GAPC2*	TCAGGAACCCTGAGGACATC	CGTTGACACCAACAACGAAC
At1g51710	*UBP6*	GAAAGTGGATTACCCGCTG	CTCTAAGTTTCTGGCGAGGAG-
REVERSED GMF EXPERIMENT TARGET GENES			
At1g07890	*APX1*	GAAGTTACTGGTGGCCCTGA	AGAGGGTTTGATGTCCATGC
At1g20620	*CAT3*	TCACATGGTGCTGGATGTTT	GGGTAGTTGCCAGATGCAAT
At5g52760	*COPT1*	CCGTTTCTCGATTTTCAGGA	GCTGGTTTCTCAGGTTCAGG
At4g28520	*CRU3*	CTCTAAGACAGCCCTACGAGAG	CTCTAAGACAGCCCTACGAGAG
At4g25100	*FeSOD1*	TGGAGGAAAACCATCAGGAG	GGATTCACAGCATTGGGAGT
At5g47910	*RbohD*	CCTATGAGCCGATGGAAAAA	TACCAAAAGGCGTTGAAACC
At4g34410	*RRTF1*	CTCAACTTCCCCTTTGTGGA	CTCAACTTCCCCTTTGTGGA
At1g77490	*TAPX*	TGGAGAAGCAGGAGGACAGT	GCAGCCACATCTTCAGCATA
PHOTOMORPHOGENIC EXPERIMENT TARGET GENES			
At4g22880	*ANS*	CTAACAACGCGAGTGGACAA	ACCGACAGAGAGAGCCTTGA
At5g13930	*CHS*	GGCTCAGAGAGCTGATGGAC	CATGTGACGTTTCCGAATTG
At5g15840	*CO*	ATTCTGCAAACCCACTTGCT	CCTCCTTGGCATCCTTATCA
At1g10370	*GST*	AACCGGTGAGTGAGTCCAAC	AGCGACAAACCACTTTTCGT
At3g17609	*HYH*	TGATGAGGAGTTGTTGATGG	TGTTGCGCTGATACTCTGTT
At5g11260	*HY5*	ATCAAGCAGCGAGAGGTCAT	ATCAAGCAGCGAGAGGTCAT
At4g25560	*LAF1*	ATGGCGAAGACGAAATATGG	ATGGCGAAGACGAAATATGG
At5g63310	*NDPK2*	TCCGTCTTTTCTCTCGCAAT	TGCTCCTCAGCCAATTCTTT

At1g09530	*PIF3*	GACTATGGTGGACGAGATCCCTAT	GACAGTAACAGGAGACGACACATC
At1g73590	*PIN1*	AACCACCACGCCGAATTACTC	CACCGTCCGTTGCCAATACT
At1g70940	*PIN3*	GCCGAAGCAAGTCAACGAAA	AGCGACGAGAGCCCAAATAA
At2g02950	*PKS1*	TTGGTGTGTTTGGAGCTGAG	TTGGTGTGTTTGGAGCTGAG
FLOWERING EXPERIMENT TARGET GENES			
At4g24540	*AGL24*	GCGGCTGGAGAAACTACTTG	GCCTCTTTAAGCGTCGTCAG
At1g69120	*AP1*	GCAAGCAATGAGCCCTAAAG	AAGCATGCTGTTTTGCTCCT
At2g46830	*CCA1*	TCAGAAAGGCAAGAGGATGG	ATTCGACCCTCGTCAGACAC
At5g15840	*CO*	ATTCTGCAAACCCACTTGCT	CCTCCTTGGCATCCTTATCA
At4g35900	*FD*	CATCACCTCTCAAACGCTCA	GGAACGAGCTGCAGATTCTC
At1g68050	*FKF1*	CTAAGGTCAGGGGAGGCATAC	ACAGTTGCGAAGGAGAGTGAA
At5g10140	*FLC*	AGCCAAGAAGACCGAACTCA	GGGAGAGTCACCGGAAGATT
At4g00650	*FRI*	ATGCCTGATCGTGGTAAAGG	CGCAGCTAATCCTCCTTCAG
At1g65480	*FT*	CTTGGCAGGCAAACAGTGTA	AGCCACTCTCCCTCTGACAA
At1g78440	*GA2ox*	GACCAAAACACGGACTCGAT	GGAGGGACAGAGATCCATGA
At4g25420	*GA20ox1*	GCCTTCAAGTCTTTGTGGAA	ATGCAAGTGATTTCCTCTCG
At5g51810	*GA20ox2*	TCGAACGGGATATTCAAGAG	GGTGGTTTCACCACTTTGTC
At1g22770	*GI*	ACGCAGAGACTTCTTCTTGGAC	CAGTTCCTGGGTAGCCTTACAC
At4g20400	*JMJ14*	GTGCTTGACCCAACAAACCT	ACCATTTGCCAGCACTTTTC
At5g61850	*LFY*	GCTCTCCACTGCCTAGACGA	CATGACGACAAGCGATGTTC
At1g01060	*LHY*	GCCATTGGCTCCTAATTTCA	TGTTCCCAACTTGGCTCTCT
At3g10480	*NAC050*	CTCCAATGGACATCGAACCT	GGACGCTCATCTTCTTCTGC
At3g10490	*NAC052*	TCGGACCAACAGAATCATCA	CGCTCCTCTTCTTCCATCTG
At2g45660	*SOC1*	ATCGAGGAGCTGCAACAGAT	GCTTTCATGAGATCCCCACT
At1g76710	*SDG26*	TCGCTCAGAAGCATGTTGAC	TGCTGCTTCCTTCTTCACCT

At1g62360	*STM*	GTCATCCGAGGAAGAAGTCG	GTAGTGACGGCTCCACCAAT
At2g22540	*SVP*	AGAAGGCCCTTGAAACTGGT	CGCTCGTTCTCTTCCGTTAG
At5g03840	*TFL1*	CAAGGCCAAGCATAGGGATA	GTGCAGCGGTTTCTCTTTGT
At5g61380	*TOC1*	TGATCTCCCAATGGCTAAGG	CATGCGTCTTCTTCTCCACA
At4g20370	*TSF*	CAACCCTCACCAACGAGAAT	ACCGTTTGTCTTCCGAGTTG
At2g17950	*WUS*	ACAACGTAGGTGGAGGATGG	CGCCACCACATTCTTCTTCT
CLOCK EXPERIMENT TARGET GENES			
At1g01060	*LHY*	GCCATTGGCTCCTAATTTCA	TGTTCCCAACTTGGCTCTCT
At5g02810	*PRR7*	GGGCCATATGGAAGCAGTAA	CAAAGCAGCTTCCCTTTGAG

Immunoblotting

Protein extraction and phosphatase treatment

Forty 3-day-old etiolated seedlings were harvested after the light treatment and then ground directly in 100 µl of Sodium Dodecyl Sulphate (SDS) 2X buffer. After 4 minutes of incubation at 100°C, samples were centrifuged at 13,000 x *g* for 8 min and then the collected supernatant was directly used for SDS-page analysis. To verify the actual nature of slow-migrated bands generated by CRY1 and PHOT1 phosphorylation, we collected even a negative control performing λ-phosphatase treatment according to Shalitin (2003).

SDS-page and Western blotting

Thirty µl of each sample were loaded on a 7.5% SDS-polyacrylamide (40% Acrylamide/Bis Solution, 37.5:1, Biorad) gel and separated at 200 V for 40 minutes. Gel-run proteins were transferred on a nitrocellulose membrane at 100 V for 60 minutes. After 1 h blocking in 8% milk, membranes were probed with the primary antibodies overnight (anti-PHYA 1:2000 (Agrisera); anti-PHYB from Nagatami's lab, 1:8000; anti- CRY1 from Ahmad's lab, 1:10000; anti-CRY2 from Batschauer's lab, 1:5000; anti-NPH3 from Sakai's lab, 1:8000; anti-PHOT1 polyclonal antibody (Cho *et al.*, 2006), 1:50000 and anti-UGPase 1:20000 (Newmarket Scientific) as a loading control). Three Tris Buffer Saline, 0.1% Tween 20 (TBS-T) 1X washings of 10 minutes each were performed before the incubation with the secondary antibodies (anti-rabbit and anti-mouse horseradish peroxidase (HRP)-conjugated secondary antibody (Promega)) at room temperature for one hour. All membranes were developed in a Xograph imaging system using Pierce® ECL Plus Western blotting substrate (Thermo Fisher Scientific) as a fluorescent method. The same membranes were stripped and re-probed more than once to detect all the proteins.

Statistical analyses

All our experiments were performed at least three times (three biological replicates) and all our data were expressed as mean values ± standard deviation (SD) or standard error (SE) (as specified for all the table and graphs in the result section). Ninety-five (95%) confidence level ($p<0.05$) was adopted to judge the statistical significance of all our data, using SYSTAT 10.

For morphometric measurements, at least 10 plates or 15 pots were used for each biological replicate. The statistical significance between treatment and control groups for all the analysed morphological variables was assessed by a two-tailed paired t-test analysis.
Considering gene expression analysis, each biological replicate was analysed using three technical replicates. All data are expressed as fold changes with respect to the control condition (i.e. reversed GMF/normal GMF; NNMF/GMF; GMF/NNMF). Normality test Kolmogorov-Smirmov confirmed normality of all the results. ANOVA and the following Tukey and Bonferroni *post-hoc* tests were used to assess significant differences between the treatment and the control. The cluster analysis for the flowering experiment was calculated by using Euclidean distances with median linkage.
Concerning protein analysis, the ImageJ software was used to quantify the blotted protein bands relatively to the UGPase level and then the significance of the results was verified by t-test.

RESULTS

The GMF polarity affects Arabidopsis growth and gene expression

To substantiate the hypothesis of GMF reversal influence on plant evolution, the response of plants to normal and reverse magnetic field conditions was investigated. After 10 days exposure to normal or reverse GMF conditions, Arabidopsis morphology was monitored and then compared to changes in gene expression induced by the GMF polarity. The analysed genes were selected based on studies previously carried out by our group (unpublished results), which highlighted a GMF influence on genes directly related to plant growth and oxidative response. Roots and shoots were separately analysed to discriminate the role of the two organs in mediating the possible response to GMF polarity.

After 10 days exposure to normal or reversed GMF conditions, the phenotype of plants showed evident morphological alterations. As reported in Table 2, roots of plants grown under normal GMF were significantly longer with respect to those of plants exposed to reversed GMF. Under reversed GMF conditions, the morphology of leaves was also altered by showing a reduced development of leaflets expansion (Table 2). Therefore, reversed GMF negatively affected both root length and leaf area.

Table 2: Effects of the geomagnetic field reversal on Arabidopsis morphology. (A) root lengths; (B) leaf area.

A	Normal GMF		Reversed GMF		Significativity
	Mean (±SE) mm	n. of seedlings	Mean (±SE) Mm	n. of seedlings	
Root lenght	29.41(±1.04)	32	17.53(±0.58)	36	*

B	Normal GMF		Reversed GMF		Significativity
	Mean (±SE) mm^2	n. of seedlings	Mean (±SE) mm^2	n. of seedlings	
Leaf area	4.95(±0.03)	32	3.71 (±0.03)	36	*

*=significant differences between plants exposed to reversed and normal GMF conditions: for (A) $p = 0.003$; df = 26; for (B) $p = < 0.001$; df = 53.

These morphological changes occurred along with an altered expression of genes connected to Arabidopsis growth : *CRU3*, that encodes a 12S seed storage protein that is tyrosine-phosphorylated and whose phosphorylation state is modulated in response to ABA in *Arabidopsis thaliana* seeds (Kagaya *et al.*, 2005; Wan *et al.*, 2007); *COTP1*, that encodes an heavy metal transport/detoxification superfamily protein with the predominant function in soil Cu acquisition and pollen development (Sancenon *et al.*, 2003) and *RRTF1*, that encodes a member of the ETHYLENE RESPONSE FACTOR (ERF) subfamily B-3 of ERF/AP2 transcription factor family that contains one AP2 domain that facilitate the synergistic co-activation of gene expression pathways and confer cross tolerance to abiotic and biotic stresses (Foyer, Karpinska and Krupinska, 2014).

All the three genes (*CRU3*, *COTP1*, *RRTF1*) were affected by the GMF dependently from its polarity (Figure 6). In particular, shoots of plants exposed to reversed GMF conditions showed a significantly increased (> 2 fold changes, $p<0.05$) mRNA level with respect to normal GMF

conditions. In roots, the GMF reversal significantly (p<0.05) decreased the number of *CRU3* transcripts. The opposite was found for *COTP1* and *RRTF1*, whose root expression level was slightly upregulated by the exposure to reversed GMF.

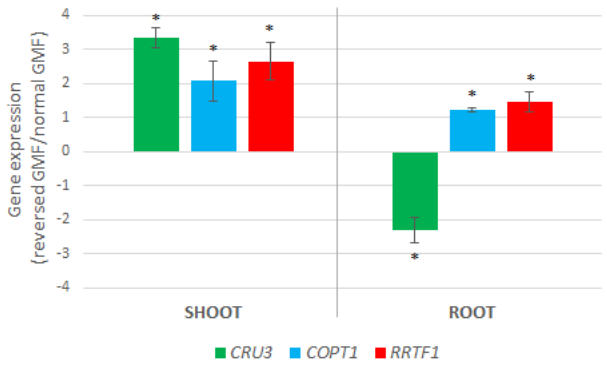

Figure 6: Effects of the geomagnetic field reversal on Arabidopsis gene expression. Bars indicate standard deviation; asterisk indicates significant (p<0.05) differences between plants exposed to reversed and normal GMF conditions.

Interesting results were obtained by analyzing five genes directly involved in the response to oxidative stress: *FSD1*, that encodes a cytoplasmatic enzyme that rapidly converts superoxide (O_2^-) and water (H_2O) to hydrogen peroxide (H_2O_2) and molecular oxygen (O_2) (Myouga *et al.*, 2008); *CAT3*, that encodes an enzyme that catalyzes the breakdown of H_2O_2 into water and oxygen (Contento and Bassham, 2010; Mhamdi *et al.*, 2010); *TAPX*, that encodes a chloroplastic thylakoid peroxidase that scavenges H_2O_2 (Kangasjarvi *et al.*, 2008); *APX1*, that encodes a cytosolic peroxidase that scavenges H_2O_2 (Begara-Morales *et al.*, 2014); and *RbohD* that encodes a NADPH oxidase that plays pivotal roles in regulating growth, development and stress responses in Arabidopsis and whose activity is related to the production of superoxide (Miller *et al.*, 2009; Jiménez-Quesada, Traverso and Alché, 2016).

In general, all the genes analysed in shoots did not show significant differences (p>0.05) with respect to GMF polarity (Figure 7 and Figure 8). However, a significant down-regulation of all the five genes was observed in roots of plants exposed to reversed GMF conditions. In particular, *CAT3* showed a dramatic downregulation (Figure 8), followed in order of downregulation by *APX1*, *RbohD, FSD1*, and *TAPX* (Figure 7).

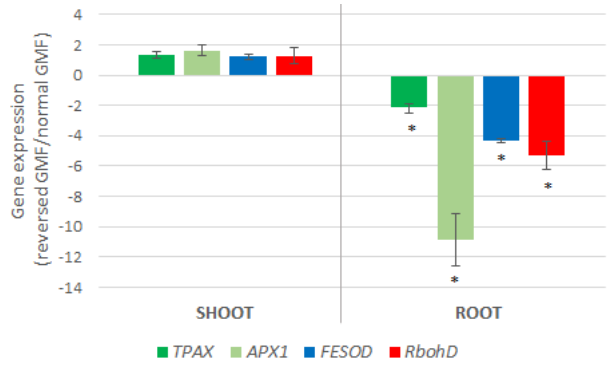

Figure 7: Effects of the geomagnetic field reversal on Arabidopsis antioxidant-related gene expression. Bars indicate standard error; asterisk indicates significant (p<0.05) differences between plants exposed to reversed and normal GMF conditions.

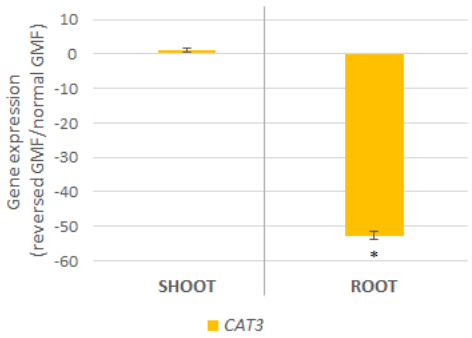

Figure 8: Effects of the geomagnetic field reversal on Arabidopsis *CAT3* expression. Bars indicate standard deviation; asterisk indicates significant (p<0.05) differences between plants exposed to reversed and normal GMF conditions.

Molecular basis of NNMF-induced flowering delay in *Arabidopsis thaliana*

To provide some new information on the mechanism downstream plant magnetoreception, the molecular basis of NNMF-induced flowering delay was investigated under LD white light conditions.

Arabidopsis WT plants were grown until full bloom under GMF and NNMF conditions and time course experiments were performed to analyze the rosette and flowering meristem expression of the key genes from all the major pathways responsible for the control of flowering, according to Fornara, de Montaigu and Coupland (2010). Hence, the effect of NNMF was evaluated on the expression of genes involved in the circadian clock and photoperiod pathway, vernalization pathway, temperature pathway and gibberellin pathway and on the expression of genes encoding NAC transcription factors, histone methylation regulators, shoot apical meristem differentiation factors and flowering effectors and integrators genes. The plant switching from the vegetative to the reproductive stage was monitored along time in terms of rosette leaf area index, stem length and time of occurrence of all the reproductive growth phenological phases. A generation experiment was used to test the persistence of the different flowering time in GMF with respect to NNMF conditions in WT plants grown by seeds produced by WT NNMF-exposed plants. *Cry1cry2* mutant plants were also grown until fool bloom both under GMF and NNMF conditions, just to monitor their flowering time so to discriminate cryptochrome involvement in NNMF-induced flowering delay under long day conditions.

NNMF delays the transition to flowering both in wild type (WT) and cry1cry2 *mutant plants*

Exposure of *A. thaliana* WT plants to NNMF and long day conditions caused a significant delay in flowering time. NNMF-exposed plants started flowering about 4 days later with respect to control plants (GMF) and reached full bloom about 5 days later than controls. WT plants grown by seeds produced under NNMF conditions (F_1- WT NNMF) started to flower about one day later with respect to parent plants grown in NNMF conditions. A second generation of seeds produced by F_1WT NNMF (F_2WT NNMF), did not show any significant difference in flowering time with respect to parent plants F_1-WT NNMF. However, F_2 WT NNMF plants showed a delayed flowering time with respect to GMF. Seeds of F_2-NNMF grown in GMF conditions recovered the normal phenotype (F2 WT NNMF→GMF) (Figure 9). As expected, the flowering time of the *cry1cry2* mutant was severely delayed with respect to the WT when plants were grown in GMF conditions. Surprisingly, exposure of the double mutant to NNMF conditions

caused the same delay found in WT plants with respect to the beginning of flowering, while the full blooming was reached 4 days later than under GMF conditions.

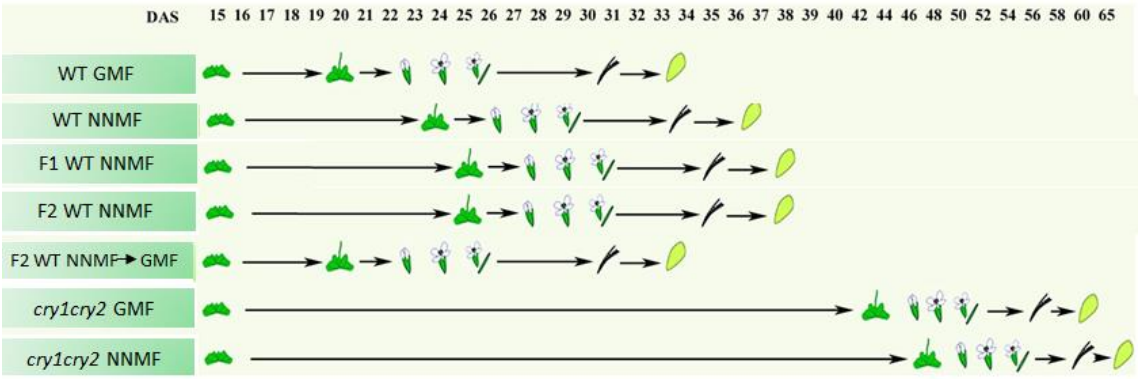

Figure 9: Phenological phases of *Arabidopsis thaliana* development and flowering in WT and *cry1cry* plants exposed to local GMF and to NNMF conditions. DAS= days after sowing

The time of flowering in WT plants was also monitored in terms of number of rosette leaves at bolting time. This parameter was not significantly different in control plants with respect to NNMF-exposed plants (Figure 10).

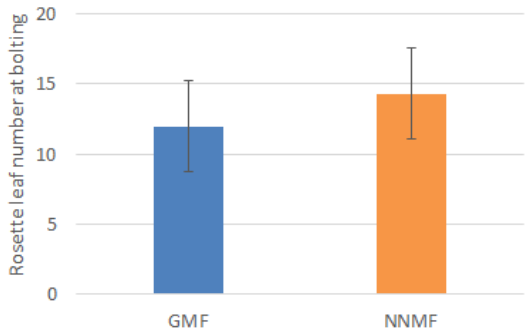

Figure 10: Rosette leaf number at bolting of *Arabidopsis thaliana* WT plants exposed to local GMF and NNMF conditions. Metric bars indicate standard deviation.

However, WT flowering stem length (Figure 11) as well as WT leaf area index (Figure 12) were negatively affected by NNMF starting from 24 DAS, when the bolting of NNMF-exposed plants and thereby their switching to the reproductive stage occurred.

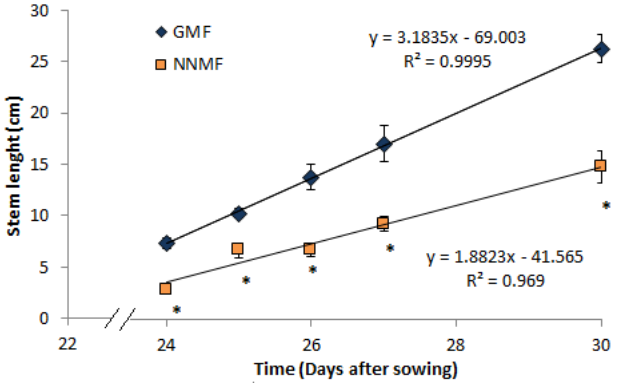

Figure 11: Length of the flowering stem of WT plants exposed to normal (GMF) and treated (NNMF) conditions. Metric bars indicate standard deviation; asterisks indicate significant (p< 0.05) differences between controls and NNMF-exposed plants.

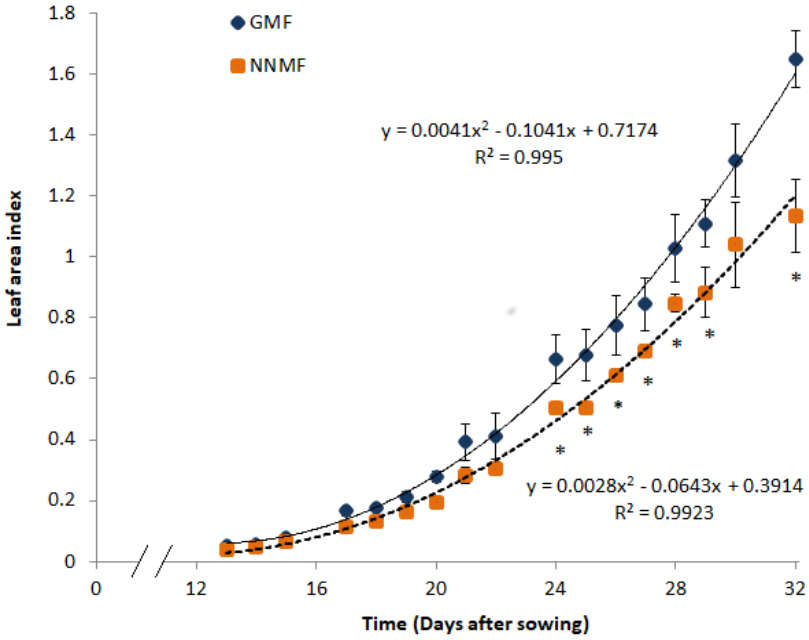

Figure 12: Leaf area index of WT plants exposed to normal (GMF) and treated (NNMF) conditions. Metric bars indicate standard deviation; asterisks indicate significant (p< 0.05) differences between controls and NNMF-exposed plants.

NNMF alters the expression of WT rosette genes involved in flowering transition

To dissect the effect of NNMF conditions on the transition to flowering, the expression of several genes involved in this process was separately analysed in WT rosette and flowering meristem tissues.

The following genes were assayed: *CCA1, LHY* and *TOC1*, encoding proteins which constitute the morning and evening circadian clock loops (De Caluwé *et al.*, 2016); *CO*, encoding a flowering promoting transcription factor whose protein and transcript levels are regulated dependently from the photoperiod (An, 2004; Shim, Kubota and Imaizumi, 2017); *GI* and *FKF1,* encoding an evening internal clock component and a flavin-binding Kelch repeat F-box protein, which together promote CO transcription under long day conditions (Song *et al.*, 2014); *FLC,* encoding a MAD box flowering transcriptional repressor whose transcription is negatively regulated by cold; it contributes to temperature compensation of the circadian clock (Helliwell *et al.*, 2015); *FRI,* encoding a protein that increases *FLC* transcript level, thus negatively affecting flowering time (Caicedo *et al.*, 2004); *SVP,* encoding a protein that interact with FLC in repressing the promotion of flowering and functions in the thermo-sensory pathway (Mateos *et al.*, 2015); *Ga2ox1,* encoding a gibberellin oxidase enzyme that acts on C19 gibberellins and negatively regulates flowering transition (Rieu *et al.*, 2008); *GA20ox1* and *GA20ox2* ,encoding two gibberellin oxidases that are involved in the later steps of the gibberellin biosynthetic pathway and in the promotion of the transition to flowering (Rieu *et al.*, 2008); *NAC050* and *NAC052,* encoding two NAC transcription factors that repress the flowering process by associating with JMJ14 (Ning *et al.*, 2015); *JMJ14,* encoding a JmjC domain-containing histone H3K4 demethylases which represses floral transition (Ning *et al.*, 2015); *SDG26,* encoding an histone methylase involved in the activation of flowering (Berr *et al.*, 2015); *WUS*, an homeodomain gene whose expression is essential for maintaining the pool of stem cells in an undifferentiated state at the indeterminate shoot apical meristem level

(Schoof *et al.*, 2000); *STM*, encoding a class I knotted-like homeodomain protein that is essential for the maintenance of indeterminate development of apical and axillary meristems during all phases of the plant life (Lenhard, Jürgens and Laux, 2002); *AGL24,* encoding a MADS-box transcription factor found to promote flowering by regulating the expression of *SOC1* (Pérez-Ruiz *et al.*, 2015); *AP1,* floral homeotic gene encoding a MADS domain protein required for the transcriptional activation of *SVP*, *SOC1* and *AGL24* (Valentim *et al.*, 2015)*; FD,* encoding a bZIP protein that interacts with FT to positively regulate flowering (Abe *et al.*, 2005); *FT*, encoding a protein which promotes flowering together with LFY during long day (Notaguchi *et al.*, 2008; Song, 2016); *LFY,* encoding a transcription factor that lays a key role in parallel with FT to activate floral meristem identity genes (Schultz, 1991); *SOC1,* integrator gene encoding a MADS box transcription factor that promotes the transition to flowering (Moon *et al.*, 2003)*; TFL1*, encoding a protein that controls inflorescence meristem identity, by repressing *LFY* and *AP1* (Liljegren *et al.*, 1999); *TSF,* encoding an FT homologous floral inducer and whose expression is influence by the vernalization and the photoperiod (Yamaguchi *et al.*, 2005; Jang, Torti and Coupland, 2009) pathways.

Table 3 summarized NNMF-induced regulation of rosette genes involved in the transition to flowering. In the rosette, *Ga20ox2* was the most dramatically downregulated gene in the early flowering induction (17-19 DAS) under NNMF conditions. Differently, *TOC1, FKF1, GA20ox1* and *FD* showed a consistent downregulation in *Arabidopsis thaliana* plants exposed to NNMF from 17 to 22 DAS. *CO*, *FRI, WUS* and *FT* exhibited a similar trend with an early (17-19 DAS) and a late (28 DAS) NNMF-induced downregulation. NNMF significantly reduced *AP1* and *STM* transcript level starting from 19 DAS to later flowering developmental stages. *LFY* and *TSF* exhibited a general downregulation, except for their upregulation at 23 DAS and 19 DAS, respectively. *CCA1* and *LHY* showed a general NNMF-induced downregulation trend during all the flowering transition phases. On one hand, a significant upregulation was found for *FLC* during early floral induction with a progressive downregulation during later stages of floral development. On the other hand, *GI* showed an opposite trend, being downregulated at 22 DAS and then upregulated at 28 DAS. Finally, while *NAC050* expression was not affected by NNMF, *SVP, SD26* and *TFL1* were significantly upregulated in the early flowering.

In order to clarify the pattern of expression of rosette genes, a cluster analysis was calculated on the data of Table 3 by using Euclidean distances and median linkage (Figure 13). *TSF* and *GA20ox2* compose two separate clusters because of late and early down-regulation, respectively, whereas *CCA1* and *FLC* form distinct clusters because of their very early (*CCA1*) and late (*FLC*) down-regulation. These clusters are separated by genes with late up-regulation (*GI*, *SDG26* and *SVP*), whereas the remaining genes are gathered for early and late down-regulation (*FRI*, *CO*, *WUS*, *FT*, *LHY*), only moderate early down-regulation (*TOC1*, *FKF1*) and irregular regulation (all remaining genes).

Table 3. Time-course expression of rosette genes in *Arabidopsis thaliana* exposed to NNMF conditions. Values are expressed as fold change (± SD) with respect to control plants growing in GMF conditions.

Function	***Gene***	**DAYS AFTER SOWING**					
		17	**19**	**21**	**22**	**23**	**28**
Circadian clock	*CCA1*	**-5.25** (± 0.11)	**-1.57** (± 0.06)	-1.02 (± 0.08)	**-1.65** (± 0.03)	**-2.94** (± 0.03)	**-1.77** (± 0.11)
	LHY	**-2.91** (± 0.04)	**-1.73** (± 0.04)	-1.28 (± 0.09)	**-1.77** (± 0.05)	-1.04 (± 0.05)	**-2.01** (± 0.07)
	TOC1	**-2.16** (± 0.03)	**-1.54** (± 0.04)	**-1.39** (± 0.09)	-1.13 (± 0.12)	-1.23 (± 0.02)	-1.13 (± 0.03)
Photoperiod pathway	*CO*	**-2.72** (± 0.01)	**-1.74** (± 0.13)	1.25 (± 0.4)	-1.13 (± 0.20)	1.16 (± 0.11)	**-2.70** (± 0.04)
	FKF1	**-1.45** (± 0.09)	**-1.67** (± 0.02)	**-1.38** (± 0.01)	**-1.43** (± 0.06)	-1.07 (± 0.05)	-1.12 (± 0.01)
	GI	1.04 (± 0.09)	1.07 (± 0.11)	1.01 (± 0.02)	**-1.32** (± 0.50)	-1.04 (± 0.04)	**1.51** (± 0.05)
Vernalization and temperature pathways	*FLC*	**1.98** (± 0.17)	-1.12 (± 0.03)	-1.10 (± 0.11)	**-1.75** (± 0.11)	**-2.22** (± 0.28)	**-3.81** (± 0.08)
	FRI	**-1.80** (± 0.09)	**-1.61** (± 0.05)	1.27 (± 0.57)	-1.32 (± 0.04)	**1.71** (± 0.07)	**-1.75** (± 0.16)
	SVP	-1.08 (± 0.13)	-1.01 (± 0.1)	-1.31 (± 0.20)	1.32 (± 0.18)	-1.15 (± 0.15)	**1.41** (± 0.08)
Gibberellin pathway	*GA20ox1*	**-3.11** (± 0.28)	**-2.43** (± 0.36)	**-1.24** (± 0.21)	**-2.29** (± 0.09)	1.22 (± 0.27)	-1.20 (± 0.12)
	GA20ox2	**-5.58** (± 0.66)	**-6.81** (± 0.34)	1.19 (± 0.12)	1.16 (± 0.23)	1.38 (± 0.18)	-1.02 (± 0.11)
NAC transcription factors	*NAC050*	-1.11 (± 0.15)	-1.5 (± 0.23)	-1.44 (± 0.12)	-1.14 (± 0.06)	1.05 (± 0.09)	-1.03 (± 0.12)
Histone methylation regulators	*SDG26*	-1.26 (± 0.07)	-1.11 (± 0.09)	-1.16 (± 0.15)	**2.09** (± 0.27)	-1.44 (± 0.23)	**3.23** (± 0.54)
Shoot apical meristem differentiation	*STM*	-1.47 (± 0.18)	**-2.68** (± 0.13)	1.15 (± 0.49)	**-1.80** (± 0.04)	1.35 (± 0.15)	**-1.47** (± 0.08)
	WUS	**-3.09** (± 0.10)	**-2.41** (± 0.05)	-1.12 (± 0.33)	-1.16 (± 0.06)	1.01 (± 0.10)	**-1.73** (± 0.01)
Flowering effectors and integrator genes	*AP1*	-1.04 (± 0.01)	**-1.71** (± 0.11)	**-1.93** (± 0.31)	**-3.01** (± 0.12)	**-1.40** (± 0.04)	1.14 (± 0.02)
	FD	**-1.40** (± 0.03)	-1.23 (± 0.09)	**-1.86** (± 0.19)	-1.12 (± 0.16)	1.18 (± 0.09)	-1.14 (± 0.18)
	FT	**-3.09** (± 0.02)	**-2.26** (± 0.05)	-1.25 (± 0.08)	-1.37 (± 0.05)	1.03 (± 0.03)	**-2.35** (± 0.02)
	LFY	**-2.07** (± 0.15)	**-1.71** (± 0.15)	**-2.15** (± 0.23)	1.15 (± 0.07)	**1.56** (± 0.20)	**-1.66** (± 0.27)
	TFL1	-1.52 (± 0.18)	-1.11 (± 0.16)	-1.33 (± 0.13)	1.09 (± 0.05)	**2.16** (± 0.05)	-1.43 (± 0.13)
	TSF	**-2.30** (± 0.13)	**2.83** (± 0.67)	1.14 (± 0.50)	**-5.13** (± 0.02)	**-6.13** (± 0.01)	**-1.70** (± 0.24)

Bold faced numbers indicate a significant ($p < 0.05$) difference between NNMF and GMF treatment.

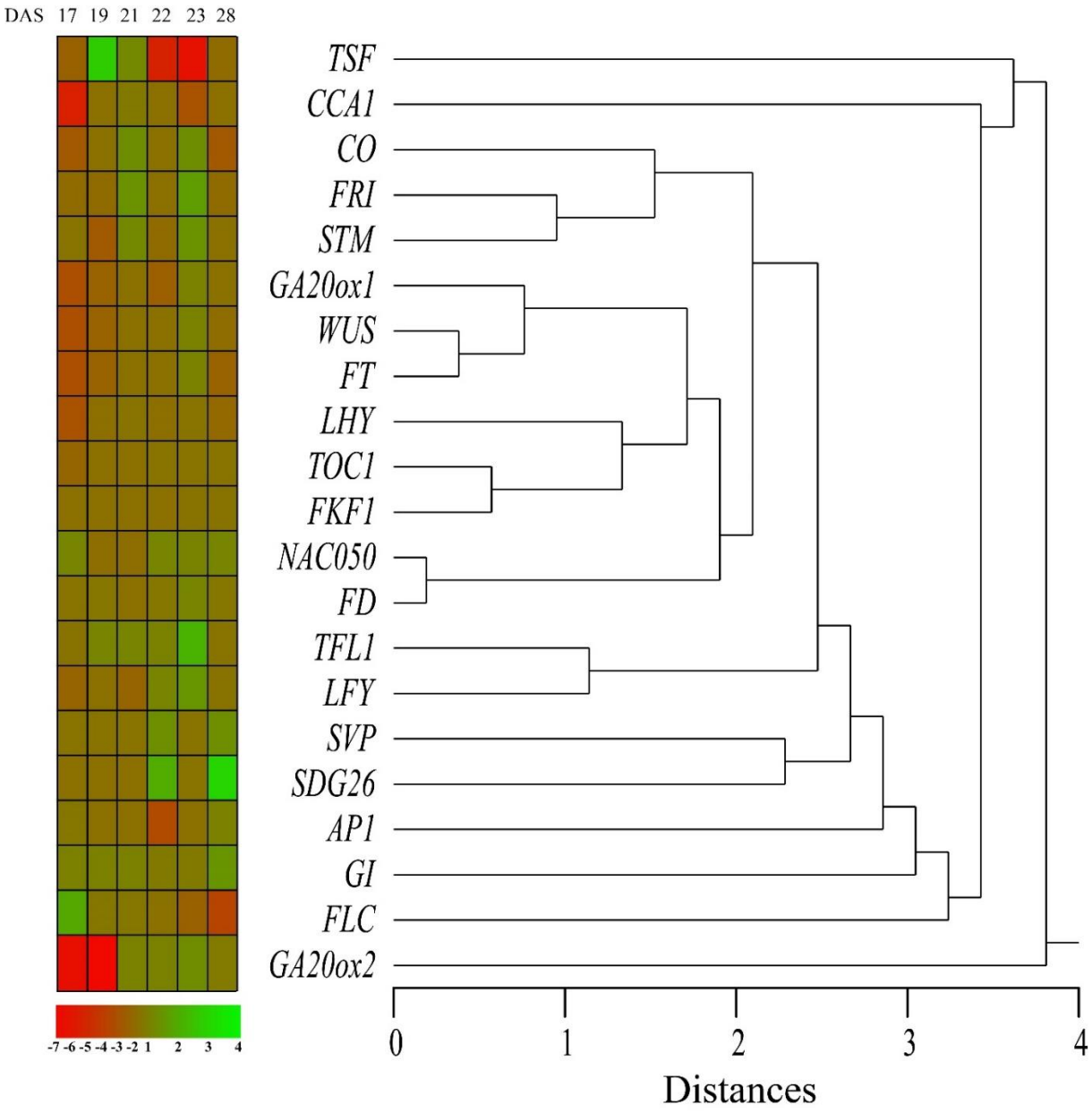

Figure 13: Pattern of expression of genes involved in flowering in *Arabidopsis thaliana* rosette. The cluster analysis was conducted by using Euclidean distances and median linkage. DAS, days after sowing. The different shades of green and red correspond to the expression levels reported in the figure colour bar.

NNMF alters the expression of WT flowering meristem genes involved in flowering transition

Table 4 summarized NNMF-induced regulation of flowering meristem genes involved in the transition to flowering. In the flowering meristem of *A. thaliana* plants exposed to NNMF, *GA20ox1* showed a slight downregulation during early times of flowering. Differently*, Ga2ox1, GA20ox2* and *FLC* were significantly down-regulated from 21 to 28 DAS. In particular, *Ga20ox2* downregulation was dramatic at 21, 22 and 28 DAS, whereas that of *FLC* at 22 DAS. NNMF induced a significant decrease in *NAC050* and *NAC052* mRNA level starting from 22 DAS, whereas *SOC1* was only downregulated during late flowering. *SVP*, *SDG26*, *LFY* and, particularly, *FD* showed a significant up-regulation at 21 DAS, but then they were all downregulated with different trends. *SVP* was downregulated only at late flowering time (28 DAS), while *SDG26* both at late (28 DAS) and early (22 DAS) flowering time. Differently, *FD*

downregulation occurred at early flowering time (22 DAS), whereas *LFY* was downregulated at 23 and 28 DAS. NNMF affected the transcription level of *AGL24* by down-regulating its expression in early flowering times (22 DAS) and up-regulating its expression during flowering (23, 28 DAS). Finally, *AP1* showed a significant downregulation at 21, 23 and 28 DAS and a significant upregulation at 22 and 30 DAS, whereas *JMJ14* did not show any significant regulation.

The cluster analysis built on the data reported in Table 4 by using Euclidean distances and median linkage (Figure 14) shows a clear distinction between the pattern of expression of *GA20ox2*, *FLC,* and all other genes. A cluster gathers the expression patterns of *AP1* and *GA2ox1*, whereas another cluster groups genes showing early up-regulation. The two *NAC* genes (*NAC050* and *NAC052*) show similar patterns, which gather them in a cluster, whereas the pattern of expression of *AGL24* is separated from the other clusters because of its late up-regulation.

Table 4. Time-course expression of flowering meristem genes in *Arabidopsis thaliana* exposed to NNMF conditions. Values are expressed as fold change (± SD) with respect to control plants growing in GMF conditions.

Function	***Gene***	**DAYS AFTER SOWING**				
		21	**22**	**23**	**28**	**30**
Gibberellin pathway	*GA2ox1*	**-2.72** (± 0.02)	1.03 (± 0.05)	**-3.54** (± 0.01)	**-3.44** (± 0.02)	1.19 (± 0.15)
	GA20ox1	**-1.83** (± 0.21)	**-1.92** (± 0.25)	-1.39 (± 0.23)	1.04 (± 0.08)	1.03 (± 0.33)
	GA20ox2	**-23.87** (± 5.82)	**-53.65** (± 1.23)	**-3.11** (± 0.38)	**-47.49** (± 5.73)	-1.25 (± 0.24)
Vernalization and temperature pathways	*FLC*	**-5.00** (± 0.07)	**-14.39** (± 0.01)	**-5.54** (± 0.03)	**-3.28** (± 0.07)	1.75 (± 0.18)
	SVP	**2.10** (± 0.30)	-1.31 (± 0.20)	1.16 (± 0.25)	-1.13 (± 0.19)	**-3.62** (± 0.34)
NAC transcription factors	*NAC050*	1.15 (± 0.25)	**-5.79** (± 0.96)	1.06 (± 0.18)	**-1.95** (± 0.35)	-1.42 (± 0.22)
	NAC052	-1.19 (± 0.03)	**-4.06** (± 0.63)	-1.00 (± 0.13)	**-1.60** (± 0.10)	**-1.38** (± 0.04)
Histone methylation regulators	*JMJ14*	1.10 (± 0.32)	-1.17 (± 0.21)	1.10 (± 0.11)	-1.04 (± 0.25)	1.30 (± 0.12)
	SDG26	**1.59** (± 0.02)	**-3.31** (± 0.75)	1.48 (± 0.18)	-1.32 (± 0.27)	**-1.61** (± 0.32)
Flowering effectors and integrator genes	*AGL24*	-1.06 (± 0.08)	**-3.30** (± 0.23)	**1.96** (± 0.15)	**1.97** (± 0.36)	-1.37 (± 0.22)
	AP1	**-1.72** (± 0.03)	**1.99** (± 0.22)	**-4.75** (± 0.01)	**-2.76** (± 0.03)	**1.80** (± 0.47)
	FD	**3.41** (± 0.55)	**-1.56** (± 0.19)	1.39 (± 0.02)	-1.16 (± 0.13)	-1.02 (± 0.03)
	LFY	**1.45** (± 0.01)	1.27 (± 0.14)	**-1.97** (± 0.06)	**-2.00** (± 0.08)	-1.89 (± 0.26)
	SOC1	1.44 (± 0.11)	1.69 (± 0.20)	-1.15 (± 0.06)	**-2.63** (± 0.07)	-1.04 (± 0.07)

Bold faced numbers indicate a significant ($p<0.05$) difference between NNMF and GMF treatment.

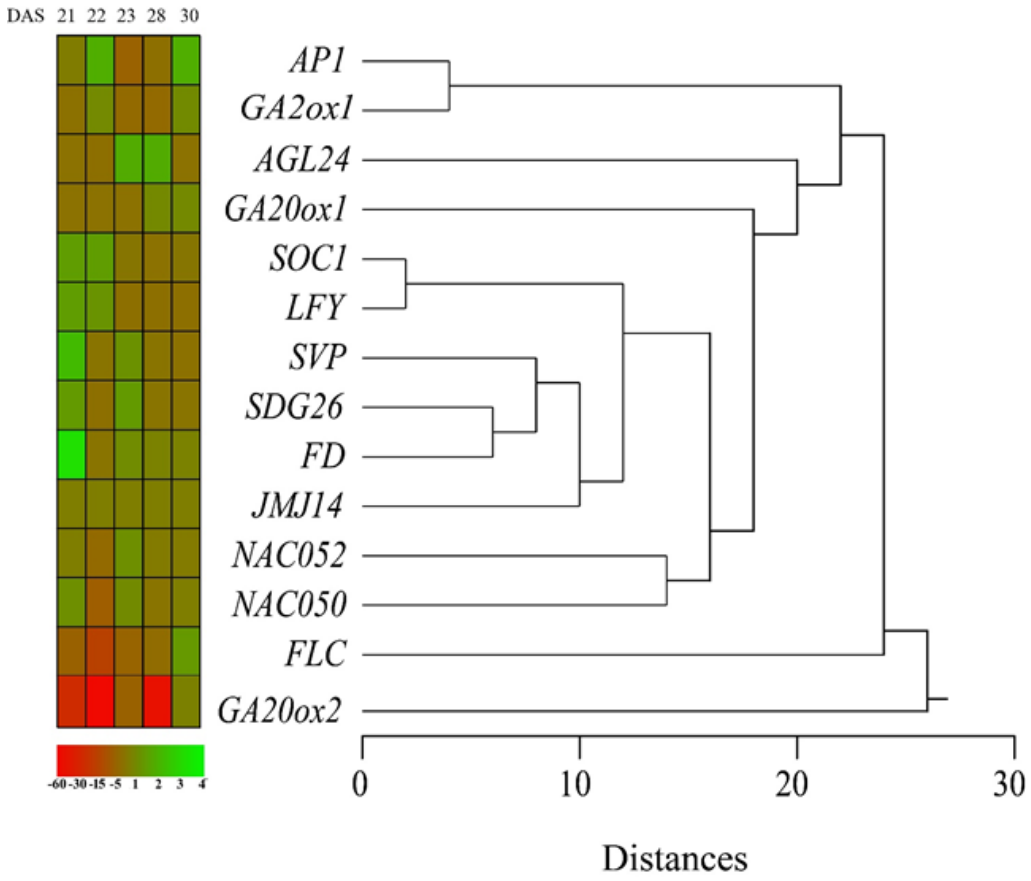

Figure 14: Pattern of expression of genes involved in flowering in *Arabidopsis thaliana* flowering meristem. The cluster analysis was conducted by using Euclidean distances and median linkage. DAS, days after sowing. The different shades of green and red correspond to the expression levels reported in the figure colour bar.

Influence of the GMF on light-dependent responses along the photomorphogenic process

To assess whether the GMF effects on Arabidopsis are light dependent and to discriminate the contribution of photoreceptors to this response, the influence of the GMF on different photomorphogenesis-related responses was evaluated. Three-day-old etiolated WT seedlings were compared to *cry1cry2, phot1* and *phyAphyB* mutant seedlings in the response after 72 h exposure to GMF or NNMF coupled with different light conditions. The long-day white light condition reproduced the natural activation and de-activation status of the plant photoreceptors, when they can synchronize the circadian clock under a light/darkness cycle. The continuous white light condition stimulated photoreceptors continuously, whereas continuous red and blue light conditions selectively activated the red light-responsive (phytochrome) and blue light-responsive (cryptochrome, phototropins, ZTL/FKF1/LKP2 family and phytochrome, partially) photoreceptors, respectively. The continuous darkness condition was used as a negative control, to test whether magnetoreception could be light independent. The GMF influence on photomorphogenesis was evaluated by monitoring plant morphology and the expression of light-related gene pathways, discriminating between root and shoot responses. We decided to separately analyse the two plant organs since roots appear to be the main site of response to the GMF as above mentioned.

The influence of the GMF on photoreceptor activation was then investigated, considering photoreceptors phosphorylation and degradation status. The role of the cross talk between photoreceptors in mediating these responses was also discussed.

The GMF does not affect Arabidopsis root and hypocotyl growth under dark and light exposure

From a morphological point of view, GMF and NNMF effects on Arabidopsis 3-day-old etiolated WT seedlings were verified on hypocotyl and root length after 72 h treatment with continuous darkness (D), continuous white light (CW) and long-day white light (LD) (Figures 15). The skotomorphogenic phenotype under D conditions, as well as the photomorphogenic phenotype under all white light treatments were not affected by the GMF both in the hypocotyl (15a) and in the root (15b). Hypocotyl growth was indeed inhibited by light, while primary root growth was promoted by light.

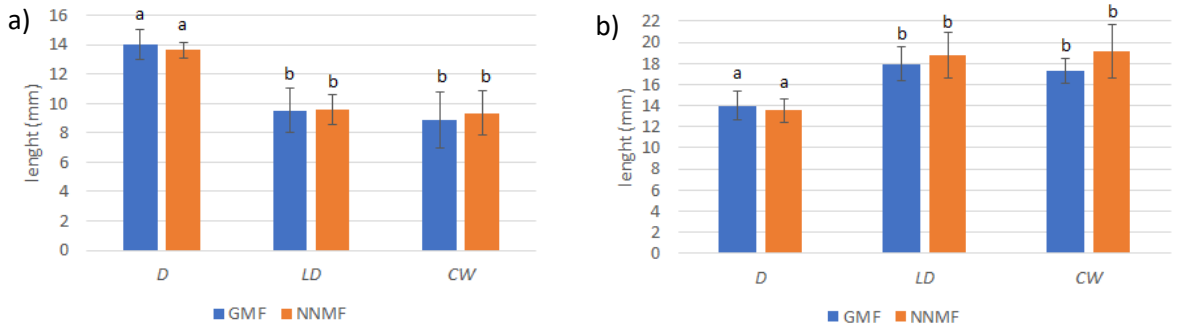

Figure 15. Morphometric measurements of *Arabidopsis thaliana* **WT** seedlings grown under different light conditions for 72 h either in GMF or in NNMF conditions. Hypocotyl (a) and root (b) length is reported as mean values (± SD). *D* (continuous darkness); *LD* (Long -day white light); *CW* (continuous white light). Different letters in the same group indicate a significant difference ($p < 0.05$).

Same results were found when Arabidopsis WT, *cry1cry2*, *phot1* and *phyAphyB* seedlings were exposed to GMF and NNMF and grown under either blue light (Figure 16) or red light (Figure 17). Even in this case NNMF exposed seedlings showed the same phenotype of GMF exposed plants. Therefore, the GMF does not interfere with CRY1, CRY2, PHYA and PHYB function in mediating hypocotyl length reduction under blue light (Figure 16a) as well as with PHYA and PHYB function in mediating hypocotyl length reduction under red light (Figure 17a). Moreover, the function of all the analysed blue light photoreceptors in mediating root length elongation under blue light (Figure 16b) as well as that of phytochrome in mediating root length elongation under red light (Figure 17 b) was not affected by GMF.

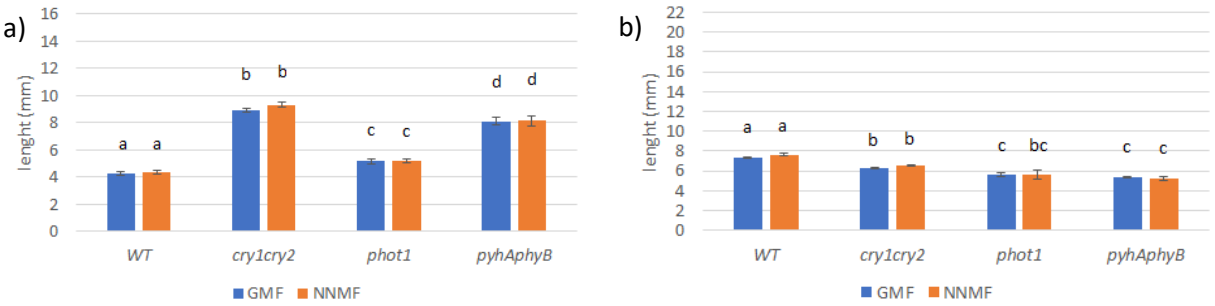

Figure 16: Morphometric measurements of *Arabidopsis thaliana* WT, *cry1cry2*, *phot1* and *phyAphyB* seedlings grown under **blue** light for 72 h either in GMF or in NNMF conditions. Hypocotyl (a) and root (b) length is reported as mean values (± SD). Different letters in the same group indicate a significant difference ($p < 0.05$).

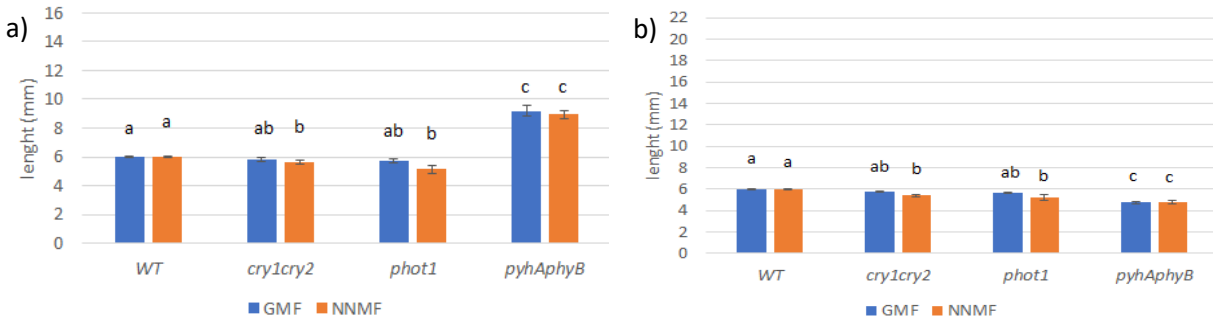

Figure 17: Morphometric measurements of *Arabidopsis thaliana* WT, *cry1cry2, phot1* and *phyAphyB* seedlings grown under **red** light for 72 h either in GMF or in NNMF conditions. Hypocotyl (a) and root (b) length is reported as mean values (± SD). Different letters in the same group indicate a significant difference ($p < 0.05$).

The GMF regulates the expressions of light-related genes under different light conditions

To assess whether the retention of Arabidopsis photomorphogenic and skotomorphogenic morphology is in fact related to the absence of GMF influence on the light-dependent signaling cascade, the expression of several key genes regulated downstream photoreceptor activation was analysed. Therefore, the level of expression of the following genes directly related to the photomorphogenic response was measured: genes encoding transcription factors regulated by the COP1/SPA1 complex that operate downstream of multiple photoreceptors and whose transcriptional regulation is mediated by different light wavelengths (*CO*, *HYH*, *HY5* and *LAF1*) (Sellaro *et al.*, 2009; Su *et al.*, 2017) , genes encoding molecules mainly regulated by downstream phytochrome signals and whose expression is mediated by light (*PKS1*, *PIF3* and *NDPK2*) (Montgomery, 2016), anthocyanin biosynthesis genes which are transcriptionally regulated by cryptochromes and phytochromes (*ANS* and *CHS*) (Shin, Park and Choi, 2007; Wang, 2015; Gangappa and Botto, 2016); genes encoding auxin transporters whose localization and transcriptional regulation is under cryptochrome and phytochrome control (*PIN1* and *PIN3*) (Halliday and Martı, 2009; Park *et al.*, 2011) and genes involved in oxidative stress responses (*GST* and *NDPK2*) (Jiang *et al.*, 2010; Kim *et al.*, 2011).

To provide evidence of a possible light-independent response to the GMF in Arabidopsis, the GMF influence on gene expression was evaluated in WT seedlings exposed to dark conditions. After 72 h exposure to D, GMF conditions prompted an up-regulation of *HYH* in WT shoots, whereas in WT roots the GMF caused a significant up-regulation of *CO* and *HYH,* a slightly down-regulation of *LAF1* and a 3-fold change downregulation of *NDPK2.*

To confirm the presence of a light-dependent response to the GMF in Arabidopsis, the expression of light-related gene was evaluated under LD and CW conditions in WT plants (Table 5). In seedlings grown under LD, the presence of the GMF significantly ($p< 0.05$) down-regulated *HY5*, *NDPK2*, *CHS* and in particular *GST* in the shoot and significantly ($p < 0.05$) up-regulated *PIF3, NDPK2* and *CO* in the root (Table 5).

Under CW, the GMF prompted a significant down-regulation of *HYH* and *PKS1* expression level and a significant ($p < 0.05$) up-regulation of *GST* and *ANS* transcripts in WT shoots (> 2-fold changes), with respect to NNMF conditions. In WT roots, GMF conditions significantly ($p < 0.05$) down-regulated *HYH, HY5* and in particular *NDPK2* and *GST*, whereas *PIN3* was up-regulated (Table 5).

Table 5. GMF contribution to **shoot** and **root** gene expression of 3-day-old etiolated Arabidopsis **WT** seedlings grown for 72 h under either GMF or NNMF conditions using different light exposures. Data are expressed as fold changes (mean ± SD) with respect to NNMF conditions (i.e., GMF/NNMF).

Function	***Gene***	**Continuous darkness**		**Long day white light**		**Continuous white light**	
		Shoot	*Root*	*Shoot*	*Root*	*Shoot*	*Root*
Transcription factors regulated by COP1/SPA1 complex	*CO*	-1.36 (±0.59)	**1.33** (± 0.11)	1.27 (± 0.29)	**1.79** (± 0.01)	-1.12 (± 0.24)	**1.30** (± 0.19)
	HYH	**2.00** (± 0.00)	**1.45** (± 0.36)	1.06 (± 0.05)	-1.08 (± 0.25)	**-1.58** (± 0.06)	**-1.41** (± 0.12)
	HY5	-1.35 (± 0.47)	1.22 (± 0.19)	**-1.45** (± 0.01)	1.01 (± 0.12)	1.08 (± -0.13)	**-1.61** (± 0.06)
	LAF1	n.e.	**-1.30** (± 0.09)	n.e.	1.2 (± 0.17)	n.e.	1.06 (± -0.16)
Phytochrome -related factors	*PKS1*	-1.28 (± 0.03)	-1.08 (± 0.11)	-1.17 (± 0.02)	-1.12 (± 0.17)	**-1.91** (± 0.03)	1.23 (± -0.15)
	PIF3	1.32 (± 0.26)	1.08 (± 0.1)	-1.04 (± 0.03)	**1.30** (± 0.22)	-1.10 (± 0.12)	-1.07 (± 0.18)
	**NDPK2*	-1.50 (± 0.26)	**-3.42** (± 0.51)	**-1.29** (± 0.05)	**1.47** (± 0.02)	1.14 (± -0.17)	**-2.09** (± 0.35)
Anthocyanin biosynthesis	*ANS*	n.e.	1.11 (± 0.19)	-1.85 (± 0.42)	1.30 (± 0.40)	**3.85** (± -1.04)	-1.02 (± 0.12)
	CHS	n.e.	1.16 (± 0.41)	**-2.59** (± 0.26)	-1.40 (±0.43)	-1.43 (± 0.13)	-1.70 (± 0.13)
Auxin signaling	*PIN1*	-1.03 (± 0.04)	1.22 (± 0.09)	-1.38 (± 0.08)	1.19 (± 0.43)	-1.09 (± 0.41)	-1.17 (± 0.07)
	PIN3	1.72 (± 0.48)	1.02 (± 0.04)	-1.10 (± 0.14)	1.19 (± 0.24)	1.01 (± -0.2)	**1.25** (± -0.05)
Oxidative response	*GST*	-1.59 (± 0.44)	-1.59 (± 0.44)	**-5.06** (± 0.07)	-1.45 (± 0.36)	**2.04** (± -0.17)	**-2.68** (± 1.01)

Boldfaced numbers indicate a significant (p<0.05) difference between NNMF and GMF treatment. *= this gene is associated to the oxidative response either.

To discriminate whether GMF influence on light-related signaling pathways is blue or red-light dependent, we monitored GMF effects on gene expression under blue and red light separately. To simplify data presentation, we only plotted those genes whose expression showed a significant ($p < 0.05$) difference in WT plants in the GMF vs. NNMF comparison under blue and red-light exposure. To discriminate whether the GMF-induced gene regulation was dependent from a specific photoreceptor, the gene expression level was also evaluated on photoreceptor mutant lines.

Under blue light conditions (Figure 18), the GMF modulated the expression of 5 genes in WT shoots (Figure 18a) and 7 genes in WT roots (Figure 18b). In WT shoots, the GMF down-regulated the expression of *HYH*, *PKS1*, *PIN1* and *PIN3*, whereas *PIF3* was up-regulated (Figure 18a). When compared to WT, *cry1cry2* shoots showed an opposite trend for *HYH*, *PKS1* and *PIN3* and the same trend for *PIF3*, whereas *PKS1* was not significantly regulated by the GMF. *Phot1* shoots showed the same trend of WT plants, with the sole exception of *PKS1* and *PIN3* whose expression levels were not significantly affected by the GMF. Finally, the *phyAphyB* mutant showed a down-regulation similar to WT seedlings in the shoot for *HYH* and *PKS1*, an opposite trend for *PIN3*, and no GMF-dependent regulation for *PIF3* and *PIN1*.

In the roots, the GMF upregulated the expression of *HYH*, *PIF3*, *CHS*, *PIN1* and *PIN3* in WT plants, whereas the expression of *PKS1* and *NDPK2* was down-regulated (Figure 18b). The roots of the *cry1cry2* showed the same trend of the WT for *PIF3* and *PIN3*, whereas *HYH* and *CHS* were not significantly regulated by the GMF. When compared to WT, the *cry1cry2* mutant and the *phot1* mutant showed an opposite trend for *NDPK2*. Whereas, the *phot1* mutant showed the same modulation trend of WT plants for *HYH,* the opposite regulation for *CHS* with respect to WT plants and no regulation for *PKS1, PIN1* and *PIN3*. Finally, the *phyAphyB*

mutant showed the same gene expression trend of WT plants for *PIF3* and *NDPK2*, an opposite trend for *PIN1* and *CHS*, while no GMF-induced regulation for*PKS1* and *PIN3* was observed.

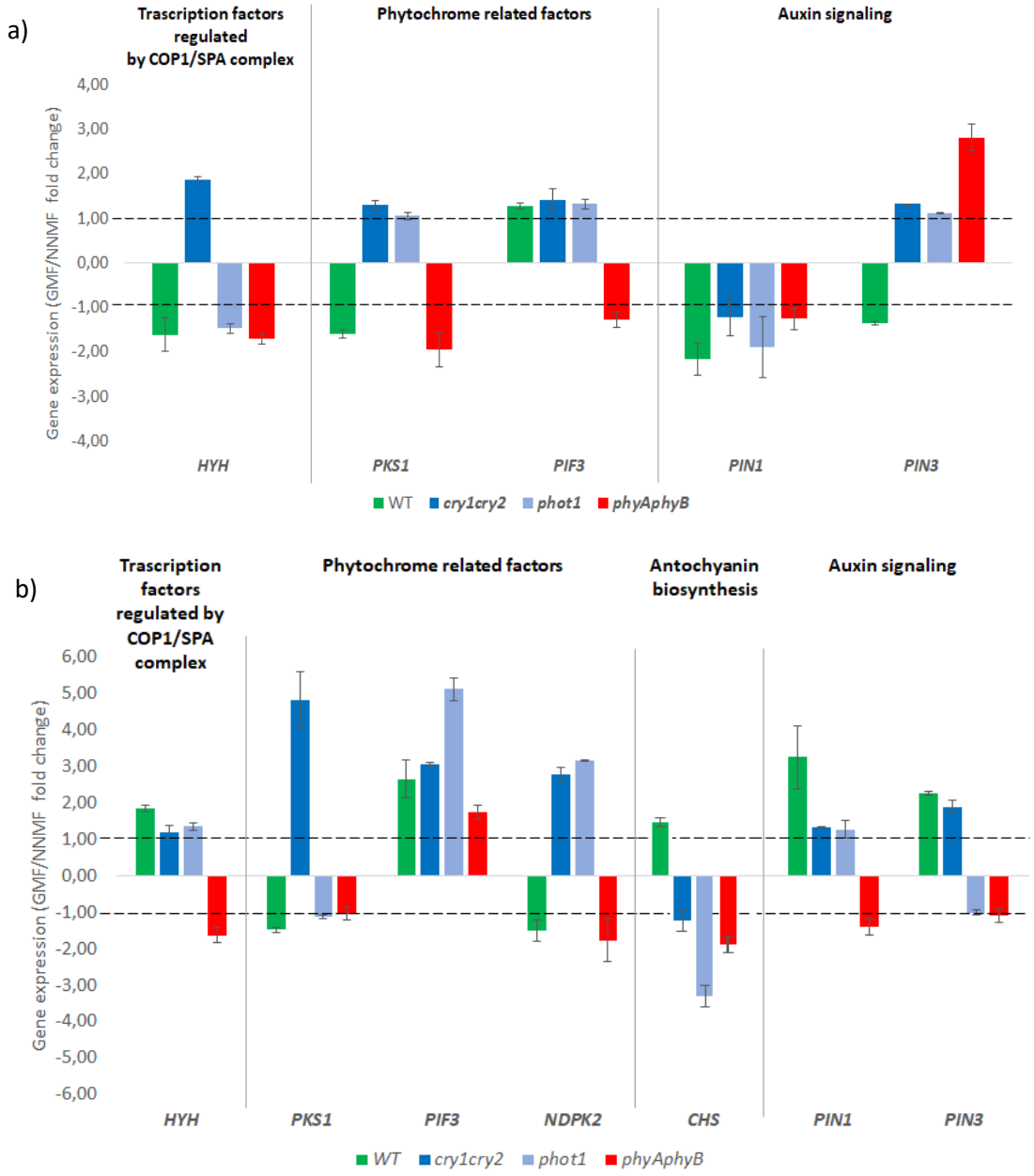

Figure 18: GMF contribution to **shoot** (a) and **root** (b) gene expression of 3-day-old etiolated Arabidopsis *WT, cry1cry2, phot1* and *phyAphyB* seedlings grown for 72 h under either GMF or NNMF conditions using **blue** light exposure. Data are expressed as fold changes (mean ± SD) with respect to NNMF conditions (i.e., GMF/NNMF). The two dotted lines highlight the range of absence of GMF-dependent regulation (between 1 and -1 fold change; $p<0.05$).

Exposure to red light differentially regulated the transcription level of 5 genes in the shoot (Figure 19a) and 9 genes in the root (Figure 19b) of WT seedlings exposed to GMF vs NNMF conditions. In WT shoots, GMF down-regulated *PKS1*, *PIF3* and *GST*, and up-regulated *ANS* and *CHS*. The same trend of WT plants was observed in *cry1cry2* mutants for *PIF3* and *ANS*, whereas *PKS1, CHS* and *GST* expression was not significantly affected by the GMF (Figure 19a). With respect to *WT* plants, the *phot1* mutant showed the same trend for *PIF3* and *GST* and an opposite trend for *PKS1*, *CHS* and *ANS*. The *phyAphyB* mutant showed an opposite trend

compared to WT plants for *ANS* and *CHS* while *PKS1, PIF3* and *GST* were not significantly regulated by the GMF.

Under red light, in WT roots the GMF caused a significant ($p < 0.05$) up-regulation of *LAF1,* no regulation of *HYH* and a significant down-regulation of the other genes, especially the phytochrome related factors *PIF3* and *NDPK2* (Figure 19b). When compared to WT, *cry1cry2* roots showed an opposite trend for *HY5*, *LAF1* and *PIN1,* whereas all the other genes showed the same trend except for *CHS* and *PIN3* whose expression was not significantly affected by the GMF. When compared to the WT, the *phot1* mutant showed an opposite trend for *LAF1* and *PIN3,* whereas all the other genes showed the same trend apart from *PIF3* and *NDPK2,* whose expression was not modulated by the GMF. *PhyAphyB* root gene expression level was similar to that of *cry1cry2* seedlings, with the sole exception of *CHS* that was downregulated and *GST* that showed no regulation (Figure 19b).

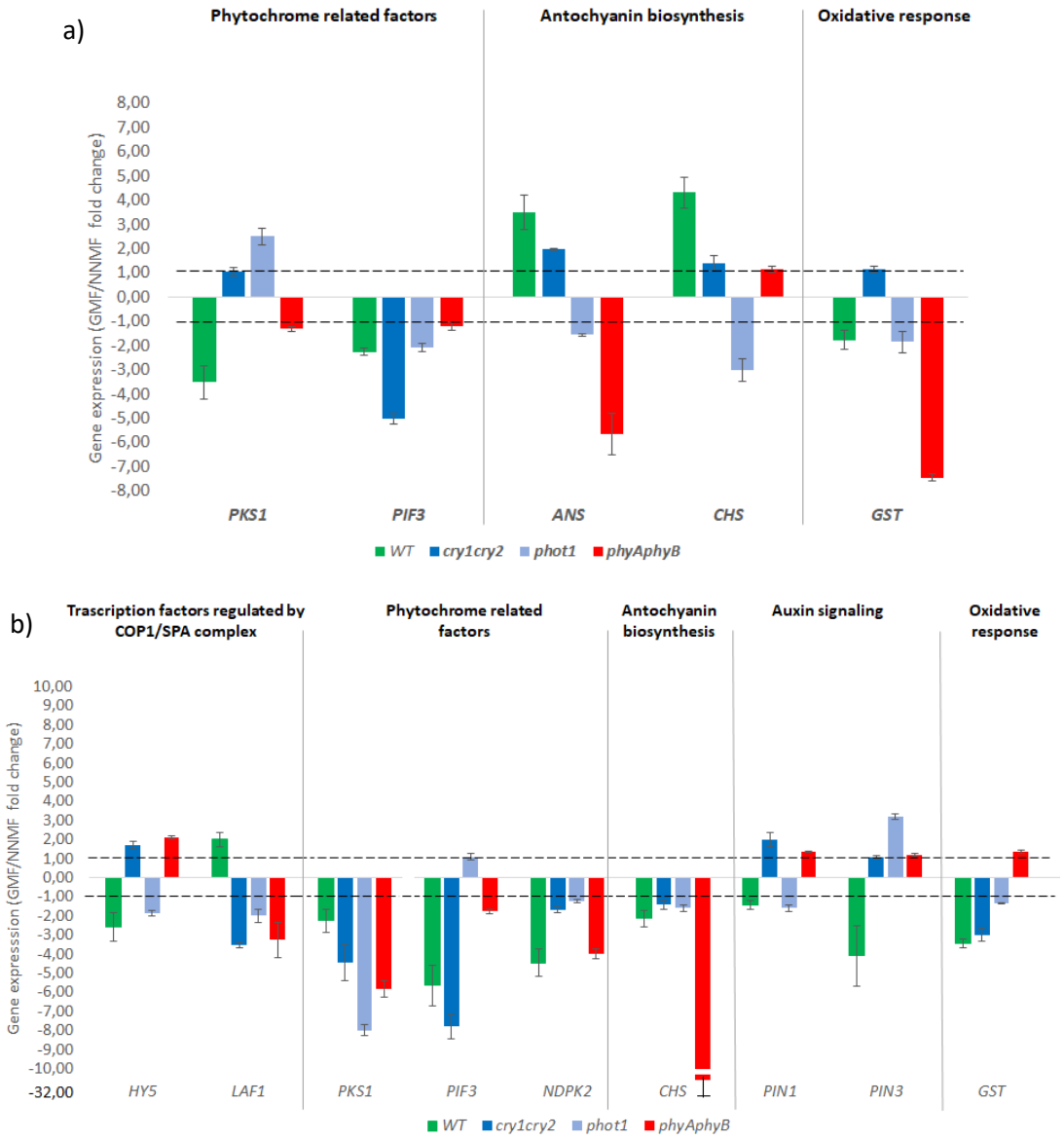

Figure 19: GMF contribution to **shoot (a)** and **root (b)** gene expression of 3-day-old etiolated Arabidopsis WT, *cry1cry2, phot1* and *phyAphyB* seedlings grown for 72 h under either GMF or NNMF conditions using **red** light exposure. Data are expressed as fold changes (mean ± SD) with respect to NNMF conditions (i.e., GMF/NNMF). The two dotted lines highlight the range of absence of MF-dependent regulation (between 1 and -1 fold change, $p<0.05$).

The GMF influences blue and red-light photoreceptors activation level

Having assessed that the GMF effect on gene expression is both blue and red- light dependent and that photoreceptors contribute in mediating this response, the GMF influence on photoreceptor activation was then evaluated. All the blotting analyses were performed in Prof. Christie's laboratory, at the University of Glasgow.

CRY1, CRY2 and PHOT1 activation level was tested under blue light. As for cryptochrome, CRY1 activation level was assayed by monitoring the blue light-induced CRY1 phosphorylation (Shalitin, 2003), while CRY2 degradation was used as an indirect indicator of CRY2 activation (Weidler *et al.*, 2012) by exposing seedlings to blue light. Furthermore, *phot1, phyA* and *phyAphyB* mutant lines were used to evaluate the role of phytochromes and PHOT1 in mediating cryptochrome activation in the absence of the GMF. Under NNMF conditions, CRY1 phosphorylation was practically absent in WT seedlings, with respect to GMF-exposed plants, thus suggesting a GMF role in promoting CRY1 activation (Figure 20). Moreover, CRY2 degradation was significantly reduced under NNMF conditions, thus implying its lower activation level in the absence of the GMF in WT plants (Figure 21). Both the processes seem to be independent from PHOT1 and phytochromes, because NNMF conditions did not significantly affect CRY1 phosphorylation and CRY2 level in *phyAphyB, phyA* and *phot1* seedlings with respect to WT plants (Figure 20 and 21).

Figure 20: CRY1 phosphorylation level of 3-day-old WT, *phot1, phyAphyB* etiolated seedlings exposed to GMF or NNMF conditions coupled with 20 µmol m^{-2} sec^{-1} blue light for 15 min. *cry1cry2* was used as negative control. The phosphatase treated sample was used to verify the actual nature of the phosphorylation shift. D=darkness; BL=blue light; red arrow=phosphorylated protein

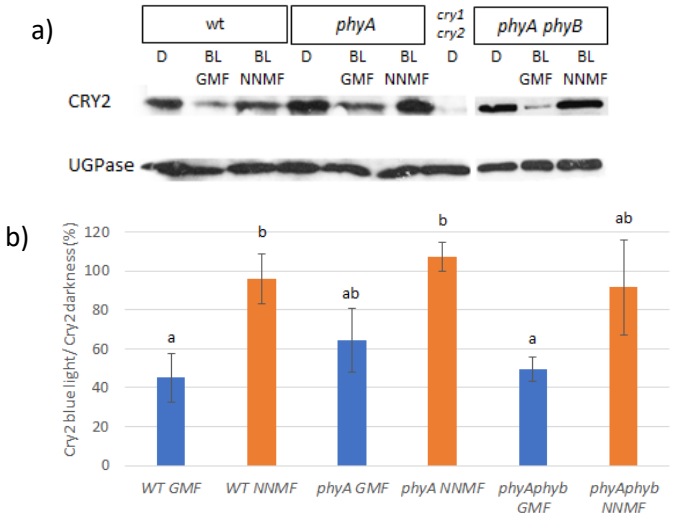

Figure 21: CRY2 degradation level of 3-day-old WT, *phyA* and *phyAphyB* etiolated seedlings exposed to GMF or NNMF conditions coupled with 0.5 µmol m^{-2} sec^{-1} blue light for 8 hours. (a) example of a gel. *cry1cry2* was used as negative control. D=darkness; BL=blue light; (b) histogram; data are expressed as percentage of CRY2 protein quantity after the blue light treatment with respect to the dark control condition. Error bars indicate the SD. Different letters associated with a statistically significant regulation ($p<0.05$).

To evaluate PHOT1 activation under blue light, the occurrence of its phosphorylation was monitored along with de-phosphorylation level of NON-PHOTOTROPIC HYPOCOTYL 3 (NPH3) as an indirect indicator of PHOT1 phosphorylation (Inoue *et al.*, 2008, Pedmale *et al.*, 2010), since PHOT1 degradation accidentally occurred in some samples. Phytochrome and cryptochrome KNOCK OUT (KO) mutants were used to focus on the role of phytochromes and cryptochrome in mediating PHOT1 activation. Our results highlighted the persistence of PHOT1 phosphorylation as well as NPH3 dephosphorylation under NNMF conditions in WT, *cry1cry2* and *phyAphyB* seedlings (Figure 22). Thereby, the GMF appears not to affect the occurrence of PHOT1 phosphorylation.

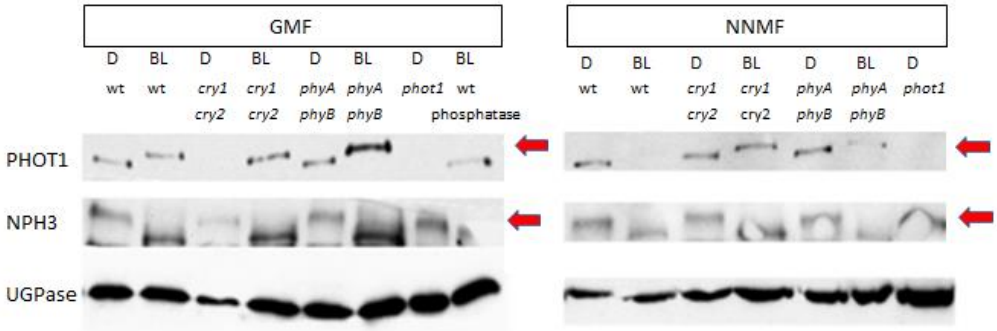

Figure 22: PHOT1 phosphorylation level and NPH3 dephosphorylation level of 3-day-old WT, *phot1, phyAphyB* etiolated seedlings exposed to GMF or NNMF conditions coupled with 20 µmol m^{-2} sec^{-1} blue light for 15 min. *phot1* was used as negative control. The phosphatase treated sample was used to verify the actual nature of the phosphorylation shift. Considering the PHOT1 proteolysis during protein extraction, NPH3 de-phosphorylation was used as an indirect indicator of PHOT1 phosphorylation. D=darkness; BL=blue light; red arrow=phosphorylated protein.

The GMF effect on PHYA and PHYB activation was assessed by monitoring their degradation level under red light (Ni *et al.*, 2014). The involvement of PHOT1, CRY1 and CRY2 in mediating these responses was assessed using *phot1* and *cry1cry2* mutant lines.

After 3 hours exposure to red light, PHYA was less degraded in WT seedlings exposed to GMF with respect to NNMF conditions (Figure 23), thus suggesting a lower activation of PHYA in the presence of the GMF. In *cry1cry2* and *phot1* seedlings, PHYA degradation was not significantly different between plants exposed to GMF and NNMF conditions. These results indicate that the lower PHYA activation level in the presence of the GMF is associated to PHOT1, CYR1 and CRY2.

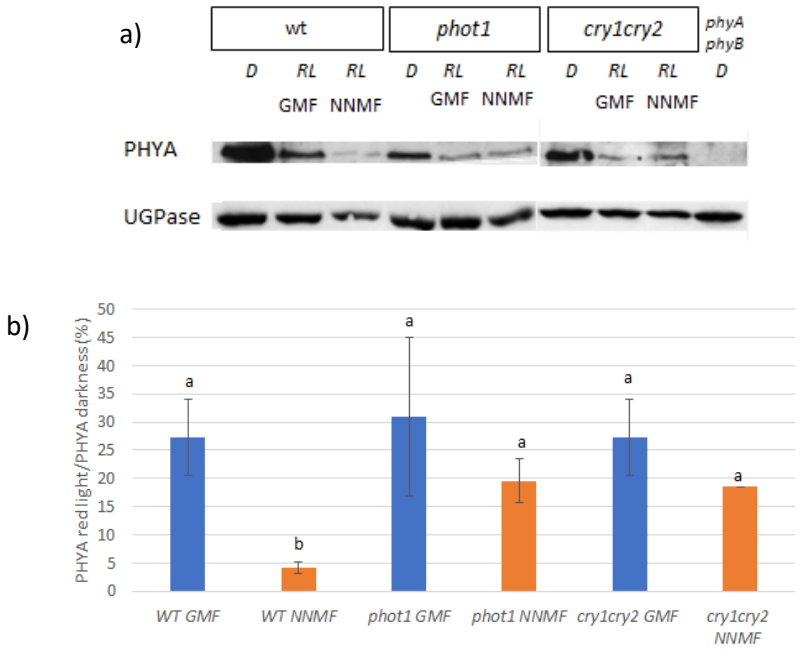

Figure 23: PHYA degradation level of 3-day-old WT, *cry1cry2,* and *phot1* etiolated seedlings exposed to GMF or NNMF conditions coupled with 60 µmol m^{-2} sec^{-1} red light for 3 hours. (a) example of a gel. *phyAphyB* was used as negative control. D=darkness; RL=red light; (b) histogram; data are expressed as percentage of PHYA protein quantity after the red-light treatment with respect to the dark control condition. Error bars indicate the SD. Different letters associated with a statistically significant regulation (p<0.05).

As for PHYB degradation (Figure 24) under red light, a significantly higher PHYB degradation occurred in WT plants exposed to GMF with respect to NNMF conditions. In both *cry1cry2* and *phot1* seedlings PHYB degradation was almost absent in the presence of the GMF (Figure 23). Thereby, the presence of the GMF appears to enhance PHYB activation level in a mechanism mediated by PHOT1, CRY1 and CRY2.

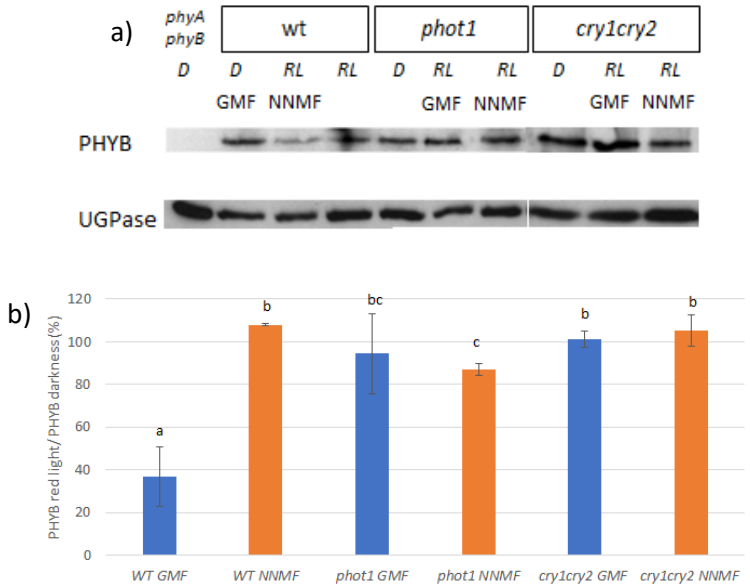

Figure 24: PHYB degradation level of 3-day-old WT, *cry1cry2* and *phot1* etiolated seedlings exposed to GMF or NNMF conditions coupled with 60 µmol m^{-2} sec^{-1} red light for 9 hours. (a) example of a gel. *phyAphyB* was used as negative control. D=darkness; RL=red light; (b) histogram; data are expressed as percentage of PHYB protein quantity after the red-light treatment with respect to the dark control condition. Error bars indicate the SD. Different letters associated with a statistically significant regulation (p<0.05).

The GMF stabilizes the circadian clock amplitude

The possible influence of the GMF on Arabidopsis circadian clock was evaluated even by discriminating the involvement of light in this process. Seven-day-old seedlings grown under long day (LD) and normal GMF conditions were exposed at ZT (dawn) to the darkness or left in LD conditions for 4 days and contemporary exposed to NNMF or GMF.

The expression of *LHY* and *PRR7* was evaluated every 4 hours starting from the beginning of the treatment. *LHY* is the morning gene encoding the Myb-domain transcription factor that acts together with CCA1 as repressor of PPRs and the evening clock factors (Alabadí *et al.*, 2001), whereas *PRR7* peak of expression occurred 6 h after dawn and its corresponding protein acts as a repressor of *LHY* and *CCA1* (Hayama *et al.*, 2017). *LHY* expression was measured both in dark and LD conditions, while PRR7 was successfully assayed only under LD conditions. All the results are plotted as relative gene expression as a function of time.

As clearly shown in Figure 25, under both GMF (Figure 25 a) and NNMF (Figure 25 b) conditions the switching to the darkness caused the internal clock resetting to its natural period length. After the first permanence of the light stimulus to the clock, *LHY* expression peak was indeed moved 4 hours later under CD with respect to LD conditions. While the dark exposure normally reduced the amplitude of the clock rhythm under GMF conditions (Figure 25 a), this behavior was not observed in absence of the GMF (Figure 25 b).

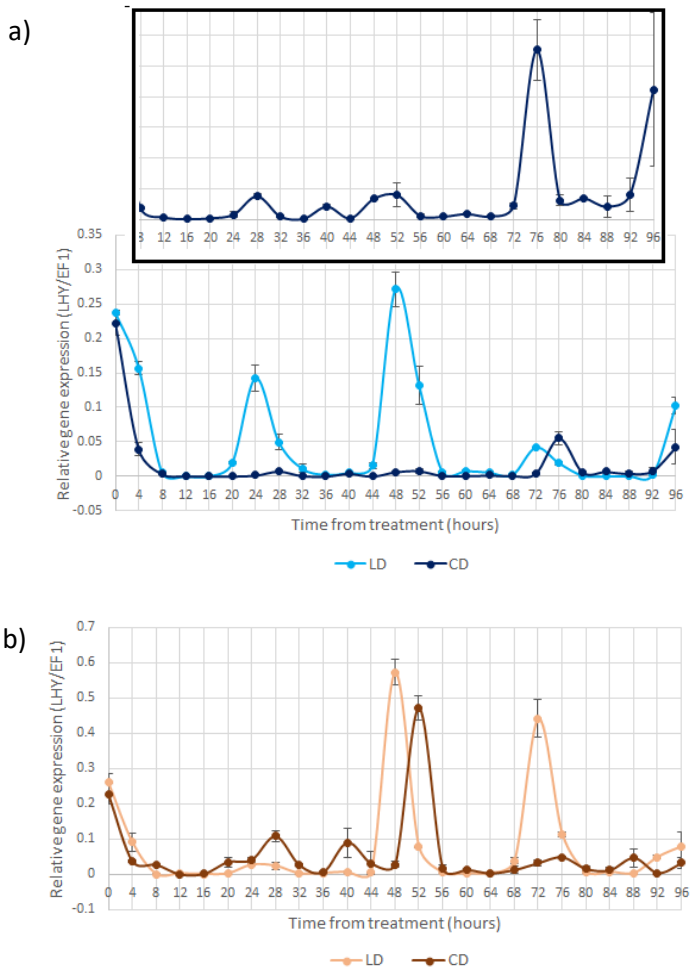

Figure 25: *LHY* relative expression starting from ZT when plants were exposed under GMF (a) or NNMF (b) conditions. The dark-shaped box in (a) reproduces LHY rhythm under CD coupled with GMF conditions using a lower scale. LD=long day white light; CD= continuous darkness; EF1= *eEF1Balpha2.*

A direct comparison between GMF and NNMF treatments clearly highlighted the GMF influence on *LHY* rhythm amplitude that appears to occur not only under CD conditions (Figure 26b), but even under LD exposure (Figure 26a).

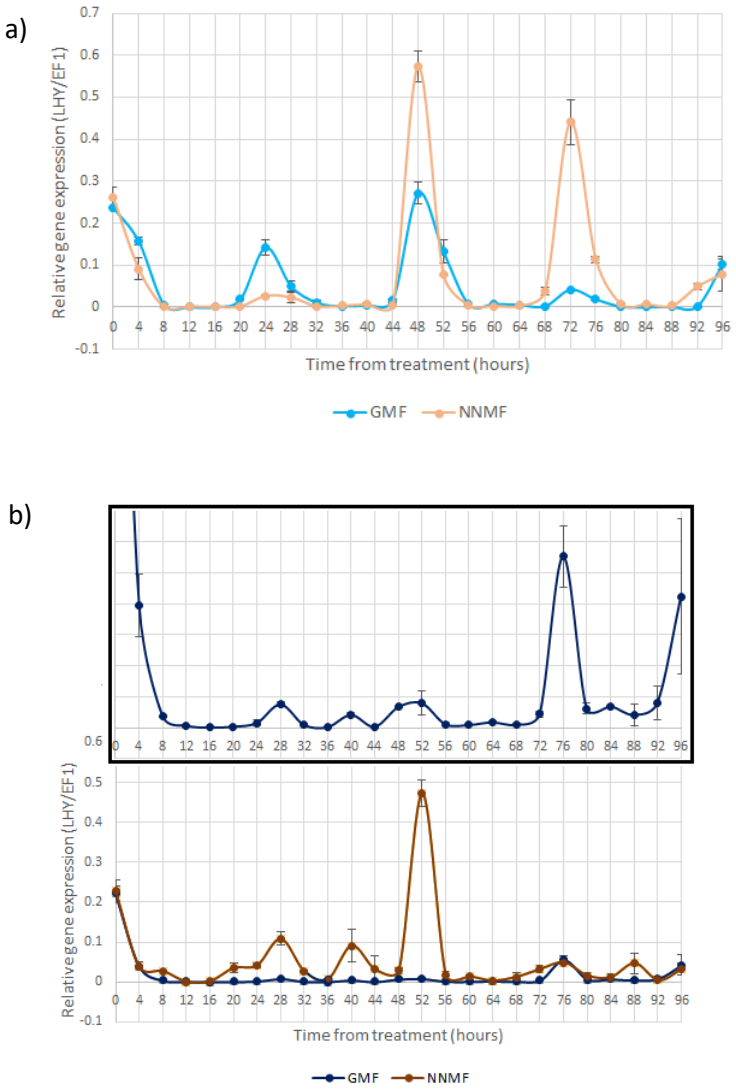

Figure 26: *LHY* relative expression starting from ZT when plants were exposed under long day white light (a) or continuous darkness (b) conditions. The dark-shaped box in (b) reproduces LHY rhythm under GMF conditions coupled with CD using a lower scale. GMF=Earth's magnetic field; NNMF= Near Null Magnetic field; EF1= *eEF1Balpha2.*

PPR7 rhythm was even affected by NNMF treatments under LD conditions (Figure 27) by showing a higher amplitude starting from 24 h after ZT.

Based on these preliminary results, we can hypothesize that the GMF appears to have a role in stabilizing the internal clock rhythm amplitude.

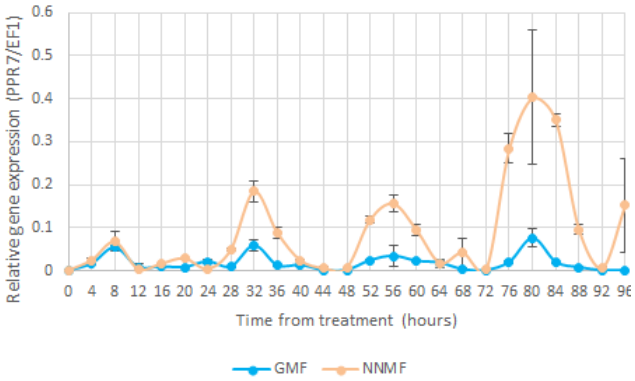

Figure 27: *PRR7* relative expression starting from ZT when plants were exposed under long day white light conditions coupled with GMF or NNMF treatment. GMF=Earth's magnetic field; NNMF= Near Null Magnetic field; EF1= *eEF1Balpha2.*

DISCUSSION

An accurate comparison between paleomagnetic data and Angiosperm fossils highlighted the occurrence of Angiosperm speciation during normal phase magnetic field polarity, thus implying a possible role of GMF polarity in plant evolution (Occhipinti, De Santis and Maffei, 2014). During polarity transitions, the GMF is reduced to a maximal mean intensity about 10% of the stable field, thus being comparable to NNMF conditions (Crain, 1971). Interestingly, NNMF delays Arabidopsis flowering time (Xu *et al.*, 2012), thus suggesting a correlation between Angiosperm speciation after a GMF reversal and its influence on timing of plant reproduction. Along with flowering time alteration, many other light and clock dependent plant processes appear to be influenced by MF variations, including photomorphogenesis (Maffei, 2014).

In this thesis work, the role of the GMF as a plant evolutionary driving force has been substantiated by monitoring the influence of reversed magnetic field and NNMF on Arabidopsis growth and gene expression. The study of the molecular bases related to NNMF-induced flowering delay under LD conditions along with the assessment of the GMF influence on the photomorphogenesis gene targets under different light conditions (by using photoreceptors mutant lines along with wild type plants) allow us to better understand the signals downstream Arabidopsis magnetoreception and their light and eventually clock dependence. The evaluation of the GMF influence on photoreceptor activation and on the circadian clock rhythm give us further information about the mechanism of GMF sensing upstream gene expression alteration.

The reversed GMF acts as an abiotic stress factor on plants

Plant development, productivity and overall fitness are dependent on the optimal shoot and root system architecture (Szymanowska-Pulka, 2013). The reduced root length and leaf size of plants exposed to reversed GMF conditions with respect to normal GMF polarity corroborates the hypothesis that GMF reversals may affect plant growth acting as an abiotic stress factor on plants. Furthermore, this evidence suggests the presence of an Arabidopsis sensing system able not only to perceive variations in magnetic field intensity (Maffei, 2014), but also to respond to magnetic field vector direction and polarity, as already seen in other living organisms (Deutschlander, Phillips and Borland, 1999).

Our gene expression data confirm the negative influence of the reversed GMF on plant growth and its role as an abiotic stress factor on plants. Cruciferin (a 12 S globulin) is the most abundant storage protein in the seeds of *A. thaliana* and without its phosphorylation and consequent degradation, embryos cannot develop properly (Job, 2005; Wan *et al.*, 2007). Moreover, its transcription level is under the control of abscisic acid (Kagaya *et al.*, 2005), which is usually involved in the response to abiotic stress (Lin and Tang, 2014). The GMF reversal affects the expression of the gene encoding for cruciferin 3; *CRU3* leaf upregulation correlates with a lower leaf expansion, whereas its significant root downregulation correlates with a reduced root length.

Copper is an essential cofactor for key processes in plants, but it exerts harmful effects when in excess or in low quantities (Printz *et al.*, 2016). COPT1 is the main transporter involved in Cu acquisition at the root level and it is upregulated in Cu-deficient plants in order to increase the absorption capacity at systemic level (Ravet and Pilon, 2013; Perea-García *et al.*, 2016;

Printz *et al.*, 2016). The effect of GMF reversal is a significant overexpression of *COPT1* in both shoots and roots, thus explaining the reduced plant growth. In particular, the transition metals Fe and Cu take a central role in redox control and electron transport in the cell. When the electron transport capacity in the chloroplast is limited, electrons can alter the redox state of the cell (Ravet and Pilon, 2013). In Arabidopsis the expression of the transcription factor *RRTF1* is specifically regulated by redox signals from the photosynthetic electron transport (Matsuo and Oelmüller, 2015), which derived from dynamic changes in pO_2 (Haddad, 2002). RRTF1 facilitates the synergistic co-activation of gene expression pathways and confer cross tolerance to abiotic and biotic stresses (Khandelwal *et al.*, 2008; Foyer, Karpinska and Krupinska, 2014). The reversal of the GMF induces a significant transcriptional overexpression of RRTF1, which acts in response to the production of a higher rate of reactive oxygen species (ROS) (Matsuo and Oelmüller, 2015). The altered plant capability to scavenge ROS and the enhancement of plant ROS level have been already demonstrated under MF intensities higher than that of the GMF (Sahebjamei, Abdolmaleki and Ghanati, 2007; Alemán *et al.*, 2014). The upregulation of *RRTF1* correlates with the downregulation of root scavenging enzymes in plants exposed to reversed GMF conditions, thus indicating that the alteration of oxygen scavenging is not only dependent from MF intensity, but also from its direction. The dramatic root downregulation of *CAT3*, *APX1* and *TAPX* indicates the reduced ability of root cells to scavenge H_2O_2, which is coupled to the reduced ability to dismutate the superoxide anion by downregulation of *FSD1*. Moreover, the root downregulation of *RbohD* correlates with the downregulation of genes encoding for scavenging enzymes, since *RbohD* activity promotes the activation of the ROS-scavenging response (Yao *et al.*, 2017). Therefore, the oxidative stress induced by the GMF reversal is higher in roots, which appear to be the main site of the response to reversed GMF. Alternatively, the observed different gene expression response in roots with respect to leaves could assess the presence of an independent mechanism of GMF polarity perception in different plant organs.

The reduced growth in reversed magnetic field conditions together with the enhancement of the oxidative stress and the reduced antioxidant response at the root level could be directly related to the observed major speciation of Angiosperms during normal phase GMF polarity (Occhipinti, De Santis and Maffei, 2014). Thereby, these results provide a compelling evidence in support of the hypothesis that the GMF reversals might have been one of the driving forces for plant evolution.

NNMF induces a delay in flowering by globally slowing down the transition to the plant reproductive stage

Successful reproduction ensures a species' survival. The reproductive success of flowering plants depends on flowering at the right moment. Hence, plants have evolved genetic and molecular networks integrating various environmental cues with endogenous signals in order to flower under optimal conditions (Fornara, de Montaigu and Coupland, 2010). NNMF-induced delay in Arabidopsis flowering time is maintained in our generation experiment, when plants are constantly grown under NNMF conditions, and is recovered when plants are grown in GMF conditions. This clearly demonstrates that the effect of NNMF exposure occurs in the growing plant and is due to the presence of a plant magnetoreceptor (Occhipinti, De Santis and Maffei, 2014). Interestingly, the NNMF starts acting on the plant development from the transition to the reproductive phase, such as already reported by Xu *et al.* (2013). Since that

time, the leaf area index as well as the stem length are reduced. However, the number of rosette leaves at bolting time is not influenced by NNMF. Thereby, these morphological data suggest that NNMF delays Arabidopsis reproductive transition but does not alter the plant development status at the flowering transition time though. Interestingly, despite the absence of NNMF-induced flowering delay in *cry1cry2* mutant plants exposed to 10 µmol m^{-2} s^{-1} blue light for 6 h in a 12 h photoperiod (Xu *et al.*, 2015), the NNMF delays flowering time even in *cry1cry2* mutant lines under our adopted LD white light conditions. Therefore, this observation suggests the presence of actors different from cryptochrome in mediating this response under LD conditions. The time-course analysis of WT rosette and flowering meristem genes allowed the evaluation of the influence of NNMF on the expression of the flowering integrator genes and on the upstream signal transduction pathways, thus discriminating those factors mostly involved in the observed delay in flowering (Figure 27).

NNMF-flowering delay is correlated to the downregulation of flowering integrator genes in the rosette

The transition to flowering is mediated by FT, which acts as a mobile molecule in plants, transferring the flowering signal from the rosette to the meristem. Its function is similar to that of TSF and both of them usually form a complex with FD (Tsuji, 2017). By analyzing the gene expression data, the flowering delay seems directly related to the rosette early downregulation of the flowering integrators *FT* and *TSF* together with *FD.* A similar expression pattern was already observed by Xu *et al.* (2012) for *FT* under long day white light.

The maintenance of the pool of stem cells and the indeterminate development of apical and axillary meristems is related to the homeodomain gene *WUS* and the *STM* gene, respectively (Lenhard, Jürgens and Laux, 2002). The center of the shoot apical meristem (SAM) is maintained in a vegetative state by the key floral repressor TFL1*,* which acts by repressing *LFY* and *AP1* (Liljegren *et al.*, 1999)*.* LFY plays a key role in the integration of flowering signals in parallel with FT to activate floral meristem identity genes, such as *AP1* (Liljegren *et al.*, 1999). Under NNMF conditions, the observed delay in flowering is correlated to a downregulation of rosette *LFY*, *AP1* and *FD* in the floral induction period, an upregulation of rosette *TFL1* during early flowering and a downregulation of rosette *WUS* and *STM* transcript level which occurs at the beginning of the flowering transition. A similar expression pattern was already observed by Xu *et al.* (2017) for *LFY* under 6 h blue light/6 h dark exposure.

NNMF downregulates the expression of Arabidopsis circadian clock and photoperiod gene pathways in the rosette

Under long day conditions, Arabidopsis flowering time is correlated to the interaction between the circadian clock and the photoperiod pathway, mediated by the late afternoon expression peak of *CO* and the corresponding higher protein concentration. CO promotes flowering by initiating transcription of the integrator genes *FT* and *TSF* (Tsuji, 2017). Similarly to what observed by Xu *et al.* (2012), NNMF conditions down-regulate *CO* under long day white light conditions. We also observed a correlation between CO transcript level and *FT*, since their downregulation stops at 22 DAS, two days before the bolting of NNMF-exposed plants. During LD, blue light promotes the interaction between GI and FKF1 in the late afternoon. These interactions stabilize the F-box proteins, allowing them to promote the degradation of a set of transcriptional repressors of *CO* (Song *et al.*, 2014). In Arabidopsis exposed to NNMF, a significant down-regulation of *FKF1* transcript level in the rosette is

correlated to *CO* downregulation in the early floral induction period. *FKF1* transcription is repressed by LHY and CCA1, which also negatively regulate *TOC1* expression (Endo, Araki and Nagatani, 2016). LHY and CCA1 are known to oppositely act as transcriptional activators of PPRs factors, whose peak transcript level occurs 8 after ZT, a time close to our plant material sampling. PPRs repress *LHY* and *CCA1* in a feedback loop (Hayama *et al.*, 2017). Therefore, the down-regulation of *LHY* and *CCA1* induced by the NNMF might be related to a higher transcription repression mediated by PPRs. Moreover, the lower *FKF1* and *TOC1* transcript level might be related to a higher LHY level under NNMF conditions. Interestingly, light is able to influence the transcription of *CCA1*, *LHY* and *GI* (Harmer, 2009). Therefore, the action on the circadian clock expression mediated by the NNMF might be light-dependent.

The circadian clock and the photoperiod pathways also interact to promote CO accumulation at the end of the day under LD conditions. PPRs are known to stabilize CO protein level during the early afternoon (Hayama *et al.*, 2017). Moreover, a complex composed by CRY2, CRY1 and PHYA promotes CO accumulation in the afternoon, under blue light. Differently, PHYB is known to reduce CO level in the morning in a red light dependent manner, while PHYA stabilizes CO under far-red light conditions (L. J. Liu *et al.*, 2008; Sarid-Krebs *et al.*, 2015). However, all the photoreceptors are constitutively expressed during the day (Golembeski *et al.*, 2014). It is the key function of the blue light promoted complex composed by FKF1 and CO to determine CO stabilization in the evening, allowing flowering under LD conditions (Golembeski *et al.*, 2014; Song *et al.*, 2014). As a consequence of CO stabilization at the end of the day, *FT* transcription is activated (L. J. Liu *et al.*, 2008). Although CO protein level was not monitored in our experiment, the observed reduced accumulation of *FT* transcripts under NNMF conditions could be also related to an influence of NNMF on photoreceptor activation. Moreover, FKF1 directly repress *FT* transcription, while a complex composed by CRY2 and CIB1 protein is able to promote *FT* expression (Endo, Araki and Nagatani, 2016). Therefore, photoreceptors could be involved in the mechanism of NNMF-induced flowering delay. Xu *et al.* (2015) suggested the absence of NNMF-promoted delay in flowering under specific red-light photoperiods and fluences, while blue light seems to be involved in this process in a cryptochrome dependent manner. However, the observed persistence of a NNMF-induce flowering delay in *cry1cry2* mutant plants under white light long day conditions suggests that cryptochrome is not the only actor in the promotion of this mechanism. Future experiments should aim to evaluate the flowering time even using other photoreceptor and internal clock mutant lines under our experimental conditions, considering the time of CO accumulation in the evening as a key point for discriminating clock and photoperiod pathway involvement in NNMF-induced flowering delay.

NNMF downregulates the expression of Arabidopsis gibberellin and thermo-sensory gene pathways in the rosette

Recently, photoreceptors (mainly cryptochrome and phytochromes) have been discovered to interact dependently from the light quality and intensity with the gibberellin and the thermosensitive flowering promoting pathways at the leaf level (Endo, Araki and Nagatani, 2016). Moreover, the circadian clock directly interferes with the expression of some genes belonging to both the gibberellin and thermo-sensory flowering promoting pathways (Imaizumi, 2010). Interestingly, while the genes belonging to the autonomous pathways (*NA050* and *SDG26*) seem not to be affected by the reduction of the GMF, NNMF conditions

influence the expression of the genes belonging to the gibberellin and the thermo-sensory pathways in the rosette.

The gibberellin pathway is composed by GA biosynthetic genes, called *Ga20ox1* and *Ga20ox2*, whose mutation reduces bioactive GA_4 and thus delays flowering under long day conditions (Rieu *et al.*, 2008). NNMF induces a down-regulation of *GA20ox2* immediately prior to floral induction under our experimental conditions. Similarly, *Ga20ox2* transcript level is reduced by NNMF under 12 h photoperiod of blue light (6 h/6 h) and is not affected in *cry1cry2* mutant under the same exposure conditions, thus suggesting a cryptochrome dependent downregulation of this gene (Xu *et al.*, 2017). However, the flowering delay persists in *cry1cry2* mutant lines under LD white light conditions. Interestingly, even the phytochrome mediated pathway is known to interact with the gibberellin pathway by the action of SENSITIVITY TO RED LIGHT REDUCED (SRR1), whose mutant showed an early flowering (Staiger *et al.*, 2003). Moreover, under LD conditions, *GA20ox1* and *GA20ox2* transcripts assume circadian rhythms, reaching the peak 8 h after ZT (Filo *et al.*, 2015), close to the time of our plant material sampling.

The vernalization pathway activates flowering by silencing *FLC* in response to prolonged exposure to low temperatures (Fornara, de Montaigu and Coupland, 2010). FLC acts together with SVP in repressing the transcription of *FT* (Mateos *et al.*, 2015). While *SVP* showed no significant regulation in plant exposed to NNMF, the early downregulation of *FT* might be therefore linked to *FLC* upregulation. *FRI* encodes a protein with two coiled-coil motifs and is required to increase *FLC* transcript level (Caicedo *et al.*, 2004). A slight but significant down-regulation of *FRI* was observed in Arabidopsis exposed to NNMF conditions only in early and late phase of floral induction, thus implying the absence of correlation between its downregulation and *FLC* transcription level under NNMF conditions. Thereby, changes in *FLC* expression could be related to other regulation mechanism induced by NNMF conditions. Interestingly, a phytochrome-mediated pathway is known to enhance *FLC* expression level and cryptochrome and phytochrome are generally involved in regulating flowering in a thermo-sensory pathway (Blázquez, Ahn and Weigel, 2003).

NNMF acts on the expression of flowering integrator genes and downregulates GA 20 OXIDASE 2 *and* FLOWERING LOCUS C *in the flowering meristem*

The floral induction is necessary to transform the shoot apical meristem from a vegetative meristem to an inflorescence meristem, which forms flowers. This morphological variation is associated with dramatic changes in gene expression, including increased expression of the integrator gene *SOC1*, encoding a MADS box transcription factor (Denay *et al.*, 2017). Activation of *SOC1* during long days requires FT and may be a direct response to the translocation of FT from the leaf to the flowering meristem. Oppositely*, SOC1* expression is repressed by FLC that acts as a potent repressor of flowering together with SVP (Hepworth *et al.*, 2002). Xu *et al.* (2017) already observed a *SOC1* downregulation promoted by NNMF under a blue light photocycle. In Arabidopsis flowering meristems of plants exposed to NNMF, *SOC1* downregulation occurs only during late flowering, at 28 DAS. However, the observed strong downregulation of *FT* in the rosette is indirectly related to a lower FT protein able to reach the flowering meristem (Shim, Kubota and Imaizumi, 2017). Therefore, the absence of NNMF-dependent regulation of *SOC1* in the early flowering stages might be related to a

compensation between the FT lower protein level at the flowering meristem and the downregulation of *FLC*, particularly at 22 DAS.

The interaction of FT with FD directly promotes the transcription of *AP1* and *LFY* (Shim, Kubota and Imaizumi, 2017), which are floral meristem identity genes encoding MADS box factor. The commitment to flower is ascertained by a direct positive feed-back interaction between *AP1* and *LFY* (Irish, 2010). *LFY* transcription is under direct control of SOC1, SVP and AGL24 (Wils and Kaufmann, 2017). The latter promoted the transition to the flowering meristem identity towards the reproductive phase (Smith *et al.*, 2011). The NNMF-induced flowering delay could be linked to *AP1* downregulation, excepting for its upregulation at 22 DAS, probably due to the previous *LFY* upregulation. *FD* expression level seems to be directly related to *AP1* level in the early flowering, since AP1 is known to negatively regulate its expression and that of all the genes involved in the control onset of flowering (Wils and Kaufmann, 2017). Interestingly, *LFY* is only found upregulated by NNMF when *SVP* is upregulated at 21 DAS, whereas it is significantly down-regulated after 23 DAS. *AGL24* is up-regulated during flowering at the same time when *AP1*, *LFY* and *SOC1* are down-regulated. Upregulated levels of *AGL24* expression correspond to the degree of precocious flowering and the reduction in *AGL24* expression is related to the degree of late flowering, suggesting that AGL24 is a dosage-dependent promoter of flowering (C. Liu *et al.*, 2008). In this regard, alteration of AGL24 activity determines Arabidopsis flowering time partially independently from SOC1, and vice versa (C. Liu *et al.*, 2008). Since *AGL24* is significantly down-regulated in NNMF exposed Arabidopsis in early phases of floral development and is significantly upregulated during flowering, this pattern of expression seems to be the most linked to the observed NNMF- promoted delay in flowering.

In Arabidopsis, the H3K4 demethylase JMJ14 is involved in repression of the floral integrator genes *FT* and *SOC1* by interacting with the NAC transcriptional repressors NAC050 and NAC052 (Ning *et al.*, 2015). In the floral meristem of NNMF exposed plants *JMJ14* did not show any significant regulation, whereas a slight and similar down-regulation was found for *NAC050* and *NAC052*. These results indicate that demethylation might not be involved in the delayed transition to flowering caused by exposure to NNMF.

On the other hand, active gibberellins are growth regulators that promote flowering in Arabidopsis. While GA2ox1 represses flowering, by reducing the content of active gibberellins, GA 20 oxidases (in particular GA20ox1 and GA20ox2) promote flower initiation redundantly, by affecting also other reproductive phenological phases such as the development of stem internodes (Rieu *et al.*, 2008; Campos-Rivero *et al.*, 2017). Differently from Xu *et al.* (2017) observations, NNMF causes not only a reduction in *GA20oxidases* transcript level, but even a reduction in *GA2ox1* mRNAs. However, the dramatic downregulation of *GA20x2* makes its pattern of expression unique in our cluster analysis. This regulation might be correlated to the upregulation of *SVP* in the early flowering stages, because SVP is involved in repressing *Ga20ox2* expression (Andrés *et al.*, 2014). In the late flowering stages *Ga20ox2* downregulation is even related to the delay in stem elongation. Xu *et al.* (2017) correlated NNMF-induced changes in the *GA20 oxidases* transcription to cryptochrome during flowering time. On the one hand, the persistence of NNMF-induced flowering delay in *cry1cry2* plants under LD white light suggests that the altered gibberellin level could not be the only factor which promotes this process under our experimental conditions. On the other hand, the

gibberellin pathway could be regulated even by molecules other than cryptochromes in a possible photoperiod and light dependent or independent manner.

The response to the GMF is not only light-dependent and differs between roots and shoots

During early photomorphogenesis, all photoreceptors play a key role in the genome-wide reprogramming of light signaling (Chen, Chory and Fankhauser, 2004; Kirchenbauer *et al.*, 2016; Lee *et al.*, 2017). Thereby, considering the GMF effect on different responses related to this process has been useful to investigate the light dependence of GMF influence on Arabidopsis and to discriminate photoreceptor involvement in this process.

Our morphological observations disagree with Xu and co-workers (Xu *et al.*, 2012) who found an increased hypocotyl growth induced by NNMF under long day white light conditions. Under blue light, CRY1 and CRY2 function in mediating hypocotyl length reduction and root elongation (Yao *et al.*, 2017) is not influenced by the GMF. Our results are in accordance with previous reports (Harris *et al.*, 2009), but in disagreement with the observations by Ahmad *et al.* (2007) who reported a cryptochrome enhanced activity in promoting hypocotyl growth inhibition under MF intensity 10 times higher than the GMF. Under red light, the MF intensity does not compromise phytochrome role in mediating the photomorphogenic response, as already reported (Ahmad *et al.*, 2007). In accordance with previous studies (Ahmad *et al.*, 2007; Harris *et al.*, 2009), even the hypocotyl and root growth of dark-exposed Arabidopsis seedlings is not influenced by MF intensity.

Although the GMF does not affect Arabidopsis photomorphogenic and skotomorphogenic phenotype, Arabidopsis seedlings respond to the GMF under both dark and light exposure by altering their gene expression. Thus, early Arabidopsis growth stages are able to perceive the GMF.

Roots respond to the GMF also in absence of light

Gene expression analyses surprisingly highlight the occurrence of a light-independent response to the GMF in WT roots mainly at the oxidative level, as previously showed in the reversal experiment. Root light-independent behavior in response to MF variations has been already reported in a high gradient MF continuous application where a magnetophoretic plastid displacement and a consequent induction of root curvature was found (Kuznetsov *et al.*, 1999). Further analyses are needed to better understand the possible involvement of roots in light-independent magnetoreception.

Interestingly, *CO* expression in roots was similarly affected under dark, long day and continuous WL conditions in WT plants, thus implying that the GMF influence on its expression is independent from light and may be related to other mechanisms. Interestingly, *CO* expression level is directly controlled by the endogenous clock, as mentioned above (Imaizumi, 2010).

The GMF influences the expression of photomorphogenesis-promoting genes under white light

Gene expression analyses under long day white light and continuous white light conditions ascertain the influence of light on the response to the GMF. The GMF influence on *CO* hypocotyl expression has been already reported in literature on 7-day-old seedlings under LD

white light, whereas *HY5* expression was not found affected under the same experimental conditions (Xu *et al.*, 2012). Differently, *HY5* expression level is affected by the GMF under LD conditions in the shoot and under white continuous light in the root, thus implying a role of active photoreceptors in promoting this process.

HY5 shoot mRNA level regulation is interestingly related to the GMF influence on *CHS* transcription, which is regulated by HY5 itself in leading to the photomorphogenic response (Lee *et al.*, 2007). Furthermore, both under long day and continuous white light exposure the GMF-influence on the expression of auxin signaling (*PIN3*) and anthocyanin biosynthesis (*ANS* and *CHS*) genes could be related not only to changes in the expression of their promoting transcription factors (Shin, Park and Choi, 2007; Sassi *et al.*, 2012), but even to the strong GMF affection on the transcription of *GST*, whose participation to the photomorphogenic response is mediated by multiple photoreceptors (Jiang *et al.*, 2010).

The GMF appears to independently influence root and shoot gene expression under blue and red light

As already reported (Xu *et al.*, 2017, 2018) the GMF affects gene expression under blue light (Figure 28). In WT plants, the opposite trend in *HYH, PIN1* and *PIN3* shoot expression with respect to roots underlines the individual shoot and root response to GMF under blue light. In particular, the GMF-induced reduction in *PIN1* shoot transcription level is correlated to the downregulation of *HYH* (Sassi *et al.*, 2012) whose level is regulated by blue light (Jiao *et al.*, 2003). On the opposite, *PIN1* higher expression level in the root could be related to the GMF-induced upregulation of *HYH*, whose expression occurred autonomously in the root with respect to the shoot (Zhang *et al.*, 2017).

Differently from previous studies (Harris *et al.*, 2009), our analyses show an influence of MF on root *CHS* transcripts during blue light exposure, thus implying a possible MF effect on anthocyanin expression levels under this light treatment. In this regard, blue light influence on anthocyanins has been already demonstrated at the protein level in a MF ten times higher than the GMF (500 μT) (Ahmad *et al.*, 2007). Our data suggest that anthocyanin accumulation is MF-dependent even at the gene expression level during the photomorphogenesis process induced by blue light. Last but not least, the reduction in *PKS1* shoot expression under blue light enlightens MF-influence on this process, since blue light normally enhances *PKS1* expression level (Lariguet *et al.*, 2006).

Considering the active cryptochrome key role in promoting photomorphogenesis by modulating auxin signaling and anthocyanin biosynthesis gene expression (Ma *et al.*, 2001; Cluis, Mouchel and Hardtke, 2004), cryptochrome involvement in the GMF-induced regulation of both *PIN1* and *CHS* transcript level implies the GMF influence on cryptochrome mediated photomorphogenesis. The cryptochrome dependence of GMF regulation of *PIN1* expression was already observed in 15-day-old Arabidopsis plants grown under a blue light photocycle (Xu *et al.*, 2018).

HYH gene expression is known to be enhanced by cryptochrome in a blue light dependent manner (Jiao *et al.*, 2003). The observed *HYH* cryptochrome - dependent upregulation in the presence of the GMF highlights the possible influence of the GMF on cryptochrome activation. Despite the prevalent rapid PHOT1-mediated influence on gene expression due to blue light (Jiao *et al.*, 2003), our data highlight that *PKS1* and *PIN3* regulation in WT plants is mediated by PHOT1 both in roots and shoots in a GMF-dependent manner. In this regard, *PKS1*

expression is known to be regulated by blue light to mediate the phototropism response linked to PHOT1 (Lariguet *et al.*, 2006), while PIN3 is involved in the phototropic response both in the shoot (Zhaojun *et al.*, 2011) and in the root (Zhang *et al.*, 2013).
Despite the reduced influence of PHYA on gene expression under blue light (Jiao *et al.*, 2003), phytochromes mediate the regulation of shoot *PIF3* and *PIN1* mRNA level and root *PKS1* and *PIN3* transcript quantity in the presence of MF. Interestingly, PHYA is known to induce *PKS1* transcription under blue light (Lariguet *et al.*, 2006).

Surprisingly, the gene expression is affected by the GMF not only under blue light, but also under red light (Figure 29). In WT plants, the GMF affects not only *HY5* mRNA level but even that of *LAF1*, *PKS1* and *PIF3*, whose expression is specifically connected to red light (Tepperman, Hwang and Quail, 2006). Therefore, the GMF can influence the red-light perception signal cascade. Moreover, the red-light-induced change in the expression of genes related to the auxin signaling and anthocyanin biosynthesis pathway confirms the GMF-influence on genes targeted by PIF3, HY5 and LAF1 transcription factors during photomorphogenesis (Shin, Park and Choi, 2007). In particular, the opposite GMF-induced trend of *CHS* expression in the root with respect to the shoot suggests the independent response to the GMF in the two plant organs even under red light exposure. In this regard, *HY5* expression level is affected by the GMF in the root only, thus confirming the presence of a root-autonomous HY5 photomorphogenic pathway in accordance with data reported in literature (Chen *et al.*, 2016).

Althougth *GST* transcript level is influenced even by blue light exposure (Jiang *et al.*, 2010), our results highlighted that the GMF interferes with *GST* shoot and root expression only under red light, thus corroborating the hypothesis of a red light dependent response to the GMF.

The gene expression data of *phyAphyB* seedlings suggest a potential partial role of phytochromes in mediating the response to the GMF under red light. In particular, the observed regulation of *PKS1* shoot expression might be PHYA-dependent, since this gene is known to be PHYA-specific under red light (Tepperman, Hwang and Quail, 2006). Moreover, the observed *GST* regulation at the root level could be PHYA dependent, since PHYB does not influence *GST* transcription under red light (Jiang *et al.*, 2010). Instead, *CHS* shoot up-regulation under GMF condition with respect to NNMF exposure could to be PHYB dependent. Phytochrome influence on *CHS* expression is indeed known to be PHYB dependent under red light and induced by PIF3 promoted degradation (Shin, Park and Choi, 2007).

Interestingly, our gene expression results imply that both cryptochromes and PHOT1 play a role in regulating the GMF-dependent changes in the expression of light-related genes under red light (see Figure 9 ad 10). While the change in the expression of some genes is only dependent from PHOT1 or cryptochromes (such as that of *GST* in the root, whose expression has been already reported as influenced by cryptochrome under red light (Jiang *et al.*, 2010)), other genes such as *PIN3* in the root and *PKS1* and *CHS* in the shoot are regulated by the GMF even dependently from phytochromes.

Arabidopsis light dependent response to the GMF could be partially mediated by changes in photoreceptor activation level

After having verified the GMF effect on the expression of genes downstream photoreceptor activation under both blue and red-conditions and photoreceptors contribution to this response, we demonstrated that GMF could partially mediate this response by affecting photoreceptor activation level (Figure 30).

The GMF enhances cryptochrome1 phosphorylation and cryptochrome 2 degradation

Our data confirm the influence of the GMF on cryptochrome activation. The finding that CRY1 phosphorylation is practically absent in WT, *phot1* and *phyAphyB* mutant lines exposed to blue light under NNMF conditions are in contrast with recent results that reported a lack of differences in CRY1 phosphorylation between NNMF and GMF conditions (Xu *et al.*, 2014). The higher blue light fluence used in our experiments allowed us to ascertain the GMF influence on CRY1 phosphorylation level and suggests the independence of this mechanism from phytochromes and PHOT1.

Our data show even a significant reduction in CRY2 degradation under NNMF conditions, assessing its independence from phytochromes. Previous studies showed a reduced blue light CRY2 phosphorylation rate induced by NNMF (Xu *et al.*, 2014). Moreover, CRY2 degradation level is faster under a MF higher than the GMF (Ahmad *et al.*, 2007) as a probable consequence of the demonstrated increase in CRY2 phosphorylation rate under high MF intensities (Xu *et al.*, 2014). Our data confirm the influence of MF intensity on CRY2 activation, showing its lower activation level in the absence of the GMF.

Finally, the GMF intensity appears not to affect the occurrence of PHOT1 phosphorylation and therefore its activation. However, the actual level of PHOT1 phosphorylation and consequent degradation should be better assessed in the future, especially considering PHOT1-dependent regulation of some genes in response to the GMF (Figure 28) and the general influence of MF on phosphorylation processes (Jones, 2016).

Considering the photomorphogenic experiment, the higher activation levels of CRY1 and CRY2 in the presence of the GMF could then be directly related to *HYH* and *CHS* upregulation at the root level. Therefore, the blue light response at the root gene expression level could be partially dependent from the GMF-influence on cryptochrome activation.

Comparing the blotting data with the flowering experiment, the retention of NNMF-induced flowering delay in *cry1cry2* mutant lines suggests that the influence of the GMF on cryptochrome activation is not the only player in promoting the delay in flowering. Therefore, evaluating the effect of the GMF on LOV domain containing F box photoreceptors could be useful to further investigate the role of these blue-light receptors in promoting this delay.

The GMF reduces phytocrome A degradation and enhances phytochrome B degradation

Surprisingly, the GMF even influences phytochromes activation level under red light. Under GMF conditions, PHYA degradation level in WT plants is similar to that reported by Debrieux, Trevisan and Fankhauser (2013) under a similar red light fluence and exposure time. Moreover, PHYB degradation level is higher than that observed under lower red light fluences (Ni *et al.*, 2014), but it is known that even after 4 days of exposure to continuous red light PHYB is not completely degraded, since light-stable (Ni *et al.*, 2013). However, NNMF conditions enhance PHYA degradation in WT plants, while PHYB degradation is almost absent.

Therefore, the GMF seems to positively affect PHYB activation level and negatively affect PHYA activation level. Both the responses seem to be mediated by CRY1, CRY2 and PHOT1, even if in their inactive form (Figure 29). In this regard, two CRY1 alleles (hy4-3 that encodes C-terminal 130 a.a. deleted CRY1 and hy4-6 that encodes CRY1 with a point mutation in the chromophore-binding domain) cause hyposensitivity to red light. Moreover, the dark-promoted interaction between CRY1 and PHYB is known to be disrupted by light stimulation of either photoreceptors (Hughes *et al.*, 2012), while PHYB interaction with CRY2 occurs under light conditions (Más *et al.*, 2000). Thereby, both the darkness and light promoted interactions between the photoreceptors could be on the base of this red light mediated response to the GMF. Further investigations need to be performed to understand how cryptochromes and PHOT1 could influence PHYA and PHYB activation level in their inactive form.

During the photomorphogenic experiment, the observed downregulation of *PKS1* in the shoot and *GST* in the shoot could be then correlated to a lower activation level of PHYA under GMF conditions. Moreover, *CHS* shoot up-regulation under GMF condition compared to NNMF exposure could be correlated to the higher activation level of PHYB under red light mediated by cryptochromes. Therefore, the GMF interference with the red light signaling gene pathway could partially occur by modulating PHYA and PHYB activation levels.

With regards to the flowering experiment, PHYB reduced activation level under NNMF conditions appear to be in contrast with the observed NNMF-induced flowering delay, since *phyB* mutants are known to flower earlier (Hajdu *et al.*, 2015). However, considering the high content of red light emitted by the sodium vacuum lamps used in the flowering experiment, evaluating phytochrome degradation even using different red light fluences could be useful to ascertain the GMF influence on PHYB activation under the conditions adopted in our experiment. Moreover, the influence of phytochromes other than A and B in promoting the flowering process (Sánchez-Lamas, Lorenzo and Cerdán, 2016) should be further estimate under NNMF conditions, especially considering the observed persistence of the GMF-dependent regulation of gene expression in *phyAphyB* mutant plants under red light.

The absence of the GMF destabilizes the circadian clock amplitude in a light-independent manner

Due to its diurnal rhythmicity, the GMF has been considered as a possible entrainer for the endogenous clock in animals, resetting its phase in a light dependent manner (Yoshii, Ahmad and Helfrich-Förster, 2009). In our experiments, the observed MF influence on the transcription of Arabidopsis clock genes and on the expression of genes under the control of Arabidopsis internal clock suggests that the GMF could interact with plant circadian rhythmicity. In the clock experiment, we verified for the first time the action of the GMF on Arabidopsis endogenous clock. Interestingly, the GMF seems not to act on the internal clock period, but on its amplitude, by stabilizing this parameter. The amplitude of the circadian clock clearly responds to the light environment; the clock amplitude is low in the dark and high in the light (Salome, Xie and McClung, 2008). The NNMF causes mainly an increase in *LHY* rhythm amplitude both in long day and continuous dark conditions, thus excluding the involvement of photoreceptors in this process. Apart from light, some other variables are able to act on the circadian rhythm amplitude. Increased chlorophyll, sugar and starch contents have been found to correlate with altered epigenetic regulation of the core oscillator genes *LHY* and *CCA1*, which resulted in altered amplitude of oscillations of their transcripts (Adams and Carré, 2011). Moreover, cold reduces the amplitude of cycles for clock components (Rensing and

Ruoff, 2002). In NNMF conditions *LHY* and *PPR7* rhythm amplitude appears to be mainly increased. Similarly, copper deficiency increases the amplitude in the oscillatory expression of two of the main components of the central oscillator, CCA1 and LHY, but their period remains mostly unaffected (Perea-García *et al.*, 2016). Moreover, acute perturbation in the redox status triggered by the immune signal salicylic acid does not compromise the circadian clock but rather leads to its reinforcement (Zhou *et al.*, 2015). Therefore, our observations suggest that NNMF conditions are perceived as a stress conditions by plants, such as already reported. Moreover, the observation of the GMF influence on stabilization of the amplitude of *LHY* is truly of impact, since transcripts with high-amplitude profiles in the circadian clock, such as *LHY*, might be expected to control circadian timing more effectively than those of low-amplitude profiles, such as *TOC1* (Flis *et al.*, 2015).

The amplitude of clock genes in etiolated seedlings is much lower than that seen in the light. However, the amplitude of both morning and evening loop genes increases within 24 h of illumination to values similar to the amplitudes seen in light-grown seedlings (Salome, Xie and McClung, 2008). Interestingly, the level of *CO* transcripts during the photomorphogenesis experiment is regulated in the root by the GMF under both light and dark conditions in a similar manner. Considering that CO expression is under the circadian clock control, its regulation could be related to the observed influence of the GMF on *LHY* expression, since the sampling of plants during the photomorphogenic experiment occurred at ZT time, when *LHY* peak expression occurs.

NNMF affects the expression of the internal clock genes under long day conditions during the transition to flowering. The plant collection occurred at noon, 6 hours after the light ZT. Interestingly, *CCA1, LHY* and *TOC1* transcript levels were downregulated with respect to GMF conditions. PPR factors are known to be approximately at their expression peak at that time, thus acting as repressors of *CCA1* and *LHY* expression (Harmer, 2009). Moreover, CCA1 and LHY promotes *PPR7* transcription (Oakenfull and Davis, 2017). Interestingly, our data suggests that *PPR7* transcript level is enhanced under LD conditions by NNMF, thus indicating a possible CCA1 overexpression that is known to cause late flowering (Lu *et al.*, 2012). However, the plant circadian clock is known to be different in both its amplitude and period dependently from the plant organ (Bordage *et al.*, 2016). Thereby, the different plant responses to the GMF could also depend from this aspect that must be further investigated in the future.

The circadian clock can also interact with many other networks, including responses to hormones (Hanano *et al.*, 2006), metabolic pathways (Kim *et al.*, 2017), cold signaling pathways (Rensing and Ruoff, 2002; Bieniawska *et al.*, 2008) and solute transport (Dodd et al., 2007; Haydon et al., 2011). In particular, the circadian clock directly modulates the expression of *PIF4* and *PIF5*, which encode transcription factors that regulate photomorphogenic responses in plants together with HY5 and HYH whose gene expression is dependent from light but without circadian patterns (Soy *et al.*, 2016). Therefore, when not related to HY5, the observed influence on auxin signaling in the photomorphogenesis experiment might be related to these transcription factors. Last, but not least, the strong influence of NNMF on gibberellin oxidase enzymes observed in the flowering experiment could be related to the alterations of the clock amplitude.

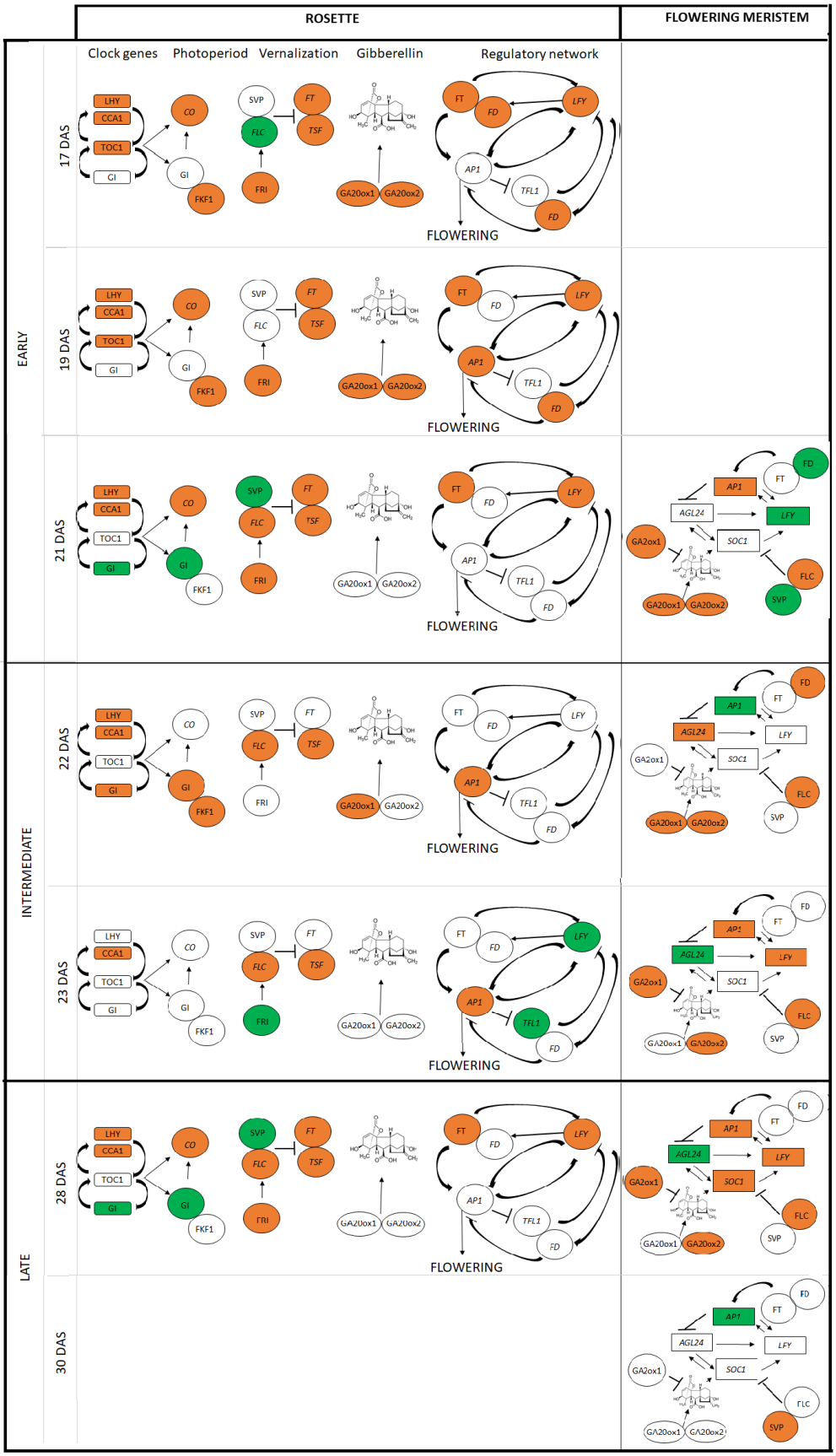

Figure 27: Representative scheme of NNMF-influence on the expression of the analysed rosette and meristem flowering genes grouped on the basis of their associated pathway. Upregulation is shown in green, downregulation in orange and no regulation in white. Italics characters indicate a regulation at gene expression level, while the normal characters a regulation at protein level.

⟶positive regulation; ⟞negative regulation; DAS=days after sowing.

a)

b)

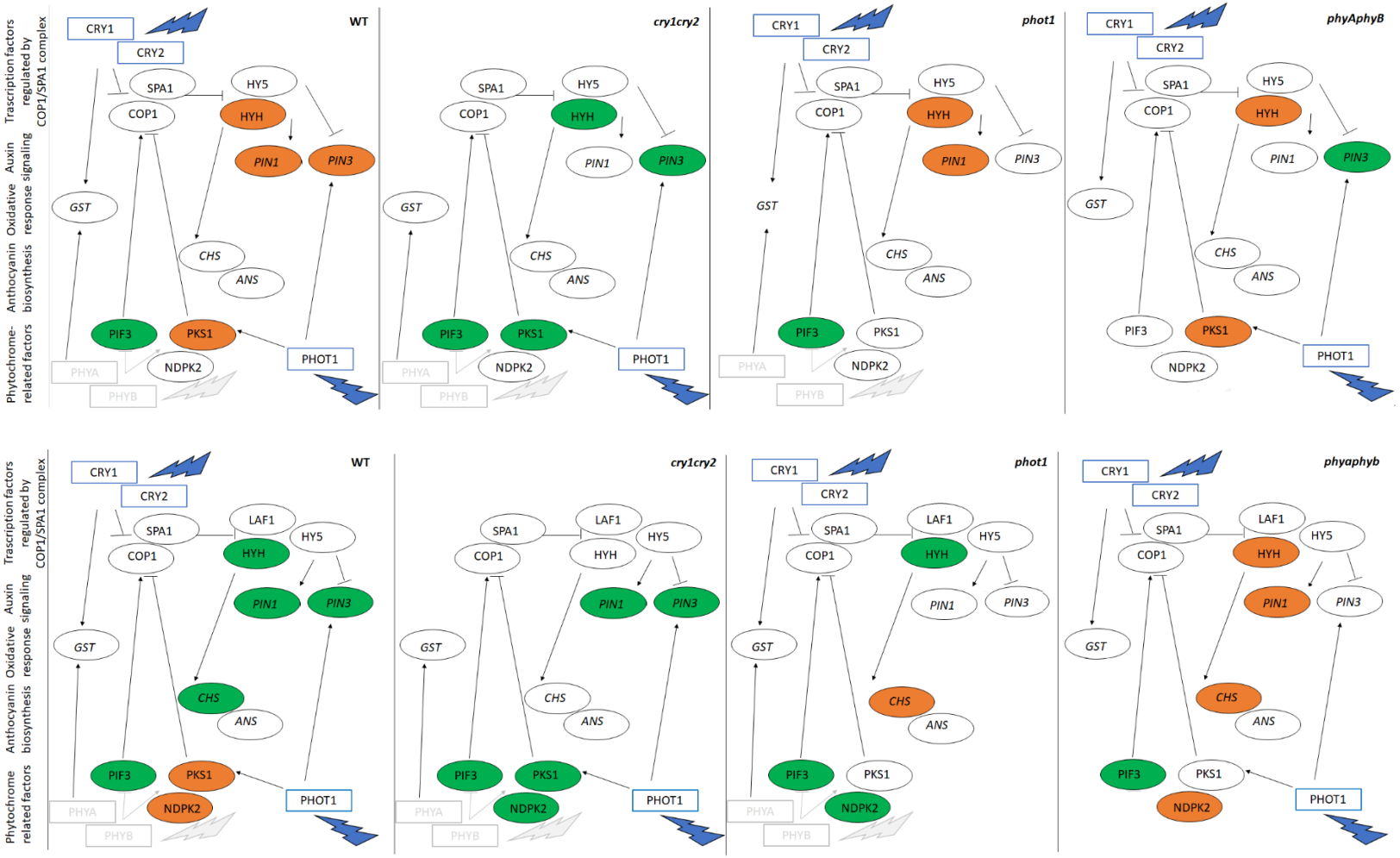

Figure 28: GMF-induced regulation of **shoot (a)** and **root (b)** light-related genes under **blue** light exposure. Squares represent photoreceptors, while the analysed genes are all in rounded shapes. Grey squares represent photoreceptors whose activation is not induced by the selected type of light. For genes, upregulation is shown in green, downregulation in orange and no regulation in white. Italics characters indicate a regulation at gene expression level, while the normal characters a regulation at protein level.

⟶ positive regulation; ⟊ negative regulatio

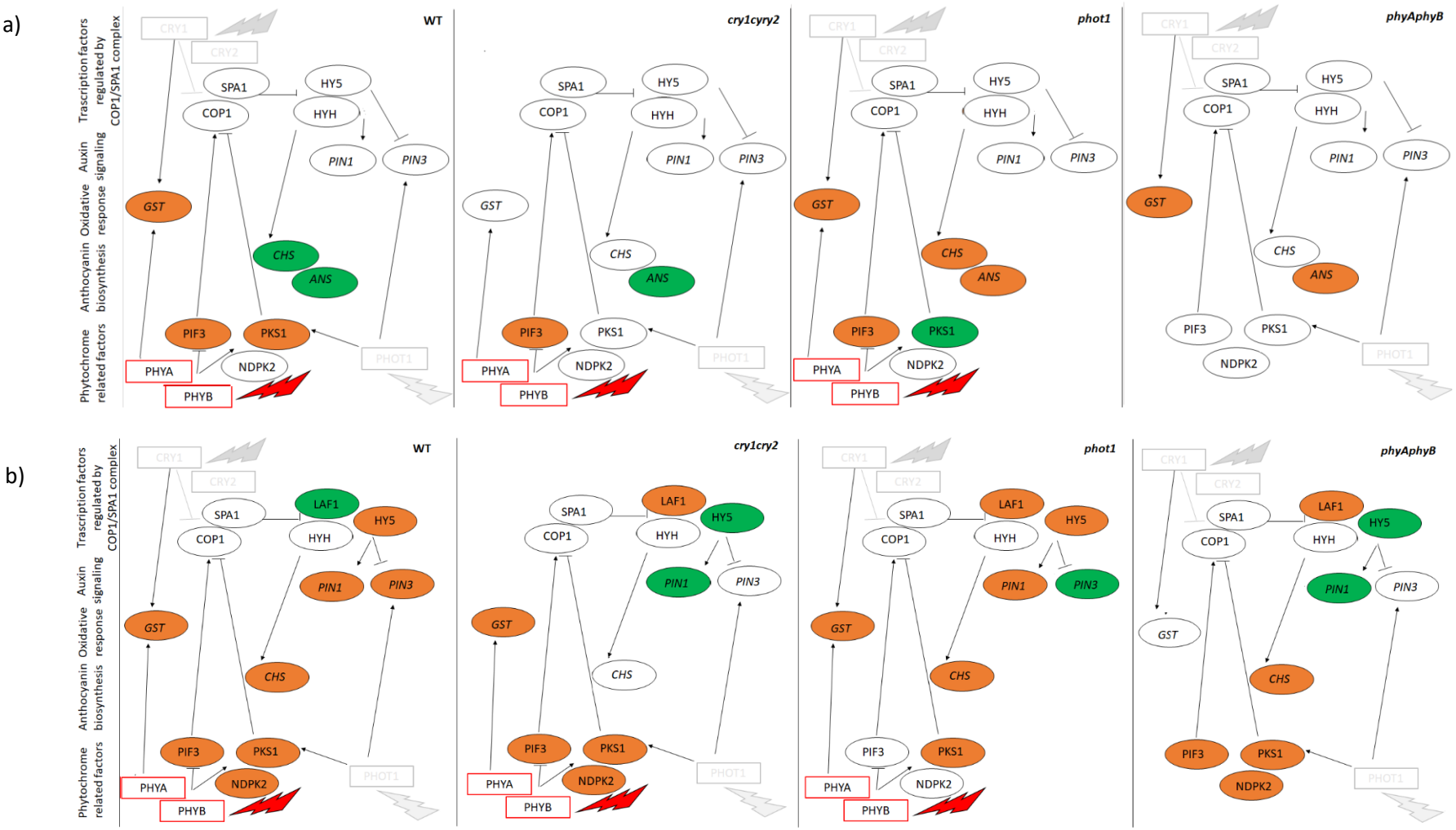

Figure 29: GMF-induced regulation of **shoot (a)** and **root (b)** light-related genes under **red** light exposure. Squares represent photoreceptors, while the analysed genes are all in rounded shapes. Grey squares represent photoreceptors whose activation is not induced by the selected type of light. For genes, upregulation is shown in green, downregulation in orange and no regulation in white. Italics characters indicate a regulation at gene expression level, while the normal characters a regulation at protein level.

→positive regulation; ⊣ negative regulation

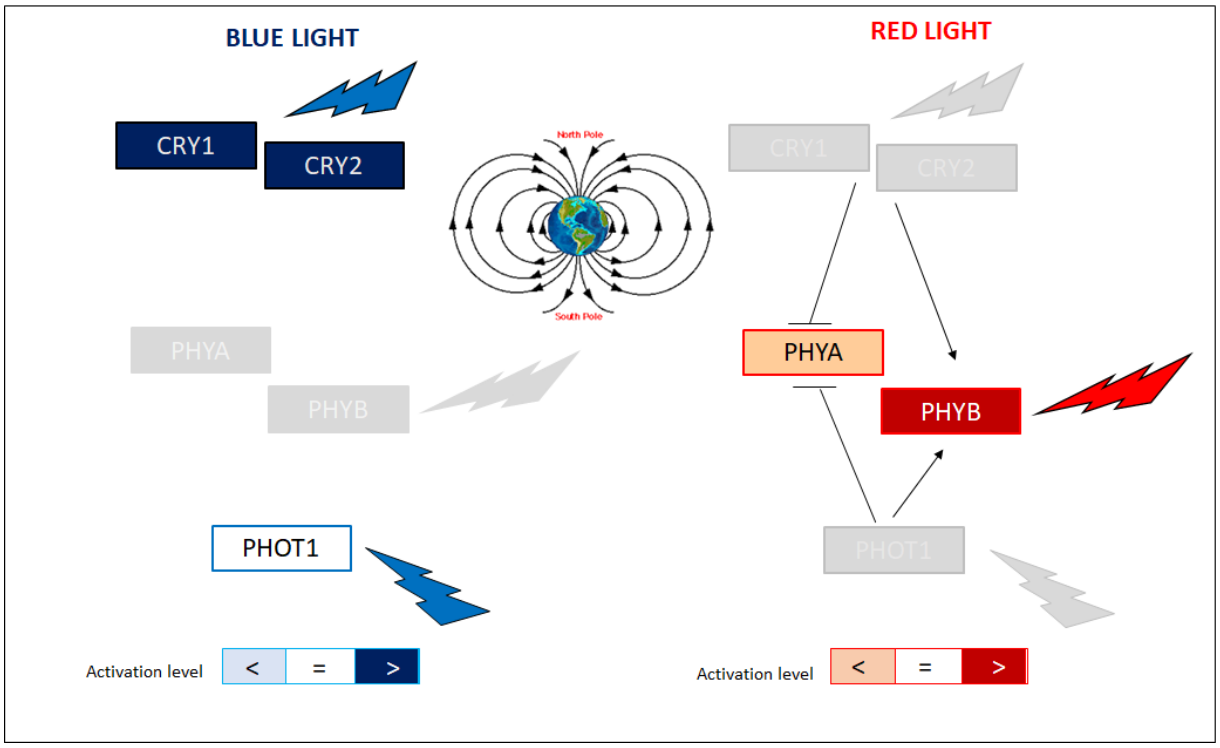

Figure 30: Summary scheme of GMF influence on photoreceptor activation under **blue** (left) and **red** (right) light exposure. Squares represent photoreceptors. Grey squares represent photoreceptors whose activation is not induced by the selected type of light. The two legends summarize the colour codes used to represent photoreceptor activation levels in GMF with respect to NNMF conditions. ⟶ positive regulation ⟊ negative regulation

CONCLUSIONS AND FUTURE PERSPECTIVES

Starting from 1960, the influence of MF intensities on plants has been deeply investigated. However, the effect of weak MF on plants has been less studied than the effect of MF intensities higher than those at the Earth's surface. Recent research advances have correlated Angiosperms evolution to period of normal GMF polarity, that occurs soon after GMF reversals characterized by NNMF intensities at the Earth's surface. However, the influence of GMF polarity on plant processes has not been investigated so far and the mechanism of GMF perception is still far from being elucidated.

In this study, investigating the effects of the current GMF values with respect to NNMF conditions and reversed GMF conditions on plants has provided new evidences on the influence of the GMF on plant growth and evolution and on the still unknown mechanism of plant magnetoreception.
In summary, the results of this work demonstrate:

- the negative influence of reserved magnetic field polarity on Arabidopsis growth;
- the differential transcriptomic response of shoots and roots to the GMF;
- the NNMF effect on Arabidopsis morphology at its late growth stages, mediated by a global delay in the transition to the plant reproductive stage by affecting gene expression;
- the capability of Arabidopsis to perceive the GMF independently from its growth stage;
- the capability of Arabidopsis to perceive not only the GMF intensity, but even its direction and polarity;
- the presence of a blue light-dependent response to the GMF partially mediated by the alteration of CRY1 and CRY2 activation level;
- the presence of a red-light response to the GMF partially mediated by the GMF-induced alteration of PHYA and PHYB activation level;
- the influence of inactive PHOT1, CRY1 and CRY2 in mediating the GMF-dependent alteration of PHYA and PHYB activation under red light, thus implying the presence of a mechanism downstream light activation in mediating this process;
- the presence of a light-independent response to the GMF (especially in the roots), based on an oxidative mechanism and an impressively fascinating effect of the GMF in stabilizing the amplitude of the internal clock rhythm.

These results confirm that the GMF can be considered as an abiotic stress factor for plants when its polarity is reversed and when its values are very low (NNMF). Arabidopsis growth is indeed affected by both GMF reversal and NNMF and the increasing of the oxidative stress occurs under both these exposures (especially at the root level). Therefore, the hypothesis of the GMF influence on plant evolution seems to be sustainable.
Despite the hypothesized role of cryptochromes as magnetoreceptors, the results of this work highlight for the first time the contribution of multiple photoreceptors and their interaction in mediating Arabidopsis response to the GMF. Future studies should be aimed to better understand the mechanism by which blue-light photoreceptors can mediate the level of phytochrome activation under red light in the presence of the GMF (i.e. by using double-hybrid yeast tests to assess the influence of the GMF in mediating photoreceptor interactions).

Moreover, the presence of a light-independent response to the GMF opens new horizons in understanding the real nature of plant magneto-sensing mechanism. In particular, the GMF-influence in stabilizing the circadian clock amplitude and the independence of this mechanism from light is to be further investigated. Considering that the internal clock is organ-dependent, future studies should separately evaluate the role of the GMF in affecting the circadian clock rhythm in different plant organs.

Having assessed an apparent different response of plant organs to the GMF, future studies should evaluate the actual independence of this response, even discriminating roots involvement in this process by studies conducted with plants in pot, thus adopting more natural experimental conditions.

Last but not least, proteomics and RNAseq analyses could help in providing a larger scale approach to study the mechanism of magneto-sensing, even by using selected mutants (for examples flowering and clock genes mutant lines).

ACKNOWLEDGEMENTS

It's been three years now, but the feeling is like it's been a minute and a thousand time at the same time. It's almost impossible to completely describe the impact of this amazing experience on my life, but I will try by thanking all the people that made that possible, hoping not to forget anyone

My sincere gratitude goes firstly to my advisor, **Prof. Massimo Maffei,** for giving me the opportunity to become a PhD student and work in his lab. I would like to thank him for choosing such a great topic for my PhD project and for always pushing me to go deeply inside its scientific meaning.

I would like to thank **Andrea Occhipinti** for having been such a special supervisor before my PhD experience. I am sure that his constant scientific and human suggestions have been crucial to make the right choice of becoming a PhD student.

My sincere gratitude goes to **Simone Bossi**, for all his technical teachings and all his suggestions during these years, since my experience as a master student. I would also like to thank **Andrea Capuzzo,** for all his advices along these years in the lab.

A special thank goes also to **Beatrice Demarchi** and **Gianpiero Vigani** for their encouraging words and their special advices in the last months of my PhD experience.

I want to thank **Cinzia Bertea** for a lot of reasons. As a "mentor", she introduced me to the molecular biology in the first year of my PhD, making me love something I was not going to appreciate so much. She has always supported me during all my experimental activities. I want to thank her for her professionality, all her suggestions, all her shared experience and mainly for her scientific enthusiasm and passion. But most of all I want to thank "Cinzia", for her humanity, her kindness, all her words to push me always towards the right direction. I might admit this experience would have been completely different without her help. Knowing her better is surely one of first reason why these three years have been so special.

I have been very lucky to meet so many people in my Italian lab during these years.

I remember with gratitude **Alberto Balocco** and **Riccardo Barbera**, since they were the first two students I could help in the lab, sharing what I was so lucky to learn from my studies and the precious teachings of all the lab. Actually, teaching is not only giving something, but also and mainly receiving something back. And this is absolutely amazing!

I am extremely happy to have met **Davide Patono**, who shared with me almost one year of my PhD, helping me with my project as a master student. I want to thank him because of his scientific enthusiasm that even pushed me to find new ideas for the development of my PhD project. It is really amazing we are still friends, my physician skier boy, and I truly hope we will never lose each other!

A special thank goes also to **Arianna Marengo** and **Francesco Molinaro**, since sharing our PhD and life experiences has been always inspiring.

I am very grateful to **Monirul Islam** for his precious help every time I need it when I was far from the lab during my abroad period and for sharing with me the scientific enthusiasm about our common PhD project.

I want to thank **Andrè Rivalta**, from the bottom of my heart. I met him in the lab when I was a first year PhD student and now he is one of my best friends. He has always been kind to me, standing right next to me during all the difficult and happy moments of this amazing experience. Thank you because I know that being your friend is truly a way to grow up, everyday!!!!

I have been super lucky for having met **Silvia Tortarolo**, a special girl who definitively made me understand what loyalty, kindness and altruism mean. I would like to thank her, because she has always been nice to me, helping me when I needed it, without asking anything in return. I am so grateful for these months together, since our friendship now is so consolidated that I'm sure I won't miss such a special person in the future.

Thank you all, **mousquetaires,** my lovely colleagues, friends and life companions! You have always been my strength, my shoulders and my anchor during these years. I cannot imagine how this experience would have been without you. All the pages of this dissertation would not be enough to explain how much I care about you, but one sentence can easily summarize what you mean for me: "One for all and all for one"! <3 **Cri, Ivo** and **Giuse**, I love you, from the very bottom of my heart!

The beauty of this amazing experience lays even in the incredible possibility of meeting people from all over the world to share science, but also life teachings. I might admit I have never completely understood the incredible power of Science before going away from my country.

My sincere gratitude goes to **Prof. John Christie** for the incredible opportunity of working in his lab at the **University of Glasgow** for seven months. I would like to thank him for his never-ending kindness, his professionality, his scientific advices and all the suggestions he has always given me so far. I even want to thank him for welcoming me and worrying about me to feel comfortable in his lab, thus making me realize the incredible luckiness of having found not only such a great scientist, but even a great scientist who could be an example for his precious humanity!

I would like to express my sincere gratitude to all my Scotland's lab mates, in particular **Jaynee, Stuart, Jan** and **Noriyuki.** Thanks for all your advices, for our talks and for all your precious teachings. I truly could have not found a better place where spending my PhD abroad period!

I want also to thank **Dr**. **Eirini Kaiserli** and all her lab, for all the precious advices they never hesitated to give and for always worrying about me to feel comfortable.

The Scotland experience has been surely the best one in my life so far. I truly can't explain all the ways it helped me to know myself better. I would like to thank **Woodside House** residents and all the people I met in the **Bower Building** for having made me realize the beauty of being a citizen of the world!!!

A special thank goes to the amazing girls who have been precious friends and confidents since we met. Thank you, **Anna**, for all the time you helped me feeling better, for all our walks together, for all the Greek sweets you made me taste, for all our teas and beers together, for our beautiful and compulsive "PRIMARK" shopping together and for sharing with me all the Glasgow's experience, form the lab stuff to the daily life. Thank you, **Elisa**, for our beautiful "ceilidh" experience together with Anna, for our long talks in the Bower Building common room, for every time you told me "You'll make it" and I fortunately actually did and especially for being my Italian best friend in Glasgow!!!! Thank you, **Tayra**, my sweet ad special Bosnian friend. I remember our three weeks together in Glasgow as a special gift life made me! Thank

you **Siyu**, my Chinese friend! It's amazing we found each other, even if in my last weeks in Glasgow. You always make me feel like I can do everything, and I truly thank you for trusting me every day, even at distance.

I want to thank from the bottom of my heart whoever supports me during all this experience even when I was far from home. I understood that loving someone doesn't mean being next to him every day but wishing him the very best and always being glad for his happiness. I would especially like to thank **Rossella** for always looking enthusiastic about my PhD experience and **Gaia** for her support and kindness all the time I felt lost!!

Thank you, **Elena**! You've been my "wonder wall" along my academic experience, literally. It's been amazing having met you at the beginning of my university path and I am impressively happy about our special friendship. Thanks a million times for being just you!

Thank you, **Ada** and **Gio'**, for being so special!!! You are my diamonds, and I truly mean that. I think that's enough to say not to fill lots of pages!!!! I love you deeply and you are an essential part of me! <3

Thank you, **Lorenzo**, for having always pushed me to believe in myself and for all your support along these years! It's amazing we are both becoming doctors in the same year, finally!!!!!

The most special thank goes to my **brother**, my **sister**, my **grandmother**, my **mum** and my **dad** for all their support, love, help, hugs, kisses, both real and virtual. All of this experience would have not been possible without you, because you have been my strength all the time I felt vulnerable, having shared with me all the happy and sad moments along these years. I am infinitely thankful to you, I am truly the luckiest sister, daughter and granddaughter in the world! The reaching of this important goal is yours, even more than mine! I should say is ours, definitely!!

Thank you all.

Chiara

REFERENCE LIST

Abe, M. *et al.* (2005) 'FD, a bZIP protein mediating signals from the floral pathway integrator FT at the shoot apex', *Science*, 309(5737), pp. 1052–1056. doi: 10.1126/science.1115983.

Adams, S. and Carré, I. A. (2011) 'Downstream of the plant circadian clock: output pathways for the control of physiology and development', *Essays in Biochemistry*, 49, pp. 53–69. doi: 10.1042/bse0490053.

Ahmad, M. *et al.* (2007) 'Magnetic intensity affects cryptochrome-dependent responses in Arabidopsis thaliana', *Planta*, 225(3), pp. 615–624. doi: 10.1007/s00425-006-0383-0.

Alabadí, D. *et al.* (2001) 'Reciprocal Regulation Between TOC1 and LHY / CCA1 Within the Arabidopsis Circadian Clock', *Science*, 293(2001), pp. 880–883. doi: 10.1126/science.1061320.

Alemán, E. I. *et al.* (2014) 'Effects of EMFs on some biological parameters in coffee plants (Coffea arabica L.) obtained by in vitro propagation', *Polish Journal of Environmental Studies*, 23(1), pp. 95–101.

An, H. (2004) 'CONSTANS acts in the phloem to regulate a systemic signal that induces photoperiodic flowering of Arabidopsis', *Development*, 131(15), pp. 3615–3626. doi: 10.1242/dev.01231.

Andrés, F. *et al.* (2014) 'SHORT VEGETATIVE PHASE reduces gibberellin biosynthesis at the *Arabidopsis* shoot apex to regulate the floral transition', *Proceedings of the National Academy of Sciences*, 111(26), pp. E2760–E2769. doi: 10.1073/pnas.1409567111.

Begara-Morales, J. C. *et al.* (2014) 'Dual regulation of cytosolic ascorbate peroxidase (APX) by tyrosine nitration and S-nitrosylation', *Journal of Experimental Botany*, 65(2), pp. 527–538. doi: 10.1093/jxb/ert396.

Belyavskaya, N. A. (2001) 'Ultrastructure and calcium balance in meristem cells of pea roots exposed to extremely low magnetic fields', *Advances in Space Research*, 28(4), pp. 645–650. doi: 10.1016/S0273-1177(01)00373-8.

Belyavskaya, N. A. (2004) 'Biological effects due to weak magnetic field on plants', *Advances in Space Research*, 34(7 SPEC. ISS.), pp. 1566–1574. doi: 10.1016/j.asr.2004.01.021.

Berr, A. *et al.* (2015) 'The trxG family histone methyltransferase SET DOMAIN GROUP 26 promotes flowering via a distinctive genetic pathway', *Plant Journal*, 81(2), pp. 316–328. doi: 10.1111/tpj.12729.

Bieniawska, Z. *et al.* (2008) 'Disruption of the Arabidopsis Circadian Clock Is Responsible for Extensive Variation in the Cold-Responsive Transcriptome', *Plant Physiology*, 147(1), pp. 263–279. doi: 10.1104/pp.108.118059.

Blázquez, M. A., Ahn, J. H. and Weigel, D. (2003) 'A thermosensory pathway controlling flowering time in Arabidopsis thaliana', *Nature Genetics*, 33(2), pp. 168–171. doi: 10.1038/ng1085.

Bliss, V. L. and Heppner, F. H. (1976) 'Circadian activity rhythm influenced by near zero magnetic field', *Nature*, 261, pp. 411–412. doi: 10.1038/261411a0.

Bordage, S. *et al.* (2016) 'Organ specificity in the plant circadian system is explained by different light inputs to the shoot and root clocks', *New Phytologist*, 212(1), pp. 136–149. doi: 10.1111/nph.14024.

Brown, F. A. (1976) 'Biological clocks: Endogenous cycles synchronized by subtle geophysical rhythms', *Biosystems*, 8(2), pp. 67–81. doi: https://doi.org/10.1016/0303-2647(76)90010-1.

Buchachenko, A. (2016) 'Why magnetic and electromagnetic effectsin biology are irreproducible and contradictory?', *Bioelectromagnetics*, 37(1), pp. 1–13. doi: 10.1002/bem.21947.

Caicedo, A. L. *et al.* (2004) 'Epistatic interaction between Arabidopsis FRI and FLC flowering time genes generates a latitudinal cline in a life history trait', *Proceedings of the National Academy of Sciences of*

the United States of America, 101(44), pp. 15670–15675. doi: https://doi.org/10.1073/pnas.0406232101.

De Caluwé, J. *et al.* (2016) 'A Compact Model for the Complex Plant Circadian Clock', *Frontiers in Plant Science*, 7(February), pp. 1–15. doi: 10.3389/fpls.2016.00074.

Campos-Rivero, G. *et al.* (2017) 'Plant hormone signaling in flowering: An epigenetic point of view', *Journal of Plant Physiology*, 214(October 2016), pp. 16–27. doi: 10.1016/j.jplph.2017.03.018.

Chen, M., Chory, J. and Fankhauser, C. (2004) 'Light Signal Transduction in Higher Plants', *Annual Review of Genetics*, 38(1), pp. 87–117. doi: 10.1146/annurev.genet.38.072902.092259.

Chen, X. *et al.* (2016) 'Shoot-to-Root Mobile Transcription Factor HY5 Coordinates Plant Carbon and Nitrogen Acquisition Report Shoot-to-Root Mobile Transcription Factor HY5 Coordinates Plant Carbon and Nitrogen Acquisition', *Current Biology*, 26(5), pp. 640–646. doi: 10.1016/j.cub.2015.12.066.

Cho, H.-Y. *et al.* (2006) 'Physiological Roles of the Light, Oxygen, or Voltage Domains of Phototropin 1 and Phototropin 2 in Arabidopsis', *Plant Physiology*, 143(1), pp. 517–529. doi: 10.1104/pp.106.089839.

Cluis, C. P., Mouchel, C. F. and Hardtke, C. S. (2004) 'The Arabidopsis transcription factor HY5 integrates light and hormone signaling pathways', *Plant Journal*, 38(2), pp. 332–347. doi: 10.1111/j.1365-313X.2004.02052.x.

Contento, A. L. and Bassham, D. C. (2010) 'Increase in catalase-3 activity as a response to use of alternative catabolic substrates during sucrose starvation', *Plant Physiology and Biochemistry*, 48(4), pp. 232–238. doi: 10.1016/j.plaphy.2010.01.004.

Crain, I. K. (1971) 'Possible direct causal relation between geomagnetic reversals and biological extinctions', *Bulletin of the Geological Society of America*, 82(9), pp. 2603–2606. doi: 10.1130/0016-7606(1971)82[2603:PDCRBG]2.0.CO;2.

Debrieux, D., Trevisan, M. and Fankhauser, C. (2013) 'Conditional Involvement of CONSTITUTIVE PHOTOMORPHOGENIC1 in the Degradation of Phytochrome A', *Plant Physiology*, 161(4), pp. 2136–2145. doi: 10.1104/pp.112.213280.

Denay, G. *et al.* (2017) 'A flower is born: an update on Arabidopsis floral meristem formation', *Current Opinion in Plant Biology*, 35, pp. 15–22. doi: 10.1016/j.pbi.2016.09.003.

Deutschlander, M. E., Phillips, J. B. and Borland, S. C. (1999) 'The case for light-dependent magnetic orientation in animals.', *The Journal of Experimental Biology*, 202(8), pp. 891–908. doi: print.

Endo, M., Araki, T. and Nagatani, A. (2016) 'Tissue-specific regulation of flowering by photoreceptors', *Cellular and Molecular Life Sciences*, 73(4), pp. 829–839. doi: 10.1007/s00018-015-2095-8.

Filo, J. *et al.* (2015) 'Gibberellin driven growth in elf3 mutants requires PIF4 and PIF5', *Plant Signaling and Behavior*, 10(3), p. e992707. doi: 10.4161/15592324.2014.992707.

Flis, A. *et al.* (2015) 'Defining the robust behaviour of the plant clock gene circuit with absolute RNA timeseries and open infrastructure.', *Open biology*, 5(10), pp. 764–776. doi: 10.1098/rsob.150042.

Fomicheva, V. M. *et al.* (1992) 'Dynamics of RNA and protein syntheses in cells of root meristems of pea, flax and lentil', *Biofizika*, 37, pp. 750–758.

Fomicheva, V. M., Govoroon, R. D. and Danilov, V. I. (1992) 'Proliferative activity and cell reproduction in meristems of seedling roots of pea, flax and lentil under conditions of screening of a geomagnetic field', *Biofizika*, 37, pp. 745–749.

Fornara, F., de Montaigu, A. and Coupland, G. (2010) 'SnapShot: Control of flowering in arabidopsis', *Cell*, 141(3), pp. 3–5. doi: 10.1016/j.cell.2010.04.024.

Foyer, C. H., Karpinska, B. and Krupinska, K. (2014) 'The functions of WHIRLY1 and REDOX-RESPONSIVE

TRANSCRIPTION FACTOR 1 in cross tolerance responses in plants: a hypothesis', *Philosophical Transactions of the Royal Society B: Biological Sciences*, 369(1640), pp. 20130226–20130226. doi: 10.1098/rstb.2013.0226.

Frankel, R. B. (1990) *Iron biominerals: an overview*.

Franklin, K. A., Allen, T. and Whitelam, G. C. (2007) 'Phytochrome A function in red light sensing', *Plant Journal*, 50(1), pp. 108–117. doi: 10.1111/j.1365-313X.2007.03036.x.

Gajdardziska-Josifovska, M. *et al.* (2001) 'Discovery of nanocrystalline botanical magnetite', *European Journal of Mineralogy*, 13(May 2000), pp. 863–870. doi: 10.1127/0935-1221/.

Galland, P. and Pazur, A. (2005) 'Magnetoreception in plants', *Journal of Plant Research*, 118(6), pp. 371–389. doi: 10.1007/s10265-005-0246-y.

Gangappa, S. N. and Botto, J. F. (2016) 'The Multifaceted Roles of HY5 in Plant Growth and Development', *Molecular Plant*, 9(10), pp. 1353–1365. doi: 10.1016/j.molp.2016.07.002.

Ghodbane, S. *et al.* (2013) 'Bioeffects of Static Magnetic Fields: Oxidative Stress, Genotoxic Effects, and Cancer Studies', *BioMed Research International*, 2013, pp. 1–12. doi: 10.1155/2013/602987.

Glatzmaiers, G. A. and Roberts, P. H. (1995) 'A three-dimensional self-consistent computer simulation of a geomagnetic field reversal', *Nature*, pp. 203–209. doi: 10.1038/377203a0.

Golembeski, G. S. *et al.* (2014) 'Photoperiodic flowering regulation in Arabidopsis thaliana', *Advances in botanical research*, 72, pp. 1–28. doi: 10.1016/B978-0-12-417162-6.00001-8.

Haddad, J. J. (2002) 'Oxygen sensing mechanisms and the regulation of redox-responsive transcription factors in development and pathophysiology', *Respir Res*, 3, pp. 26–53. doi: 10.1002/bdrb.20230.

Hajdu, A. *et al.* (2015) 'High-level expression and phosphorylation of phytochrome B modulates flowering time in Arabidopsis', *Plant Journal*, 83(5), pp. 794–805. doi: 10.1111/tpj.12926.

Hall, A. *et al.* (2001) 'Circadian Clock-Regulated Expression of Phytochrome and Cryptochrome Genes in Arabidopsis', *Plant physiology*, 127, pp. 1607–1616. doi: 10.1104/pp.010467.1.

Halliday, K. J. and Martı, J. F. (2009) 'Integration of Light and Auxin Signaling', *Cold Spring Harbor Perspectives in Biology*, 1(6), pp. a001586–a001586. doi: 10.1101/cshperspect.a001586.

Hanano, S. *et al.* (2006) 'Multiple phytohormones influence distinct parameters of the plant circadian clock', *Genes to Cells*, 11(12), pp. 1381–1392. doi: 10.1111/j.1365-2443.2006.01026.x.

Harmer, S. L. (2009) 'The Circadian System in Higher Plants', *Annual Review of Plant Biology*, 60(1), pp. 357–377. doi: 10.1146/annurev.arplant.043008.092054.

Harris, S. R. *et al.* (2009) 'Effect of magnetic fields on cryptochrome-dependent responses in Arabidopsis thaliana', *Journal of The Royal Society Interface*, 6(41), pp. 1193–1205. doi: 10.1098/rsif.2008.0519.

Hayama, R. *et al.* (2017) 'PSEUDO RESPONSE REGULATORs stabilize CONSTANS protein to promote flowering in response to day length', *The EMBO Journal*, 36(7), pp. 904–918. doi: 10.15252/embj.201693907.

Helliwell, C. A. *et al.* (2015) 'How is FLC repression initiated by cold ?', *Trends in Plant Science*. Elsevier Ltd, 20(2), pp. 76–82. doi: 10.1016/j.tplants.2014.12.004.

Hepworth, S. R. *et al.* (2002) 'Antagonistic regulation of flowering-time gene SOC1 by CONSTANS and FLC via separate promoter motifs', *EMBO Journal*, 21(16), pp. 4327–4337. doi: 10.1093/emboj/cdf432.

Hore, P. J. and Mouritsen, H. (2016) 'The Radical-Pair Mechanism of Magnetoreception', *Annual Review of Biophysics*, 45(1), pp. 299–344. doi: 10.1146/annurev-biophys-032116-094545.

Hughes, R. M. *et al.* (2012) 'Light-dependent, dark-promoted interaction between arabidopsis cryptochrome 1 and phytochrome b proteins', *Journal of Biological Chemistry*, 287(26), pp. 22165–22172. doi: 10.1074/jbc.M112.360545.

Imaizumi, T. (2010) 'Arabidopsis circadian clock and photoperiodism: time to think about location', *Current Opinion in Plant Biology*, 13(1), pp. 83–89. doi: 10.1016/j.pbi.2009.09.007.

Irish, V. F. (2010) 'The flowering of Arabidopsis flower development', *Plant Journal*, 61(6), pp. 1014–1028. doi: 10.1111/j.1365-313X.2009.04065.x.

Jacobs, J. A. and Sinno, K. (1960) 'World-Wide Characteristics of Geomagnetic Micropulsations', *Geophysical Journal of the Royal Astronomical Society*, 3(3), pp. 333–353. doi: 10.1111/j.1365-246X.1960.tb01707.x.

Jang, S., Torti, S. and Coupland, G. (2009) 'Genetic and spatial interactions between FT, TSF and SVP during the early stages of floral induction in Arabidopsis', *Plant Journal*, 60(4), pp. 614–625. doi: 10.1111/j.1365-313X.2009.03986.x.

Jiang, H.-W. *et al.* (2010) 'A Glutathione S-Transferase Regulated by Light and Hormones Participates in the Modulation of Arabidopsis Seedling Development', *Plant Physiology*, 154(4), pp. 1646–1658. doi: 10.1104/pp.110.159152.

Jiao, Y. *et al.* (2003) 'A Genome-Wide Analysis of Blue-Light Regulation of Arabidopsis Transcription Factor Gene Expression during Seedling Development', *Plant physiology*, 133, pp. 1480–1493. doi: 10.1104/pp.103.029439.chromosome.

Jiménez-Quesada, M. J., Traverso, J. Á. and Alché, J. de D. (2016) 'NADPH Oxidase-Dependent Superoxide Production in Plant Reproductive Tissues', *Frontiers in Plant Science*, 7(March), pp. 1–13. doi: 10.3389/fpls.2016.00359.

Job, C. (2005) 'Patterns of Protein Oxidation in Arabidopsis Seeds and during Germination', *Plant Physiology*, 138(2), pp. 790–802. doi: 10.1104/pp.105.062778.

Jones, A. R. (2016) 'Magnetic field effects in proteins', *Molecular Physics*, 114(11), pp. 1691–1702. doi: 10.1080/00268976.2016.1149631.

Kagaya, Y. *et al.* (2005) 'Indirect ABA-dependent regulation of seed storage protein genes by FUSCA3 transcription factor in Arabidopsis', *Plant and Cell Physiology*, 46(2), pp. 300–311. doi: 10.1093/pcp/pci031.

Kang, B. *et al.* (2008) 'Multiple interactions between cryptochrome and phototropin blue-light signalling pathways in Arabidopsis thaliana', *Planta*, 227(5), pp. 1091–1099. doi: 10.1007/s00425-007-0683-z.

Kangasjarvi, S. *et al.* (2008) 'Diverse roles for chloroplast stromal and thylakoid-bound ascorbate peroxidases in plant stress responses', *Biochemical Journal*, 412(2), pp. 275–285. doi: 10.1042/BJ20080030.

Kattnig, D. R., Solov'yov, I. A. and Hore, P. J. (2016) 'Electron spin relaxation in cryptochrome-based magnetoreception', *Physical Chemestry Chemical Physics*, 18(18), pp. 12443–12456. doi: 10.1039/C5CP06731F.

Khandelwal, A. *et al.* (2008) 'Arabidopsis Transcriptome Reveals Control Circuits Regulating Redox Homeostasis and the Role of an AP2 Transcription Factor', *Plant Physiology*, 148(4), pp. 2050–2058. doi: 10.1104/pp.108.128488.

Kim, J. A. *et al.* (2017) 'The importance of the circadian clock in regulating plant metabolism', *International Journal of Molecular Sciences*, 18(12). doi: 10.3390/ijms18122680.

Kim, Y. H. *et al.* (2011) 'Transgenic poplar expressing Arabidopsis NDPK2 enhances growth as well as

oxidative stress tolerance', *Plant Biotechnology Journal*, 9(3), pp. 334–347. doi: 10.1111/j.1467-7652.2010.00551.x.

Kirchenbauer, D. *et al.* (2016) 'Characterization of photomorphogenic responses and signaling cascades controlled by phytochrome-A expressed in different tissues', *New Phytologist*, 211(2), pp. 584–598. doi: 10.1111/nph.13941.

Krylov, V. V. (2017) 'Biological effects related to geomagnetic activity and possible mechanisms', *Bioelectromagnetics*, 38(7), pp. 497–510. doi: 10.1002/bem.22062.

Kuznetsov, O. A. *et al.* (1999) 'Curvature induced by amyloplast magnetophoresis in protonemata of the moss Ceratodon purpureus', *Plant Phisiology*, 119, pp. 645–650. doi: https://doi.org/10.1104/pp.119.2.645.

Lariguet, P. *et al.* (2006) 'PHYTOCHROME KINASE SUBSTRATE 1 is a phototropin 1 binding protein required for phototropism', *Proceedings of the National Academy of Sciences*, 103(26), pp. 10134–10139. doi: 10.1073/pnas.0603799103.

Lee, H. J. *et al.* (2017) 'Multiple Routes of Light Signaling during Root Photomorphogenesis', *Trends in Plant Science*, 22(9), pp. 803–812. doi: 10.1016/j.tplants.2017.06.009.

Lee, J. *et al.* (2007) 'Analysis of Transcription Factor HY5 Genomic Binding Sites Revealed Its Hierarchical Role in Light Regulation of Development', *the Plant Cell Online*, 19(3), pp. 731–749. doi: 10.1105/tpc.106.047688.

Lenhard, M., Jürgens, G. and Laux, T. (2002) 'The WUSCHEL and SHOOTMERISTEMLESS genes fulfil complementary roles in Arabidopsis shoot meristem regulation.', *Development (Cambridge, England)*, 129, pp. 3195–3206.

Leske, R. A. *et al.* (1995) 'Measurements of the Ionic Charge States of Solar Energetic Particles Using the Geomagnetic Field', *The Astrophysical Journal*, 452, pp. 1983–1986. doi: 10.1086/309718.

Liljegren, S. J. *et al.* (1999) 'Interactions among APETALA1, LEAFY , and TERMINAL FLOWER1 Specify Meristem Fate', *The Plant Cell*, 11(June), pp. 1007–1018. doi: 10.1105/tpc.11.6.1007.

Lin, C. (2002) 'Blue Light Receptors and Signal Transduction', *The Plant Cell*, 14(Suppl 1), pp. 207–225. doi: 10.1105/tpc.000646.S208.

Lin, R. and Tang, W. (2014) *Abscisic Acid: Metabolism, Transport and Signaling*. Edited by D. P. Zhang. doi: 10.1007/978-94-017-9424-4.

Liu, B. *et al.* (2016) 'Signaling mechanisms of plant cryptochromes in Arabidopsis thaliana', *Journal of Plant Research*, 129(2), pp. 137–148. doi: 10.1007/s10265-015-0782-z.

Liu, C. *et al.* (2008) 'Direct interaction of AGL24 and SOC1 integrates flowering signals in Arabidopsis', *Development*, 135(8), pp. 1481–1491. doi: 10.1242/dev.020255.

Liu, L. J. *et al.* (2008) 'COP1-Mediated Ubiquitination of CONSTANS Is Implicated in Cryptochrome Regulation of Flowering in Arabidopsis', *the Plant Cell Online*, 20(2), pp. 292–306. doi: 10.1105/tpc.107.057281.

Lu, S. X. *et al.* (2012) 'CCA1 and ELF3 Interact in the Control of Hypocotyl Length and Flowering Time in Arabidopsis', *Plant Physiology*, 158(2), pp. 1079–1088. doi: 10.1104/pp.111.189670.

Ma, L. *et al.* (2001) 'Light Control of Arabidopsis Development Entails Coordinated', *The Plant Cell*, 13(December), pp. 2589–2607. doi: 10.1105/tpc.010229.A.

Maffei, M. E. (2014) 'Magnetic field effects on plant growth, development, and evolution', *Frontiers in Plant Science*, 5, pp. 1–15. doi: 10.3389/fpls.2014.00445.

Martinez-Garcia, J. F., Huq, E. and Quail, P. H. (2000) 'Direct Targeting of Light Signals to a Promoter

Element-Bound Transcription Factor', *Science*, 288(5467), pp. 859–863. doi: 10.1126/science.288.5467.859.

Más, P. *et al.* (2000) 'Functional interaction of phytochrome B and cryptochrome 2', *Nature*, 408, pp. 207–211. doi: 10.1038/35041583.

Más, P. (2005) 'Circadian clock signaling in Arabidopsis thaliana: From gene expression to physiology and development', *International Journal of Developmental Biology*, 49, pp. 491–500. doi: 10.1387/ijdb.041968pm.

Mateos, J. L. *et al.* (2015) 'Combinatorial activities of SHORT VEGETATIVE PHASE and FLOWERING LOCUS C define distinct modes of flowering regulation in Arabidopsis', *Genome Biology*, 16(1), pp. 1–23. doi: 10.1186/s13059-015-0597-1.

Matsuo, M. and Oelmüller, R. (2015) 'REDOX RESPONSIVE TRANSCRIPTION FACTOR1 is involved in age-dependent and systemic stress signaling', *Plant Signaling and Behavior*, 10(11), p. e1051279. doi: 10.1080/15592324.2015.1051279.

McClean, R. G. *et al.* (2001) 'Botanical iron metals: correlation between nanocrystal structure and modes of biological self-assembly', *European Journal of Mineralogy*, 13, pp. 1235–1242. doi: https://doi.org/10.1127/0935-1221/2001/0013-1235.

Merrill, R. T. and McFadden, P. L. (1995) 'Dynamo theory and paleomagnetism', *Journal of Geophysical Research B: Solid Earth*, 100(94), pp. 317–326. doi: 10.1029/94JB02361.

Messiha, H. L. *et al.* (2014) 'Magnetic field effects as a result of the radical pair mechanism are unlikely in redox enzymes', *Journal of The Royal Society Interface*, 12(103), pp. 20141155–20141155. doi: 10.1098/rsif.2014.1155.

Mhamdi, A. *et al.* (2010) 'Catalase function in plants: A focus on Arabidopsis mutants as stress-mimic models', *Journal of Experimental Botany*, 61(15), pp. 4197–4220. doi: 10.1093/jxb/erq282.

Miller, G. *et al.* (2009) 'The plant NADPH oxidase RBOHD mediates rapid systemic signaling in response to diverse stimuli', *Science Signaling*, 2(84), pp. 1–11. doi: 10.1126/scisignal.2000448.

Montgomery, B. L. (2016) 'Spatiotemporal Phytochrome Signaling during Photomorphogenesis: From Physiology to Molecular Mechanisms and Back', *Frontiers in Plant Science*, 7, pp. 1–8. doi: 10.3389/fpls.2016.00480.

Moon, J. *et al.* (2003) 'The SOC1 MADS-box gene integrates vernalization and gibberellin signals for flowering in Arabidopsis', *Plant Journal*, 35(5), pp. 613–623. doi: 10.1046/j.1365-313X.2003.01833.x.

Murashige, T. and Skoog, F. (1962) 'A revised medium for rapid growth bioassays with tobacco tissue cultures', *Phisiologia Plantarum*, 15(3), pp. 473–497. doi: 10.1111/j.1399-3054.1962.tb08052.x.

Myouga, F. *et al.* (2008) 'A Heterocomplex of Iron Superoxide Dismutases Defends Chloroplast Nucleoids against Oxidative Stress and Is Essential for Chloroplast Development in Arabidopsis', *the Plant Cell Online*, 20(11), pp. 3148–3162. doi: 10.1105/tpc.108.061341.

Negishi, Y. *et al.* (1999) 'Growth of pea epicotyl in low magnetic field: implication for space research.', *Advances in Space Research*, 23(12), pp. 2029–2032. doi: 10.1016/S0273-1177(99)00342-7.

Ni, W. *et al.* (2013) 'Multisite Light-Induced Phosphorylation of the Transcription Factor PIF3 Is Necessary for Both Its Rapid Degradation and Concomitant Negative Feedback Modulation of Photoreceptor phyB Levels in Arabidopsis', *The Plant Cell*, 25(7), pp. 2679–2698. doi: 10.1105/tpc.113.112342.

Ni, W. *et al.* (2014) 'A mutually assured destruction mechanism attenuates light signaling in Arabidopsis', *Science*, 344(6188), pp. 1160–1164. doi: 10.1126/science.1250778.

Ning, Y. Q. *et al.* (2015) 'Two novel NAC transcription factors regulate gene expression and flowering time by associating with the histone demethylase JMJ14', *Nucleic Acids Research*, 43(3), pp. 1469–1484. doi: 10.1093/nar/gku1382.

Nohales, M. A. and Kay, S. A. (2016) 'Molecular mechanisms at the core of the plant circadian oscillator', *Nature Structural and Molecular Biology*, 23(12), pp. 1061–1069. doi: 10.1038/nsmb.3327.

Notaguchi, M. *et al.* (2008) 'Long-distance, graft-transmissible action of Arabidopsis FLOWERING LOCUS T protein to promote flowering', *Plant and Cell Physiology*, 49(11), pp. 1645–1658. doi: 10.1093/pcp/pcn154.

Oakenfull, R. J. and Davis, S. J. (2017) 'Shining a light on the Arabidopsis circadian clock', *Plant, Cell & Environment*, (July), pp. 1–15. doi: 10.1111/pce.13033.

Occhipinti, A., De Santis, A. and Maffei, M. E. (2014) 'Magnetoreception: An unavoidable step for plant evolution?', *Trends in Plant Science*. Elsevier Ltd, 19(1), pp. 1–4. doi: 10.1016/j.tplants.2013.10.007.

Osterlund, M. T. *et al.* (2000) 'Targeted destabilization of HY5 during light-regulated development of Arabidopsis', *Nature*, 405(6785), pp. 462–466. doi: 10.1038/35013076.

Park, B. S. *et al.* (2011) 'Auxin is involved in the regulation of leaf and root development by LAF1 under short day conditions', *Biologia Plantarum*, 55(4), pp. 647–652. doi: 10.1007/s10535-011-0163-y.

Perea-García, A. *et al.* (2016) 'Modulation of copper deficiency responses by diurnal and circadian rhythms in Arabidopsis thaliana', *Journal of Experimental Botany*, 67(1), pp. 391–403. doi: 10.1093/jxb/erv474.

Pérez-Ruiz, R. V. *et al.* (2015) 'XAANTAL2 (AGL14) is an important component of the complex gene regulatory network that underlies arabidopsis shoot apical meristem transitions', *Molecular Plant*, 8(5), pp. 796–813. doi: 10.1016/j.molp.2015.01.017.

Pfaffl, M. W. (2001) 'A new mathematical model for relative quantification in real time RT-PCR', *Nucleic Acids Research*, 29(9), pp. 16–21. doi: 10.1093/nar/29.9.e45.

Printz, B. *et al.* (2016) 'Copper Trafficking in Plants and Its Implication on Cell Wall Dynamics', *Frontiers in Plant Science*, 7(May), pp. 1–16. doi: 10.3389/fpls.2016.00601.

Rakosy-Tican, L., Aorori, C. M. and Morariu, V. V. (2005) 'Influence of near null magnetic field on in vitro growth of potato and wild Solanum species', *Bioelectromagnetics*, 26(7), pp. 548–557. doi: 10.1002/bem.20134.

Ravet, K. and Pilon, M. (2013) 'Copper and Iron Homeostasis in Plants: The Challenges of Oxidative Stress', *Antioxidants & Redox Signaling*, 19(9), pp. 919–932. doi: 10.1089/ars.2012.5084.

Reina, F. G., Pascual, L. A. and Fundora, I. A. (2001) 'Influence of stationary magnetic fields on water relations in lettuce seeds. Part II: Experimental Results', *Bioelectromagnetics*, 22, pp. 596–602. Available at: http://doi.wiley.com/10.1002/bem.10048.

Rensing, L. and Ruoff, P. (2002) 'Temperature effect on entrainment, phase shifting, and amplitude of circadian clocks and its molecular bases', *Chronobiology International*, 19(5), pp. 807–864. doi: 10.1081/CBI-120014569.

Rieu, I. *et al.* (2008) 'The gibberellin biosynthetic genes AtGA20ox1 and AtGA20ox2 act, partially redundantly, to promote growth and development throughout the Arabidopsis life cycle', *Plant Journal*, 53(3), pp. 488–504. doi: 10.1111/j.1365-313X.2007.03356.x.

Rozen, S. and Skaletsky, H. (2000) 'Primer3 on the WWW for general users and for biologist programmers.', *Methods Molecular Biology*, 132, pp. 365–386.

Sahebjamei, H., Abdolmaleki, P. and Ghanati, F. (2007) 'Effects of magnetic field on the antioxidant

enzyme activities of suspension-cultured tobacco cells', *Bioelectromagnetics*, 28(1), pp. 42–47. doi: 10.1002/bem.20262.

Salome, P. A., Xie, Q. and McClung, C. R. (2008) 'Circadian Timekeeping during Early Arabidopsis Development', *Plant Physiology*, 147(3), pp. 1110–1125. doi: 10.1104/pp.108.117622.

Sancenon, V. *et al.* (2003) 'Identification of a copper transporter family in Arabidopsis thaliana', *Plant Molecular Biology*, 51(4), pp. 577–587. doi: 10.1023/a:1022345507112.

Sánchez-Lamas, M., Lorenzo, C. D. and Cerdán, P. D. (2016) 'Bottom-up Assembly of the Phytochrome Network', *PLoS Genetics*, 12(11), pp. 1–24. doi: 10.1371/journal.pgen.1006413.

Sandweiss, J. (1990) 'On the cyclotroc resonance model of ion transport', *Bioelectromagnetics*, 11, pp. 203–205.

Sarid-Krebs, L. *et al.* (2015) 'Phosphorylation of CONSTANS and its COP1-dependent degradation during photoperiodic flowering of Arabidopsis', *Plant Journal*, 84(3), pp. 451–463. doi: 10.1111/tpj.13022.

Sassi, M. *et al.* (2012) 'COP1 mediates the coordination of root and shoot growth by light through modulation of PIN1- and PIN2-dependent auxin transport in Arabidopsis', *Development*, 139(18), pp. 3402–3412. doi: 10.1242/dev.078212.

Schoof, H. *et al.* (2000) 'The Stem Cell Population of Arabidopsis Shoot Meristems Is Maintained by a Regulatory Loop between the CLAVATA and WUSCHEL Genes', *Cell*, 100(6), pp. 635–644.

Schultz, E. A. (1991) 'LEAFY, a Homeotic Gene That Regulates Inflorescence Development in Arabidopsis', *the Plant Cell Online*, 3(8), pp. 771–781. doi: 10.1105/tpc.3.8.771.

Sellaro, R. *et al.* (2009) 'Synergism of Red and Blue Light in the Control of Arabidopsis Gene Expression and Development', *Current Biology*, 19(14), pp. 1216–1220. doi: 10.1016/j.cub.2009.05.062.

Shalitin, D. (2003) 'Blue Light-Dependent in Vivo and in Vitro Phosphorylation of Arabidopsis Cryptochrome 1', *the Plant Cell Online*, 15(10), pp. 2421–2429. doi: 10.1105/tpc.013011.

Shim, J. S., Kubota, A. and Imaizumi, T. (2017) 'Circadian Clock and Photoperiodic Flowering in Arabidopsis: CONSTANS Is a Hub for Signal Integration', *Plant Physiology*, 173(1), pp. 5–15. doi: 10.1104/pp.16.01327.

Shin, J., Park, E. and Choi, G. (2007) 'PIF3 regulates anthocyanin biosynthesis in an HY5-dependent manner with both factors directly binding anthocyanin biosynthetic gene promoters in Arabidopsis', *Plant Journal*, 49(6), pp. 981–994. doi: 10.1111/j.1365-313X.2006.03021.x.

Smith, H. M. S. *et al.* (2011) 'Specification of reproductive meristems requires the combined function of SHOOT MERISTEMLESS and floral integrators FLOWERING LOCUS T and FD during Arabidopsis inflorescence development', *Journal of Experimental Botany*, 62(2), pp. 583–593. doi: 10.1093/jxb/erq296.

Solov'yov, I. A., Chandler, D. E. and Schulten, K. (2007) 'Magnetic field effects in Arabidopsis thaliana cryptochrome-1', *Biophysical Journal*. Elsevier, 92(8), pp. 2711–2726. doi: 10.1529/biophysj.106.097139.

Song, Y. H. *et al.* (2014) 'Distinct roles of FKF1, GIGANTEA, and ZEITLUPE proteins in the regulation of CONSTANS stability in *Arabidopsis* photoperiodic flowering', *Proceedings of the National Academy of Sciences*, 111(49), pp. 17672–17677. doi: 10.1073/pnas.1415375111.

Song, Y. H. (2016) 'The Effect of Fluctuations in Photoperiod and Ambient Temperature on the Timing of Flowering: Time to Move on Natural Environmental Conditions.', *Molecules and cells*, 39(10), pp. 715–721. doi: 10.14348/molcells.2016.0237.

Soy, J. *et al.* (2016) 'Molecular convergence of clock and photosensory pathways through PIF3–TOC1 interaction and co-occupancy of target promoters', *Proceedings of the National Academy of Sciences*, 113(17), pp. 4870–4875. doi: 10.1073/pnas.1603745113.

Staiger, D. *et al.* (2003) 'The Arabidopsis SRR1 gene mediates phyB signaling and is required for normal circadian clock function Dorothee', *Genes & Development*, 17, pp. 256–268. doi: 10.1101/gad.244103.2002.

Su, J. *et al.* (2017) 'Coordination of Cryptochrome and Phytochrome Signals in the Regulation of Plant Light Responses', *Agronomy*, 7(1), p. 25. doi: 10.3390/agronomy7010025.

Szymanowska-Pulka, J. (2013) 'Form matters: Morphological aspects of lateral root development', *Annals of Botany*, 112(9), pp. 1643–1654. doi: 10.1093/aob/mct231.

Tepperman, J. M., Hwang, Y. S. and Quail, P. H. (2006) 'phyA dominates in transduction of red-light signals to rapidly responding genes at the initiation of Arabidopsis seedling de-etiolation', *Plant Journal*, 48(5), pp. 728–742. doi: 10.1111/j.1365-313X.2006.02914.x.

Tsuchida-Mayama, T. *et al.* (2010) 'Role of the phytochrome and cryptochrome signaling pathways in hypocotyl phototropism', *Plant Journal*, 62(4), pp. 653–662. doi: 10.1111/j.1365-313X.2010.04180.x.

Tsuji, H. (2017) 'Molecular function of florigen', *Breeding Science*, 332, p. 17026. doi: 10.1270/jsbbs.17026.

Uebe, R. and Schüler, D. (2016) 'Magnetosome biogenesis in magnetotactic bacteria', *Nature Reviews Microbiology*, 14(10), pp. 621–637. doi: 10.1038/nrmicro.2016.99.

Usami, T. *et al.* (2004) 'Cryptochromes and Phytochromes Synergistically Regulate Arabidopsis Root Greening under Blue Light', *Plant and Cell Physiology*, 45(12), pp. 1798–1808. doi: 10.1093/pcp/pch205.

Valentim, F. L. *et al.* (2015) 'A quantitative and dynamic model of the arabidopsis flowering time gene regulatory network', *PLoS ONE*, 10(2), pp. 1–18. doi: 10.1371/journal.pone.0116973.

Valet, J. P. (2003) 'Time variations in geomagnetic intensity', *Reviews of Geophysics*, 41(1), p. 1004. doi: 10.1029/2001RG000104.

Wan, L. *et al.* (2007) 'Phosphorylation of the 12 S globulin cruciferin in wild-type and abi1-1 mutant Arabidopsis thaliana (thale cress) seeds', *Biochemical Journal*, 404, pp. 247–256. doi: 10.1042/BJ20061569.

Wang, H. (2015) 'Phytochrome signaling: Time to tighten up the loose ends', *Molecular Plant*. Elsevier Ltd, 8(4), pp. 540–551. doi: 10.1016/j.molp.2014.11.021.

Weidler, G. *et al.* (2012) 'Degradation of *Arabidopsis* CRY2 Is Regulated by SPA Proteins and Phytochrome A', *The Plant Cell*, 24(6), pp. 2610–2623. doi: 10.1105/tpc.112.098210.

Wils, C. R. and Kaufmann, K. (2017) 'Gene-regulatory networks controlling inflorescence and flower development in Arabidopsis thaliana', *Biochimica et Biophysica Acta*, 1860(1), pp. 95–105. doi: 10.1016/j.bbagrm.2016.07.014.

Wiltschko, W. and Wiltschko, R. (2005) 'Magnetic orientation and magnetoreception in birds and other animals', *Journal of Comparative Physiology A: Neuroethology, Sensory, Neural, and Behavioral Physiology*, 191(8), pp. 675–693. doi: 10.1007/s00359-005-0627-7.

Winklhofer, M. and Kirschvink, J. L. (2010) 'A quantitative assessment of torque-transducer models for magnetoreception', *Journal of The Royal Society Interface*, 7, pp. S273–S289. doi: 10.1098/rsif.2009.0435.focus.

Xu, C. *et al.* (2012) 'A near-null magnetic field affects cryptochrome-related hypocotyl growth and

flowering in Arabidopsis', *Advances in Space Research*. COSPAR, 49(5), pp. 834–840. doi: 10.1016/j.asr.2011.12.004.

Xu, C. *et al.* (2013) 'Removal of the local geomagnetic field affects reproductive growth in Arabidopsis', *Bioelectromagnetics*, 34(6), pp. 437–442. doi: 10.1002/bem.21788.

Xu, C. *et al.* (2014) 'Blue light-dependent phosphorylations of cryptochromes are affected by magnetic fields in Arabidopsis', *Advances in Space Research*, 53(7), pp. 1118–1124. doi: 10.1016/j.asr.2014.01.033.

Xu, C. *et al.* (2015) 'Suppression of Arabidopsis flowering by near-null magnetic field is affected by light.', *Bioelectromagnetics*, 36(6), pp. 476–479. doi: 10.1002/bem.21927.

Xu, C. *et al.* (2017) 'Gibberellins are involved in effect of near-null magnetic field on Arabidopsis flowering', *Bioelectromagnetics*, 38(1), pp. 1–10. doi: 10.1002/bem.22004.

Xu, C. *et al.* (2018) 'Suppression of Arabidopsis flowering by near-null magnetic field is mediated by auxin', *Bioelectromagnetics*, 39(1), pp. 15–24. doi: 10.1002/bem.22086.

Xu, D., Zhu, D. and Deng, X. W. (2016) 'The role of COP1 in repression of photoperiodic flowering', *F1000Research*, 5, pp. 1–6. doi: 10.12688/f1000research.7346.1.

Yamaguchi, A. *et al.* (2005) 'TWIN SISTER of FT (TSF) acts as a floral pathway integrator redundantly with FT', *Plant and Cell Physiology*, 46(8), pp. 1175–1189. doi: 10.1093/pcp/pci151.

Yang, Z. *et al.* (2017) 'Cryptochromes Orchestrate Transcription Regulation of Diverse Blue Light Responses in Plants', *Photochemistry and Photobiology*, 93(1), pp. 112–127. doi: 10.1111/php.12663.

Yao, Y. *et al.* (2017) 'ETHYLENE RESPONSE FACTOR 74 (ERF74) plays an essential role in controlling a respiratory burst oxidase homolog D (RbohD)-dependent mechanism in response to different stresses in Arabidopsis', *New Phytologist*, 213(4), pp. 1667–1681. doi: 10.1111/nph.14278.

Yoshii, T., Ahmad, M. and Helfrich-Förster, C. (2009) 'Cryptochrome mediates light-dependent magnetosensitivity of Drosophila's circadian clock', *PLoS Biology*, 7(4), pp. 0813–0819. doi: 10.1371/journal.pbio.1000086.

Zhang, K. X. *et al.* (2013) 'Blue-light-induced PIN3 polarization for root negative phototropic response in Arabidopsis', *Plant Journal*, 76(2), pp. 308–321. doi: 10.1111/tpj.12298.

Zhang, Y. *et al.* (2017) 'Dissection of HY5 / HYH expression in Arabidopsis reveals a root-autonomous HY5- mediated photomorphogenic pathway', *PLoS ONE*, 12(7), pp. 1–15. doi: https://doi.org/10.1371/journal.pone.0180449.

Zhaojun, D. *et al.* (2011) 'Light-mediated polarization of the PIN3 auxin transporter for the phototropic response in Arabidopsis', *Nature Cell Biology*, 13, pp. 447–452. doi: doi:10.1038/ncb2208.

Zhou, M. *et al.* (2015) 'Redox rhythm reinforces the circadian clock to gate immune response', *Nature*, 523(7561), pp. 472–476. doi: 10.1038/nature14449.

Video Article

Geomagnetic Field (Gmf) and Plant Evolution: Investigating the Effects of Gmf Reversal on *Arabidopsis thaliana* Development and Gene Expression

Cinzia M. Bertea[1], Ravishankar Narayana[1], Chiara Agliassa[1], Christopher T. Rodgers[2], Massimo E. Maffei[1]

[1]Department of Life Sciences and Systems Biology, University of Turin

[2]Radcliffe Department of Medicine, University of Oxford, John Radcliffe Hospital

Correspondence to: Massimo E. Maffei at massimo.maffei@unito.it

URL: https://www.jove.com/video/53286
DOI: doi:10.3791/53286

Keywords: Developmental Biology, Issue 105, Geomagnetic field, *Arabidopsis thaliana*, plant development, gene expression, antioxidant genes, magnetic field reversal, triaxial Helmholtz coils

Date Published: 11/30/2015

Citation: Bertea, C.M., Narayana, R., Agliassa, C., Rodgers, C.T., Maffei, M.E. Geomagnetic Field (Gmf) and Plant Evolution: Investigating the Effects of Gmf Reversal on *Arabidopsis thaliana* Development and Gene Expression. *J. Vis. Exp.* (105), e53286, doi:10.3791/53286 (2015).

Abstract

One of the most stimulating observations in plant evolution is a correlation between the occurrence of geomagnetic field (GMF) reversals (or excursions) and the moment of the radiation of Angiosperms. This led to the hypothesis that alterations in GMF polarity may play a role in plant evolution. Here, we describe a method to test this hypothesis by exposing *Arabidopsis thaliana* to artificially reversed GMF conditions. We used a three-axis magnetometer and the collected data were used to calculate the magnitude of the GMF. Three DC power supplies were connected to three Helmholtz coil pairs and were controlled by a computer to alter the GMF conditions. Plants grown in Petri plates were exposed to both normal and reversed GMF conditions. Sham exposure experiments were also performed. Exposed plants were photographed during the experiment and images were analyzed to calculate root length and leaf areas. Arabidopsis total RNA was extracted and Quantitative Real Time-PCR (qPCR) analyses were performed on gene expression of *CRUCIFERIN 3* (*CRU3*), *copper transport protein1* (*COTP1*), *Redox Responsive Transcription Factor1* (*RRTF1*), *Fe Superoxide Dismutase 1*, (*FSD1*), *Catalase3* (*CAT3*), *Thylakoidal Ascorbate Peroxidase* (*TAPX*), a cytosolic *Ascorbate Peroxidase1* (*APX1*), and *NADPH/respiratory burst oxidase protein D* (*RbohD*). Four different reference genes were analysed to normalize the results of the qPCR. The best of the four genes was selected and the most stable gene for normalization was used. Our data show for the first time that reversing the GMF polarity using triaxial coils has significant effects on plant growth and gene expression. This supports the hypothesis that GMF reversal contributes to inducing changes in plant development that might justify a higher selective pressure, eventually leading to plant evolution.

Video Link

The video component of this article can be found at https://www.jove.com/video/53286/

Introduction

The Earth's magnetic field (or equivalently the geomagnetic field, GMF) is an inescapable environmental factor for all organisms living on the planet, including plants. The GMF has always been a natural feature of the Earth, so during evolution, all living organisms experienced its action. An increasing body of evidence shows that the GMF is able to influence many biological processes [1]. The GMF is not uniform and there are significant local differences in its magnitude and direction at the surface of the Earth. The GMF at the Earth's surface shows a broad range of magnitudes, ranging from less than 30 μT to almost 70 μT. The GMF protects the Earth and its biosphere from the lethal effects of solar wind by deflecting most of its charged particles through the magnetosphere[2].

Plants respond to environmental stimuli; and classical responses to abiotic factors such as light and gravity have been thoroughly described by defining the so-called phototropic and gravitropic responses. Very little, or nothing, is known on the mechanisms of perception and responses of plants to magnetic fields, despite the plethora of papers published on this topic and recently reviewed [1]. Unlike the gravitational field, the GMF changed consistently during plant evolution thereby representing an important abiotic stress factor that has been recently considered a potential driving force eventually contributing to plant diversification and speciation [2]. Geomagnetic reversals (or excursions) are changes in polarity of the GMF. During Earth's life-history, GMF reversals occurred several times. These exposed the planet to periods of reduced GMF strength during every polarity transition. Some authors have hypothesized that these transitions periods of low GMF strength might have allowed ionizing radiation from the solar wind to reach the Earth's surface, thereby inducing a consistent stress to living organisms, which could have been strong enough to induce gene alterations eventually leading to plant evolution [2].

A detailed analysis of experiments describing the effects of magnetic fields on plants shows a large number of conflicting reports, characterized by a dearth of plausible biophysical interaction mechanisms. Many experiments are simply unrealistic, while others lack a testable hypothesis and, ultimately, are unconvincing [3]. Over the past years, the progress and status of research on the effect of magnetic fields on plant has been reviewed [2,4-11]. Recently, the effect of both low and high magnetic field has been thoroughly discussed [1], with a particular focus on the involvement of GMF reversal events on plant evolution [2].

The most direct means to substantiate the hypothesis that GMF reversals affect plant evolution is to synthesize a GMF reversal in the laboratory by testing the response of plants to normal and reversed magnetic field conditions. To test the hypothesis, we therefore built a triaxial octagonal Helmholtz coil-pairs magnetic field compensation system (triaxial coils), which is able to accurately reverse the normal GMF conditions.

We used *Arabidopsis thaliana* as a model plant and we tested the effect of reversed GMF on gene expression of some important genes: *CRUCIFERIN 3* (*CRU3*), that encodes a 12S seed storage protein that is tyrosine-phosphorylated and its phosphorylation state is modulated in response to ABA in *Arabidopsis thaliana* seeds [12,13]; the *Copper Transport Protein1* (*COTP1*), that encodes a heavy metal transport/ detoxification superfamily protein with the predominant function in soil Cu acquisition and pollen development [14]; and *Redox Responsive Transcription Factor1* (*RRTF1*), that encodes a member of the ERF (ethylene response factor) subfamily B-3 of ERF/AP2 transcription factor family that contains one AP2 domain that facilitate the synergistic co-activation of gene expression pathways and confer cross tolerance to abiotic and biotic stresses [15].

Moreover we also analyzed five genes involved in oxidative stress responses: *Fe Superoxide Dismutase1*, (*FSD1*), that encodes a cytoplasmic enzyme that enzymatically and rapidly converts the superoxide anion (O_2^-) and water (H_2O) to hydrogen peroxide (H_2O_2) and molecular oxygen (O_2) [16]; *Catalase3* (*CAT3*), that that encodes and enzyme that catalyzes the breakdown of H_2O_2 into water and oxygen [17,18]; *Thylakoidal Ascorbate Peroxidase* (*TAPX*), that encodes a chloroplastic thylakoid peroxidase that scavenges H_2O_2 [19];*Ascorbate Peroxidase1* (*APX1*), that encodes a cytosolic peroxidase that scavenges H_2O_2 and represents one of the potential targets of post-translational modifications mediated by NO-derived molecules [20]; and NADPH-*Respiratory burst oxidase protein D* (*RbohD*) that encodes an enzyme that generates O_2^- and plays pivotal roles in regulating growth, development and stress responses in Arabidopsis [21].

Our field-reversal methodology provides the first evidence that GMF reversal can induce a significant change in the morphology and gene expression of *A. thaliana* roots and shoots. This protocol provides an innovative way to evaluate the effect of GMF reversal on plant morphology and gene expression and can be used to assess the potential effect of GMF reversal on other aspects of plant behavior, and thereby guide discussion of the role of GMF reversal on plant evolution.

Protocol

1. Setting of the Triaxial Coils

NOTE: **Figure 1** shows the triaxial coils used to reverse the GMF.

1. Turn on the three-axis magnetometer, whose probe is inserted in the triaxial coils.
2. Turn on the computer and launch the magnetometer software that allows data to be collected from three-axis magnetometer.
3. Use the component values reported by the magnetometer to calculate the magnitude of the GMF. For instance, with magnetometer values: Bx = 6.39 µT, By = 36.08 µT, Bz = 20.40 µT calculate a field strength of 41.94 µT by using the following equation: $B = B_{GMF} + B_{additional}$, where $B_{additional} = (Bx^2 + By^2 + Bz^2)^{½}$ (*i.e.,* 41.9 µT in the example.)
4. Turn on the three DC power supplies (dual range: 0-8V/5A and 0-20V/2.5A, 50W) each one connected to three couples of Helmholtz coils and connected to a computer via a GPIB connection (**Figure 1B**).
5. Set voltages of the power supplies to generate the desired magnetic field with a reversed magnetic field vector. For instance, with B_{GMF} as in step 1.3 and with the coil size of the instrumentation described here, set the voltages to V_x =0.00 V, V_y = 30.52 V, V_z = 0.00 V in order to generate a new resultant $B = B_{GMF} + B_{triaxial\ coils}$ = (6.38, -36.08, 20.39) µT. *i.e.,* a new field with the same magnitude as B_{GMF} but pointing to a different direction.
6. Verify the new field with the magnetometer software by using the procedure described in 1.3.
7. Expose plants to both normal and reversed GMF conditions by using Petri plates as described in section 2.
8. Perform sham exposure experiments by keeping the magnitude of the field equal to $|B_{GMF}|$ and keeping the vertical component of the field equal to that of the GMF but altering the direction (*i.e.,* "North, East or West") of the horizontal component of the field with equal currents in the triaxial coils compared to the field reversal condition. Do this by altering the voltage of the coils as described in 1.5.
   Note: This sham exposure rules out potential subtle heating or vibrational effects from either the coils themselves or from the electronics used to control the coils.
9. Run double-blind experiments by applying field conditions blinded from the personnel performing the remainder of the experiments and/or interpreting the data.

2. Preparation of Plant Materials and Conditions for Plant Growth

1. Use seeds of *Arabidopsis thaliana*, ecotype Columbia 0 (Col 0), place then into a 1.5 ml tube and surface sterilize by treatment with a 5% (w/v) calcium hypochlorite solution and 0.02% (v/v) Triton X-100 in 80% ethanol (EtOH), for 10-12 min at 25-28 °C, with continuous shaking. Then rinse twice with 80% EtOH, wash with 100% EtOH and finally rinse with sterile distilled water.
2. Prepare 1 L of Murashige and Skoog [22] (MS) modified medium by adding: 2.297 g of MS (0.5 x MS Basal Salt Mixture), 10 g Sucrose, deionized water up to 1 L, pH 5.8-6.0 adjusted with KOH. Add 16 g of agar and autoclave for 20 min, 120 °C.
3. Before solidification, pour 80 ml of medium into each (120 x 120 mm^2) square Petri plates. Sow thirty sterile seeds on plate, and then seal plates with a waxy film.
4. Vernalize the plates horizontally in darkness at 4 °C for 2 days to potentiate and synchronize germination, and then expose Petri plates to either normal or reversed GMF.
5. Expose seeds in a climate controlled environment at 22 °C in a vertical position in parallel experiments both inside the triaxial coils and outside the triaxial coils under a photoperiod schedule of 8 hr darkness and 16 hr light, using Sodium vapor lamps (220 x 10^{-6} E $m^{-2}s^{-1}$). Use a blue gelatin film for spotlight to reduce the red component of lamps.

6. Expose plants for 10 days before RNA extraction to both normal (control) and reversal (treatment) GMF conditions.
7. After exposure, take pictures of Petri dishes.
8. Use the ImageJ software to calculate root length and leaf areas.
    1. Briefly, measure the side of the Petri plate, then open the image of the Petri plate and by using the "straight" line option to draw a line that exactly crosses the plate side.
    2. In the "analyze" menu select "set scale" and insert the actual distance in the "known distance" box (*e.g.*, 120 mm), then insert the unit of length (mm); finally click the "global" option to make settings available for all measurements.
    3. For root length, follow carefully the shape of the root by using the freehand tool. Measure the length by using the "measure" option in the "analyze" menu. Continue to measure all roots in the picture and save the file for further statistical analyses.
    4. For leaf area, from the "image" menu use the adjust option and then "color threshold". Select the individual leaf and in the "analyze" menu select "analyze particles". Save the individual measurements for statistical analyses.

3. *Arabidopsis* Total RNA Extraction, Quantitative Real Time-PCR (qPCR) Reaction Conditions and Primers for *Arabidopsis*

1. Collect separately 30 shoots and 30 roots and immediately freeze in liquid nitrogen. Then grind in liquid nitrogen with mortar and pestle.
2. Isolate total RNA using a purification kit and RNase-Free DNase treatment kit by using manufacturer's instructions.
3. Check sample quality and quantity by using an RNA nano kit and capillary gel electrophoresis according to manufacturer's instructions. Confirm the quantification of RNA spectrophotometrically.
4. Use 2 µg of total RNA and random primers using a cDNA Reverse Transcription Kit to obtain first strand cDNAs according to the manufacturer's recommendations.
5. Perform all experiments on a Real-Time System using SYBR green I with ROX as an internal loading standard.
6. Perform the reaction with 25 µl of mixture consisting of 12.5 µl of 2x SYBR Green qPCR Master Mix, 0.5 µl of cDNA and 100 nM primers. Use the primers listed in **Table 1**. Include in controls non-RT controls (using total RNA without reverse transcription to monitor for genomic DNA contamination) and non-template controls (water instead of template).
7. Calculate primer efficiency for all primers pairs using the standard curve method [23].
8. Use the following PCR conditions: *CRU3*, *COTP1*, *RRTF1*. 10 min at 95 °C, 40 cycles of 15 s at 95 °C, 30 sec at 58 °C, and 30 sec at 72 °C; *UBP6*, *eEF1Balpha2*, *ACT1*, *GAPC2*, *CAT3*, *TAPX*, *APX1*, *RbohD*, *FeSOD1* 10 min at 95 °C, 40 cycles of 15 s at 95 °C, 20 sec at 57 °C, and 30 sec at 72 °C.
9. Read fluorescence following each annealing and extension phase. For all runs, perform a melting curve analysis from 55 to 95 °C by including the dissociation segment in the thermal profile. Use the dissociation curve screen, accessed through the results tab to view the dissociation profile (plot of the fluorescence as a function of temperature). Ensure that the dataset collected during the dissociation segment of the experiment is selected for analysis using the Analysis/Setup screen.
10. Determine the linear range of template concentration to threshold cycle value (Ct value) by performing a tenfold dilution series (1- to 10^3-fold) using cDNA from three independent RNA extractions analyzed in three technical replicates [24,25].
11. Analyze all amplification plots with the Real-Time PCR instrument software to obtain Ct values. Calibrate and normalize relative RNA levels with the level of the best housekeeping genes as follows: 3.11.1) Access the Amplification Plots screen through the Results tab, select the ramp or plateau for which data should be analyzed using the Analysis Selection/Setup screen, and then select the dRn (baseline-corrected normalized fluorescence) from the Fluorescence menu on the command panel. Access the Plate Sample Values screen through the Results tab to display Ct values for the sampled wells.
12. Use four different reference genes [*e.g.*, *cytoplasmic glyceraldehyde-3-phosphate dehydrogenase, (GAPC2), ubiquitin specific protease 6 (UBP6), Actin1 (ACT1) and the elongation factor 1B alpha-subunit 2 (eEF1Balpha2)*] to normalize the results of the real time PCR. Select the top ranked gene using an analysis software [26]; and use the most stable gene for normalization.
    1. Briefly, organize the input data on an Excel sheet with the first column containing the gene names and first row containing the sample names. Then select the analysis software from the menu-bar. Use the dialog box to select the input data.
    2. Next, check the fields Sample names, gene names and simple output only. Click on Go button to perform the analysis. Select the top ranked gene (which has the smallest stability value) as candidate gene most stably expressed.
13. Plot data by showing the differential fold change expression in both shoots and roots.

4. Statistical Analyses

1. Express data as mean values ± standard error. Compare the control and the treatment groups by performing analysis of variance (ANOVA) and Tukey's test with Bonferroni and Dunn-Sidak Adjusted Probability test (0.95% confidence).

Representative Results

The aim of this protocol is to provide a method to assess whether reversal of the geomagnetic field (GMF) may affect plant development and gene expression of *Arabidopsis thaliana* ecotype Col 0. Triaxial coils as shown in **Figure 1A** are used to reverse the GMF when set with the appropriate drive voltages (**Figure 1B**), obtained as described in step 1.5 in the protocol. The dimensions of the triaxial coils are ~2 x 2 x 2 m^3, which allowed sufficient space with reversed GMF conditions to host several Petri plates. Controls were grown in the same environmental conditions and at normal GMF values. After 10 days of exposure to normal and reversed GMF conditions, the phenotype of plants showed evident morphological alterations. As shown in **Figure 2**, control plants (*i.e.*, grown in normal GMF conditions) showed root lengths with significantly (Dunn-Sidak and Bonferroni Adjusted Prob <0.001; Student's t = 10.68, df = 31) higher values (29.41 mm; SEM = 1.04; N = 32) with respect to plants exposed to reversed GMF (17.53 mm; SEM = 0.58; N = 36). In GMF-reversed plants, the morphology of shoots was also altered by showing a reduced development of leaflet expansion. Plants exposed to normal conditions showed an average leaf area of 4.95 mm^2

(SEM 0.025, N = 54), whereas plants exposed to reversed GMF conditions showed significantly (Dunn-Sidak and Bonferroni Adjusted Prob = <0.001; student's t = 31.32, df = 53) lower leaf area values (3.71 mm^2; SEM = 0.032; N = 54). Therefore, exposure of Arabidopsis to reversed GMF conditions induced a reduction in both root length and leaf area.

Leaf expansion and root growth are dependent on both the division and the elongation of cells [27]. Therefore, plant development, productivity and overall fitness are dependent on an optimal shoot- and root-system architecture [28]. The reduced root length and leaf size of plants exposed to reversed GMF conditions indicate the presence of a sensing system able to not only perceive variations in magnetic field intensity, but also to respond to changes in the magnetic field "direction" compared to gravity. The hypothesis that GMF reversal may affect plant growth finds compelling evidence in our experiments, which demonstrate that GMF reversal conditions can significantly affect plant development.

The morphological changes were also accompanied by changes in gene expression. Among housekeeping genes, the most stable gene was the *elongationfactor1B alpha-subunit 2*. The first group of genes (*CRU3*, *COTP1*, *RRTF1*) showed a dramatic alteration in the gene expression (**Figure 3**). Shoot expression of all three genes was significantly increased (P <0.05) by about 2.5-fold in plants exposed to reserved GMF conditions. Root expression of *CRU3* was upregulated in the roots in plants exposed to normal GMF conditions, but was significantly (P <0.05) downregulated in reversed GMF conditions. The opposite was found for *COTP1* and *RRTF1*, which were downregulated in normal conditions and upregulated in the presence of GMF reversal (**Figure 3**).

Cruciferin (a 12 S globulin) is the most abundant storage protein in the seeds of *A. thaliana* and other crucifers and is synthesized as a precursor in the rough endoplasmic reticulum. It is then transported to the protein storage vacuoles [13]. Seedling germination requires the breakdown of cruciferin, which is used as an initial source of nitrogen. Down-regulation of cruciferin degradation reduces embryos development by impairing cell structures or cell components development [29,30]. Our results show that upregulation of *CRU3* correlates with a lower leaf expansion and a reduced root length, thus indicating that this gene in sensitive to GMF reversal and that its overexpression may contribute to the reduction of plant development. Moreover, GMF reversal induces a significant downregulation of *CRU3* in roots, which correlates with a reduced root length. Copper is an essential cofactor for key processes in plants, but it exerts harmful effects when in excess; thus, overexpressing copper transport compromises plant growth. The effect of GMF reversal was a significant overexpression of *COTP1* in both shoots and roots, thus explaining the reduced plant growth. Ion stress impairs chloroplast metabolism, which is tightly linked to the redox state of the cell. In Arabidopsis the transcription factor RRTF1 is important for the expression of genes associated to the ability to adjust to redox changes [31]. Therefore, when plants are exposed to external stimuli able to alter their physiological and developmental programs an overexpression of this important transcription factor is expected. Reversal of the GMF induced a significant overexpression of *RRTF1* in both shoots and roots, thus indicating higher oxidative stress responses of plants to reversed GMF conditions.

Interesting results are obtained by analyzing the five genes involved in oxidative stress. In general, all genes extracted and analyzed in shoots did not show significant differences (P >0.05) when plants were grown in normal or reversed GMF conditions (**Figure 4** and **Figure 5**). However, a significant down-regulation was always observed in roots of plants exposed to reversed GMF conditions. In particular, *CAT3* showed the highest downregulation (**Figure 5**), followed in order of downregulation by *APX1*, *FSD1*, *RBOHD* and *TAPX* (**Figure 4**).

Cross tolerance to abiotic and biotic stress is provided by the activation of different genes involved in several biochemical pathways. *RRTF1* transcription factor facilitates the synergistic co-activation of gene expression of these pathways [15,31], and can be potentially involved in oxidative stress [32]. Therefore, upregulation of *RRTF1* is expected when oxygen scavenging is reduced. Downregulation of root scavenging enzymes correlates with the upregulation of *RRTF1*, which acts in response to increased oxidative stress. The dramatic root downregulation of *CAT3*, *APX1* and *TAPX* indicates the reduced ability of root cells to scavenge H_2O_2, which is accompanied by the reduced ability to dismutate the superoxide anion by downregulation of *FSD1*. The oxidative stress responses is higher in roots, which appear to be the main site of reversed GMF perception.

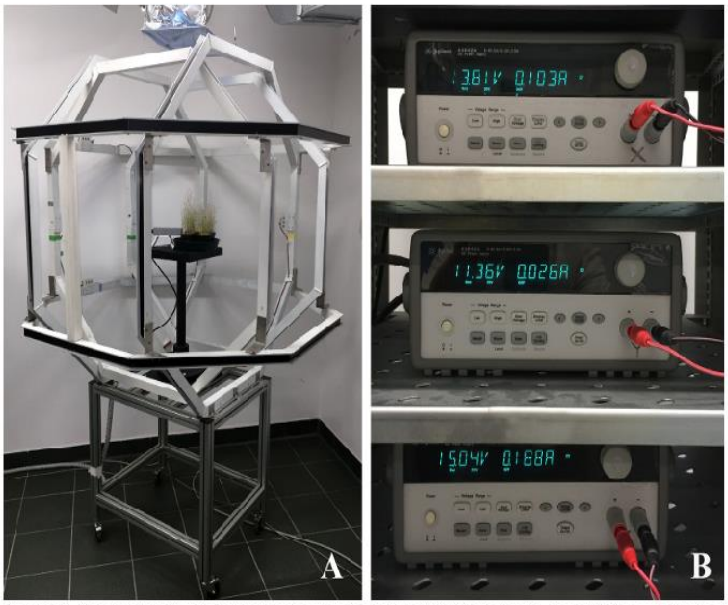

Figure 1. Geomagnetic field Compensation system. (**A**) triaxial coils (comprising a pair of octagonal coils for each of three perpendicular axes) used to reverse the geomagnetic field vector. (**B**) A computer-controlled power supply is connected to each pair of Helmholtz coils. (Voltages in these figures are arbitrary) Please click here to view a larger version of this figure.

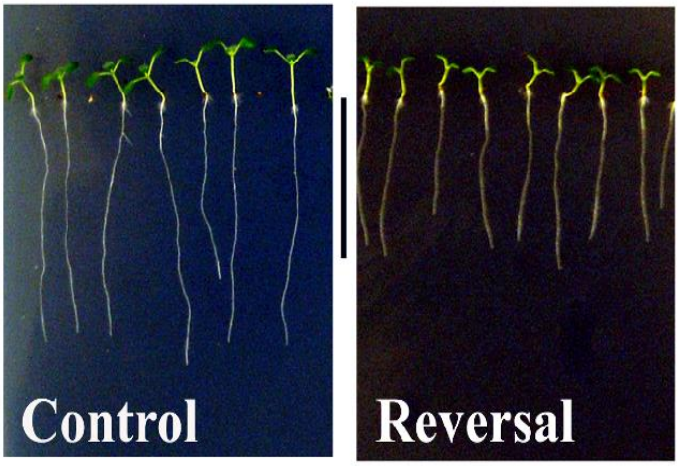

Figure 2. Effects of geomagnetic field reversal on Arabidopsis morphology. After ten days of exposure, control plants (*i.e.*, those exposed to normal GMF conditions) show a significantly greater root length and more expanded leaflets compared to plants that were exposed to reversed GMF conditions. Metric bar = 18 mm. Please click here to view a larger version of this figure.

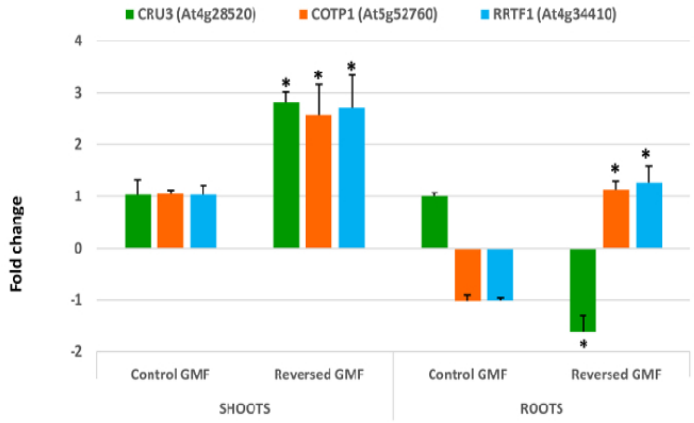

Figure 3. Effects of geomagnetic field reversal on Arabidopsis gene expression. After ten days of exposure, total RNA of control and treated plants was extracted and analysed by Real-Time PCR for expression analysis. The effect of reversal of the GMF was to induce a drastic change in the gene expression of all genes that were tested. *CRU3*, *Cruciferin 3*; *COTP1*, *Copper Transport Protein1*; *RRTF1*, *Redox Responsive Transcription Factor1*. Bars indicate standard error; asterisks indicates significant (P <0.05) differences between plants exposed to reversed and normal GMF conditions. Please click here to view a larger version of this figure.

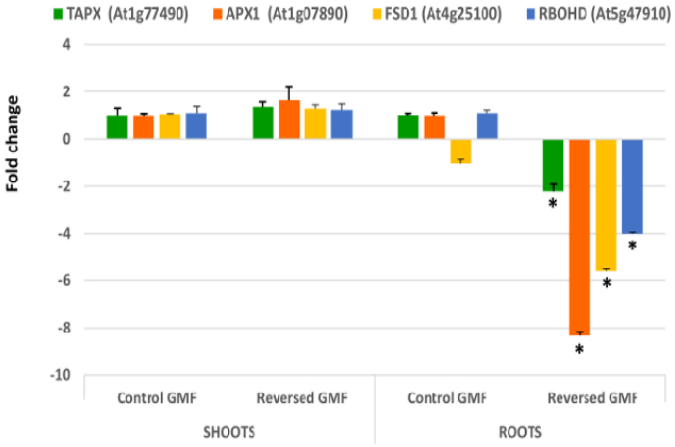

Figure 4. Effects of geomagnetic field reversal on Arabidopsis antioxidant-related gene expression. After ten days of exposure, total RNA of control and treated plants is isolated and employed for gene expression analysis using Real-Time PCR. The effect of reversal of the GMF was to induce no significant changes in shoot gene expression; however, a drastic downregulation was observed in root gene expression of plants grown under reversed GMF conditions. *TAPX*, *Thylakoidal Ascorbate Peroxidase*; *APX1*, *Ascorbate Peroxidase1*; *FSD1*, *Fe Superoxide Dismutase1*; *RbohD*, *NADPH/Respiratory burst oxidase protein D*. Bars indicate standard error; asterisks indicates significant (P <0.05) differences between plants exposed to reversed and normal GMF conditions. Please click here to view a larger version of this figure.

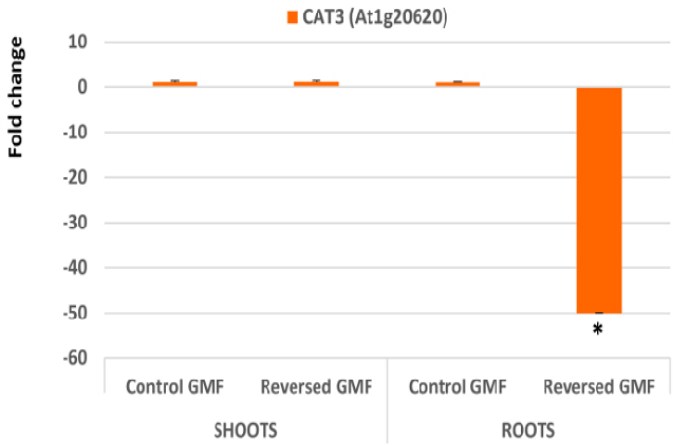

Figure 5. Effects of the geomagnetic field reversal on *Arabidopsis* Catalase 3 (CAT3) gene expression. After ten days of exposure, total RNA of control and treated plants is isolated and employed for gene expression analysis using Real-Time PCR. The effect of reversal of the GMF was to induce no significant changes in shoot gene expression; however, a drastic downregulation was observed in root gene expression of plants grown under reversed GMF conditions. Bars indicate standard error; asterisks indicates significant ($P < 0.05$) differences between plants exposed to reversed and normal GMF conditions. Please click here to view a larger version of this figure.

Discussion

We recently showed that an amazing correlation exists between GMF reversals and the time when diversion of most of the familial Angiosperm lineages occurred [2]. However, despite the stimulating hypotheses and the plethora of studies on the effect of varied GMF intensities, the assumption that GMF reversal may itself induce significant changes in plant gene expression and morphology has never been demonstrated. Here we show for the first time, a method that uses a triaxial octagonal Helmholtz coil to reverse GMF in our laboratory, and that the reversal of the ambient magnetic field can cause phenotypic changes and modulation of gene expression in plants.

In order to obtain GMF reversal (or modification) over a sufficient volume for the plant growth experiments (2 x 2 x 2 m^3), we built an octagonal Helmholtz coil system. This system is not commercially available (usually Helmholtz coils are ring-shaped and smaller) and the costs for construction were considerable. Importantly, this system delivers robust field modification, with exceptional time-stability and homogeneity in the modified magnetic fields.

The system is designed and built to reduce the value of the GMF to a thousandth of the normal conditions or to reverse any of the three dimensions of the magnetic field. However, the design of the coils does not allow to generate a high magnetic field strength. Therefore, this instrument in the present form is not suitable for experiments designed to evaluate the effect of high magnetic field strength on plants or other organisms.

In laboratory, alteration of the GMF similar to those described in this method has been obtained by different methods, including shielding by surrounding the experimental zone by ferromagnetic metal plates with high magnetic permeability, which deviate magnetic fields and concentrate them within the metal itself. The advantage of using Helmholtz coils is that the system allows plants to be exposed to more natural conditions (light, air circulation, *etc.*), thus making it ideal not only for *in vitro* studies (as with the use of Petri dishes) but also for *in vivo* plant growth and development experiments. The dimensions of our system create a space that allows a suppression up to <1/1,000th of the natural GMF throughout a 25 x 25 x 25 cm^3 spherical volume (see **Figure 1A**), thus allowing to host several Petri plates or some small pots for plant growth.

The method presented here has been applied to plant biology studies; however, the system allows a wide range of experimentation, including virology and microbiology, as well as studies on nematodes (*e.g.*, *Caenorhabditis elegans*), arthropods and small animals (including mice and rats). Therefore, tests of the hypothesis that reversal of the GMF is able to induce morphological and transcriptional changes could also be extended to many other living systems, perhaps ultimately even to human cells.

The GMF is constantly changing and fluctuating. Therefore, in our experiments one major challenge is to provide a constant compensation of the GMF in order to obtain the desired new GMF values. This can only be achieved by a continuous control of magnetic fields values through reading of magnetometer values and voltage compensation. Therefore, the system can compensate the slowly varying part of the GMF but it does nothing for higher frequency fluctuations.

In conclusion, the use of triaxial coils to reverse the GMF vector was instrumental to demonstrate that this reversal of the GMF vector is able to induce plant morphological changes and differential gene expression. The results obtained with the presented method provide a compelling evidence in support of the hypothesis that the GMF reversals might have been one of the driving forces for plant evolution over geological timescales [2].

Disclosures

The authors have nothing to disclose.

Acknowledgements

This work was supported by a grant to MEM from the Dept. of Life Sciences and Systems Biology of the University of Turin, Italy. The authors thank G. Gnavi for technical assistance during some experiments. CTR is funded by the Wellcome Trust and the Royal Society (Grant Number 098436/Z/12/Z).

References

1. Maffei, M.E. Magnetic field effects on plant growth, development, and evolution. *Front. Plant Sci.* **5,** (2014).
2. Occhipinti, A., De Santis, A., Maffei, M.E. Magnetoreception: an unavoidable step for plant evolution? *Trends Plant Sci.* **19** (1), 1-4, (2014).
3. Harris, S.R. *et al.* Effect of magnetic fields on cryptochrome-dependent responses in *Arabidopsis thaliana*. *J. Royal Soc. Interf.* **6** (41), 1193-1205, (2009).
4. Phirke, P.S., Kubde, A.B., Umbarkar, S.P. The influence of magnetic field on plant growth. *Seed Sci. Technol.* **24** (2), 375-392 (1996).
5. Abe, K., Fujii, N., Mogi, I., Motokawa, M., Takahashi, H. Effect of a high magnetic field on plant. *Biol. Sci. Space.* **11** 240-247 (1997).
6. Volpe, P. Interactions of zero-frequency and oscillating magnetic fields with biostructures and biosystems. *Photochem. Photobiol. Sci.* **2** (6), 637-648, (2003).
7. Belyavskaya, N.A. Biological effects due to weak magnetic field on plants. *Adv. Space. Res.* **34** (7), 1566-1574, (2004).
8. Bittl, R. Weber, S. Transient radical pairs studied by time-resolved EPR. *Biochim. Biophys. Acta- Bioenerg.* **1707** (1), 117-126, (2005).
9. Galland, P. Pazur, A. Magnetoreception in plants. *J. Plant Res.* **118** (6), 371-389, (2005).
10. Minorsky, P.V. Do geomagnetic variations affect plant function? *J. Atm. Solar-Terrestr. Phys.* **69** (14), 1770-1774, (2007).
11. Vanderstraeten, J. Burda, H. Does magnetoreception mediate biological effects of power-frequency magnetic fields? *Sci. Tot. Environ.* **417,** 299-304, (2012).
12. Job, C., Rajjou, L., Lovigny, Y., Belghazi, M., Job, D. Patterns of protein oxidation in Arabidopsis seeds and during germination. *Plant Physiol.* **138** (2), 790-802, (2005).
13. Wan, L.L., Ross, A.R.S., Yang, J.Y., Hegedus, D.D., Kermode, A.R. Phosphorylation of the 12 S globulin cruciferin in wild-type and abi1-1 mutant *Arabidopsis thaliana* (thale cress) seeds. *Biochem. J.* **404** 247-256, (2007).
14. Sancenon, V., Puig, S., Mira, H., Thiele, D.J., Penarrubia, L. Identification of a copper transporter family in Arabidopsis thaliana. *Plant Mol. Biol.* **51** (4), 577-587, (2003).
15. Foyer, C.H., Karpinska, B., Krupinska, K. The functions of Whirly1 and Redox-Responsive Transcription Factor 1 in cross tolerance responses in plants: A hypothesis. *Philos.Trans.Royal Soc.B-Biol.Sci.* **369** (1640), 20130226, (2014).
16. Myouga, F. *et al.* A heterocomplex of iron superoxide dismutases defends chloroplast nucleoids against oxidative stress and is essential for chloroplast development in Arabidopsis. *Plant Cell.* **20** (11), 3148-3162, (2008).
17. Mhamdi, A., Queval, G., Chaouch, S., Vanderauwera, S., Van Breusegem, F., Noctor, G. Catalase function in plants: a focus on Arabidopsis mutants as stress-mimic models. *J. Exper. Bot.* **61** (15), 4197-4220, (2010).
18. Contento, A.L. Bassham, D.C. Increase in catalase-3 activity as a response to use of alternative catabolic substrates during sucrose starvation. *Plant Physiol. Biochem.* **48** (4), 232-238, (2010).
19. Kangasjarvi, S. *et al.* Diverse roles for chloroplast stromal and thylakoid-bound ascorbate peroxidases in plant stress responses. *Biochem. J.* **412,** 275-285, (2008).
20. Begara-Morales, J.C. *et al.* Dual regulation of cytosolic ascorbate peroxidase (APX) by tyrosine nitration and S-nitrosylation. *J. Exper. Bot.* **65** (2), 527-538, (2014).
21. Li, N. *et al.* AtrbohD and AtrbohF negatively regulate lateral root development by changing the localized accumulation of superoxide in primary roots of Arabidopsis. *Planta.* **241** (3), 591-602 (2015).
22. Murashige, T. Skoog, F. A revised medium for rapid growth and bioassays with tobacco tissue cultures. *Physiol. Plant.* **15,** 473-497 (1962).
23. Pfaffl, M.W. A new mathematical model for relative quantification in real-time RT-PCR. *Nuc. Acids Res.* **29** (9), (2001).
24. Bustin, S.A. et al. The MIQE Guidelines: Minimum Information for Publication of Quantitative Real-Time PCR Experiments. *Clin. Chem.* **55** (4), 611-622, (2009).
25. Phillips, M.A., D'Auria, J.C., Luck, K., Gershenzon, J. Evaluation of candidate reference genes for real-time quantitative PCR of plant samples using purified cDNA as template. *Plant Mol. Biol. Rep.* **27** (3), 407-416, (2009).
26. Andersen, C.L., Jensen, J.L., Orntoft, T.F. Normalization of real-time quantitative reverse transcription-PCR data: A model-based variance estimation approach to identify genes suited for normalization, applied to bladder and colon cancer data sets. *Cancer Res.* **64** (15), 5245-5250, (2004).
27. Tsukaya, H. Developmental genetics of leaf morphogenesis in dicotyledonous plants. *J. Plant Res.* **108** (1092), 407-416, (1995).
28. Szymanowska-Pulka, J. Form matters: morphological aspects of lateral root development. *Ann. Bot.* **112** (9), 1643-1654, (2013).
29. Bewley, J.D. Black, M. *Seeds: Physiology of development and germination.* Plenum Press, New York (1994).
30. Kato-Noguchi, H., Ota, K., Kujime, H., Ogawa, M. Effects of momilactone on the protein expression in Arabidopsis germination. Weed *Biol. Manage.* **13** (1), 19-23, (2013).
31. Khandelwal, A., Elvitigala, T., Ghosh, B., Quatrano, R.S. Arabidopsis transcriptome reveals control circuits regulating redox homeostasis and the role of an AP2 transcription factor. *Plant Physiol.* **148** (4). 2050-2058, (2008).
32. Haddad, J.J. Oxygen-sensing mechanisms and the regulation of redox-responsive transcription factors in development and pathophysiology. *Respirat. Res.* **3** (1), (2002).